UNIVERSITEIT VAN PRETORIA
UNIVERSITY OF PRETORIA
YUNIBESITHI YA PRETORIA

GUIDELINES FOR PREDICTING THE REMAINING LIFE OF UNDERGROUND PIPE NETWORKS THAT ARE SUBJECTED TO THE COMBINED EFFECTS OF EXTERNAL CORROSION AND INTERNAL PRESSURE

Christoffel Gerhardus van Deventer

Presented in partial fulfilment of the requirements for the degree

Masters in Engineering

(Mechanical Engineering)

in the Faculty of Engineering, Build Environment and Information Technology,
University of Pretoria

Department of Mechanical and Aeronautical Engineering

2002

GUIDELINES FOR PREDICTING THE REMAINING LIFE OF UNDERGROUND PIPE NETWORKS THAT ARE SUBJECTED TO THE COMBINED EFFECTS OF EXTERNAL CORROSION AND INTERNAL PRESSURE

CHRISTOFFEL GERHARDUS VAN DEVENTER

9603997

Mentor: Dr M Heyns

Department: Department of Mechanical and Aeronautical Engineering
UNIVERSITY OF PRETORIA

Degree: Masters in Mechanical Engineering

ABSTRACT

Underground pipelines are used in various process piping systems to transport gasses or fluids and are usually subjected to the effects of external corrosion.

Corrosion can be defined as the deterioration of a material due to a reaction with its environment or the destruction of the material by means that are not mechanical (Fontana and Greene, 1967:2). External corrosion, due to the interaction between the pipe and the soil, is generally a slow process and the corrosion rate is influenced by a variety of external factors. Some of these factors include the ambient pH and salinity, the presence of moisture and bacteria, temperature, the electrical potential difference between the pipe and other structures and the implementation of preventative measures (such as cathodic protection and wrapping).

Although the external corrosion of underground pipelines is generally a slow process in mild environments, pipe degradation as a result of external corrosion remains one of the prevalent reasons for the failure of underground pipelines.

As with many mechanical systems that are prone to fail at one time or the other, the high costs involved with unforeseen failure necessitate some quantitative (or qualitative) indication of the condition of the pipe system. Some of the costs that can be expected as a result of unforeseen pipeline failure are, amongst others:

- *costs as a result of the failure of dependent systems;*
- *costs as a result of the loss of production;*
- *costs as a result of the loss of product (in distribution networks);*
- *the cost of unscheduled maintenance (logistical costs);*
- *costs as a result of damage to public property;*
- *fines imposed by customers (in distribution networks);*
- *costs related to pollution control, and*
- *the loss of life.*

The single most important parameter associated with the condition of a system is its profitable remaining life. This is the time during which a sub-system contributes to the well-being of a larger system and the organisation. Therefore, it is necessary to determine, with reasonable accuracy, the extent of the remaining life of a system so that managerial decisions (i.e. investments, cash-flow analyses, maintenance task scheduling and replacement programmes), based on this figure, can be made. Done correctly, this can directly lead to a decrease in maintenance costs and subsequently to an increase in profit.

The extent of a corrosive attack on the pipeline might be highly localised or might be fairly uniform over the length of the installation. The fact of the matter is that, since the pipe is buried, it is very difficult to quantify the external damage caused by corrosion. A variety of techniques are in use to survey pipelines and detect anomalies. However, for large pipelines, most of these techniques are either inefficient or too expensive. There will always remain some uncertainty regarding the integrity of the pipeline.

The work presented in this study is explained with valid generic examples and aims:

1. *to provide the reader with sufficient background information so that the need for determining the integrity of a pipeline becomes apparent;*
2. *to indicate why a reliability-centred approach is necessary (Chapter 1);*
3. *to explain the basic principles of corrosion and the electrochemical nature of corrosion (Chapter 2);*
4. *to indicate areas, based on the basic principles of corrosion, where severe corrosion can be expected (Chapters 2 and 7);*
5. *to provide and elaborate on information regarding pipe surveillance techniques that are currently available (Chapter 3);*
6. *to establish the criteria for pipeline failure, in the form of a limit state function, for pipes that are subjected to near-constant internal pressures (static failure domain) as well as for pipes subjected to varying internal pressures (fatigue domain) (Chapters 5 and 6);*

7. *to indicate the sensitivity of the fatigue domain solution to changes in the system variables and to indicate that a significant reduction in the system variables does not necessarily reduce the solution accuracy (Chapter 6), and*
8. *to integrate the above-mentioned into a practical and workable guideline that can be used to determine the remaining life of an underground pipe network (Chapter 7).*

Keywords:

External corrosion, internal pressure, underground, pipe networks, fatigue, Monte Carlo simulation, reliability, probability of failure, soil corrosion rate, ultrasonic inspection

SAMEVATTING

Ondergrondse pyplyne word in verskeie proses stelsels gebruik om verskeie vloeiers te vervoer en is gewoonlik blootgestel aan uitwendige korosie.

Korosie kan gedefinieer word as die verlies van materiaal integriteit as gevolg van die materiaal se wisselwerking met sy omgewing of as die vernietiging van die materiaal op 'n ander wyse as suiwer meganies (Fontana en Greene, 1967:2). Uitwendige korosie, as gevolg van die wisselwerking tussen die pyp en die grond, is gewoonlik 'n stadige proses en word deur verskeie eksterne faktore beinvloed. Van hierdie faktore sluit die volgende in: die omgewing se pH en sout vlakke, die teenwoordigheid van vog en bakterieë, temperatuur, elektriese potensiaal verskille tussen die pyp en ander strukture en die teenwoordigheid van voorkomende maatreëls.

Alhoewel uitwendige korosie van ondergrondse pype 'n stadige proses in gematigde omgewings is, is die verlies aan pyp integriteit, as gevolg van korosie, waarskynlik die grootste oorsaak van pyp falings. Soos met enige meganiese stelsel, wat verdoem is om een of ander tyd te faal, is die hoë kostes gekoppel aan onvoorsiene pyp faling die dryfveer om 'n kwantitatiewe of kwalitatiewe aanduiding van pyp integriteit te verkry. Van die kostes wat verwag word, as gevolg van onvoorsiene pyp faling, sluit die volgende in:

- *kostes as gevolg van faling van afhanklike stelsels;*
- *kostes as gevolg van produksie verliese;*
- *kostes as gevolg van produk verliese (in verspreidings netwerke);*
- *logistiese kostes as gevolg van ongeskeduleerde instandhouding;*
- *kostes as gevolg van skade aan publieke eiendom;*
- *boetes ingedien deur verbruikers (in verspreidings netwerke);*
- *kostes as gevolg van besoedelingsbeheer, en*
- *die verlies van lewens.*

Die belangrikste parameter wat geassosieer word met die integriteit van 'n stelsel is die stelsel se oorblywende winsgewende leeftyd. Hierdie is die tydperk waartydens 'n sub-stelsel bydra tot die welvarendheid van 'n grooter stelsel en die organisasie. Daarom is dit nodig om, tot 'n aanvaarbare akkuraatheid, die oorblywende lewe van só 'n stelsel te voorspel sodat bestuursbesluite aangaande beleggings, kontantvloei, instandhouding skedulering en vervanging strategieë op 'n gefundeerde grondslag geneem kan word. Sulke gefundeerde besluite lei tot 'n vermindering in instandhoudingskoste en gevolglik 'n verhoging in wins.

Die omvang van die uitwendige korosiewe aanval op die pyplyn mag hoogs gelokaliseerd wees maar mag net sowel redelik eweredig oor die lengte van die pyp versprei wees. Die feit is dat, aangesien die pyplyn begrawe is, dit ongelooflik moeilik is om die uitwendige skade, as gevolg van korosie, te kwantifiseer. Verskeie metodes en tegnieke bestaan om lokale skade te kwantifiseer maar word oneffektief of duur vir groot pyp netwerke. Daar sal dus altyd 'n mate van onsekerheid bestaan oor die integriteit van die netwerk.

Die werk wat in hierdie studie voorgelê word, word verduidelik aan die hand van geldige generiese voorbeelde en is gerig op die volgende:

1. *om die leser met genoeg agtergrond kennis te voorsien sodat die behoefte om die integriteit van pyplyne te bepaal van selfsprekend word;*
2. *om aan te dui waarom 'n betroubaarheids-gebasseerde benadering nodig en voldoende is (Hoofstuk 1);*
3. *om die basiese korosie beginsels asook die elektro-chemiese aard van korosie te verduidelik (Hoofstuk 2);*
4. *om lokale gebiede waar erge korosie verwag kan word, gegrond op die basiese korosie beginsels, uit te wys (Hoofstuk 2 en 7);*
5. *om die leser bekend te maak met die beskikbare moniterings metodes en tegnieke (Hoofstuk 3);*
6. *om 'n pyplyn falingskriterium, in die vorm van 'n grenstoestandsfunksie, vir pype wat aan konstante (statiese falings gebied) sowel as veranderende interne (vermoeidheids gebied) druk blootgestel word (Hoofstuk 5 en 6);*
7. *om die sensitiwiteit van die vermoeidheids gebied oplossing ten opsigte van veranderinge in die stelsel veranderlikes te bepaal en aan te toon dat 'n*

noemenswaardige vermindering in die stelsel veranderlikes nie noodwendig die akkuraatheid van die oplossing verlaag nie (Hoofstuk 6), en

8. *om die bogenoemde te integreer tot 'n praktiese en werkbare riglyn wat gebruik kan word om die oorblywende leeftyd van 'n ondergrondse pyp netwerk te voorspel (Hoofstuk 7).*

Sleutelterme:

Uitwendige korosie, interne druk, ondergronds, pyp netwerke, vermoeidheid, Monte Carlo simulasie, betroubaarheid, falings waarskynlikheid, grond korosie tempo, ultrasoniese inspeksie

ACKNOWLEDGEMENTS

I would like to express my gratitude towards the following persons who have contributed to, and showed interest in, this study:

1. Mr Robie Botes of *Sasol Technology* who identified the research opportunity.
2. Mr Adam Look of *Soil, Climate and Water* of the *Agricultural Research Council* who determined the soil properties used in the study.
3. Mr Len Laidlaw of *Fedhak Industrial Services* for his contributions to Chapter 3 – Available Technologies.
4. Dr Michiel Heyns for his guidance and technical input during this study.
5. Everyone at *Investmech* who supported and motivated me.
6. Mrs Lenie van der Merwe who played a great role in my understanding of mathematics.
7. My friends and family, especially my parents, who provided me with endless support and motivation.

LIST OF SYMBOLS

Symbol	Designation	Unit
A	Area	mm^2 or m^2
A_r	Amplitude ratio	-
a	Corrosion exponent that depends on the exposure conditions	-
B_d	Width of ditch of underground pipe	mm or m
b_p	Corrosion constant with value equal to the average pit depth	mm or m
b	Fatigue strength exponent	-
C	Internal pressure multiplication constant	-
C_d	Earth-pressure coefficient	-
C_t	Surface-load coefficient	-
COV	Coefficient of variation	-
c	Fatigue ductility exponent	-
D_i	Fatigue damage caused during reversal i	-
D_{total}	Total fatigue damage caused during one load block	-
d_p	Pit diameter	mm or m
d	Diameter	mm or m
E	Modulus of elasticity	GPa
E_p	Cell potential	mV
F	Force	N or kN
F_c	Faraday's constant	96.5×10^3 A.s/mol
$f(x)$	Statistical distribution function	-
$f(\underline{x}(t))$	The state function of an entity	-
ΔG	Change in free energy	J
I_c	Impact factor	-
i	Corrosion current	A
i_d, i_{CORR}	Current density	A/m^2

Symbol	Designation	Unit
J	Gradient vector	-
$K, \Delta K$	Crack-tip stress-intensity factor	$MPa\sqrt{m}$
K'	Cyclic-strength coefficient	MPa
k_d	Deflection coefficient	-
k	Corrosion multiplying constant	mm or m
k_m	Bending-moment coefficient	-
L	Length	mm or m
M	Atomic mass of corroding material	g/mol
$2N_f$	Number of reversals before failure	-
n	Corrosion exponential constant	-
n_e	Number of electrons involved with the corrosion reaction	-
n'	Strain-hardening exponent	-
P	Depth of corrosion penetration	mm or m
P_f	Probability of an event happening before a specified time	-
p_i	Internal pressure	MPa
R	Stress ratio	-
r_i	Internal pipe radius	mm or m
S_y	Yield strength of a material	MPa
T	Exposure time	Years
t_w	Wall thickness of pipe	mm or m
t_p	Depth of corrosion pit	mm or m
V	Shear force	N
Vol	Volume	mm^3 or m^3
w	Weight of corroded material	gram
$\underline{x}(t)$	A variable set that is time dependent	-
$\Delta\underline{x}(t)$	A change in the variable set that is a function of time	-

Symbol	Designation	Unit
z	Limit state function	-
$z_H(T)$	Hazard Rate Function	-
α	Thermal expansion coefficient	1/°C
γ	Unit weight of soil	-
$\Delta\theta$	Temperature differential	°C
δ	Step size	-
$\frac{\partial F(T,\underline{x})}{\partial x_i}$	Partial derivative of $F(T,\underline{x})$ with respect to x_i	-
$\Delta\varepsilon$	Strain range	m/m
$\varepsilon_f{}'$	Fatigue-ductility coefficient	m/m
ρ	Density	kg/m^3
σ_{stat}	Standard deviation	-
σ	Tensile stress	MPa
σ_a	Stress amplitude	MPa
σ_m	Mean stress	MPa
$\sigma_f{}'$	Fatigue-strength coefficient	MPa
σ_{eq}	Equivalent Von Mises stress	MPa
$\Delta\sigma$	Stress range	MPa
μ	Statistical mean	-
ν	Poisson's ratio	-
τ	Shear stress	MPa
χ	Longitudinal curvature	rad.m^{-1}

TABLE OF CONTENTS

INTRODUCTION

Pipes play an integral part in many process industries, are the preferred method of transporting liquid and suspended bulk in process plants and are extensively used in distribution networks (such as water and gas distribution networks). For this reason, it is safe to state that pipes play an integral role in the world economy.

In mild environments, pipes are subjected to very little internal or external mechanical wear and the implementation of preventative measures, such as lining, wrapping and cathodic protection, usually protects the pipes against the effects of aggressive bulk and the environment.

Pipe failure rates vary highly from location to location and from application to application. In the United States, more than 329 water and gas utilities have cast iron distribution mains with continuous service records that stretch back further than 100 years and nine have mains that are more than 150 years old (Cast Iron Soil Pipe Institute, 2000). According to the *Cast Iron Soil Pipe Institute* (CISPI), over 95 % of all cast-iron pipes that have ever been installed in underground service in the United States are still in use. However, according to a survey conducted by the *Canadian National Research Council*, each year ageing pipes rupture at a rate of 35.9 breaks for every 100 kilometres and more recently installed metallic pipes still average approximately 9.5 breaks per 100 kilometres (Chlorine Chemistry Council, 2000).

Underground pipe networks are invariably subjected to the effects of external corrosion and the CISPI states that, in the case of an underground water main buried in significantly moist soil, corrosion is a definite concern in cases where the pipe is more than 30 years old (Cast Iron Soil Pipe Institute, 2000).

Various methods and techniques are available and are in use to quantify the effects that a pipe's environment has on its integrity and some of these are presented in Chapter 3 of this study. However, no formal methodology with which the remaining life of an underground pipe network can be predicted exists. The work presented in this study aims to provide guidelines for predicting the remaining life of underground

pipe networks that are subjected to the combined effects of external corrosion and internal pressure.

Since the world in which we live and function is dynamic and ever changing, the performance required from all earth-bound systems also changes and evolves. This inherent drive for change in system performance forms the foundation of the work presented in this study. One of South Africa's leading petro-chemical companies was, at the start of this study, conducting feasibility studies for the expansion of one of their underground pipe networks. The details of this expansion remained confidential throughout the research period (and probably still are) and no access to any relevant information was granted to the author.

The main concerns expressed by the company were the following:

1. *What is the present state of the integrity of our pipe network?*
2. *What will happen if we increase the operational demand?*
3. *How will any changes affect the system's integrity?*

An underground pipe network can easily be approximated as a mechanical system in which loads acting on the load-bearing material cause structural stresses. Some of these loads can be approximated as quasi-static while others can be approximated as live or varying. These loads can cause failure in two different domains respectively, 1) the static failure domain (Chapter 5), and 2) the fatigue failure domain (Chapter 6). The structural integrity of a pipe can easily be inferred using a variety of classical theories and/or numerical techniques in both these failure domains.

However, another two aspects related to the integrity of underground pipes may be readily identified:

1. the corrosion aspect, and
2. the aspect of scale and uncertainty.

The corrosion, either internal or external, of the load-bearing material causes structural stress to increase as a function of time. This time-dependent increase in

stress can easily be incorporated into both of the above-mentioned failure domains and a reduction in life, due to corrosion, may be expected.

However, the aspect of scale and uncertainty requires more attention:

Pipe networks vary in length from a few hundred metres to hundreds of kilometres. The same pipe network may, furthermore, be subjected to varying degrees of corrosive aggression and the integrity of the system is therefore not explicitly quantifiable. Anomalies, due to soil-induced corrosion, may be highly localised and on a micro-scale ("pitting" – Chapter 2) or may be fairly uniformly present over the length of the pipeline ("uniform attack" – Chapter 2).

The differences in the scales of the anomalies therefore pose difficulties on three different conceptual levels:

1. *the mathematical model of the effect that corrosion has on the integrity of the pipe network (for both failure domains) should be similar (or at least be substitutable) for both anomaly scales;*
2. *the "chance" of detecting an uniform anomaly is possibly greater than that of detecting a localised, micro-scale anomaly, and*
3. *the techniques/methods used to detect localised anomalies might become inefficient or expensive when used to detect global effects.*

*Thus, it can be deduced that the aspect of scale will **induce and guarantee** a degree of uncertainty in the prediction of pipeline integrity whenever localised **and** uniform effects are present in the same pipe network (which is entirely possible!).*

The high probability of localised and uniform effects occurring in the same pipe network, as well as the inherent uncertainty that surrounds the magnitude of system variables (such as material and geometrical properties, load magnitude and corrosion rates), ***compel*** one to ***reconsider*** the conceptual solution.

The author is of opinion that it would be foolish to believe a prediction of pipeline integrity that yields a highly defined, singular indication of the state of the

underground pipe network. Such a solution ***is*** presented in Chapters 5 and 6 but it only forms ***the basis*** of a reliability approach. In Chapter 5 it is indicated that ***20 independent system variables*** are needed to describe and solve the static failure domain solution while in Chapters 4 and 6 it is indicated that ***26 independent system variables*** are needed to describe and solve the fatigue failure domain solution. This implies that, in order to give a highly defined, highly accurate, singular solution to the integrity problem, the magnitude of each of the 26 odd variables needs to be determined ***exactly***! (Which is, of course, highly unlikely when most of the parameters are to be measured *in situ*). It becomes evident that a probability based solution is required.

The author is of opinion that including uncertainties in predictive models is becoming more and more relevant in the various engineering disciplines as can be seen in various recent publications (for example McAllister and Ellingwood, 2002:21).

Mathematical and predictive theories are frequently tested and verified by conducting experiments or tests in highly controlled, almost sterile, laboratory environments. For these experiments, high correlations between the predicted and measured results are usually the order of the day. The correlation between the predicted and measured results tends to be lower when these controlled and sterile environments are "contaminated". This is usually of minor concern when the differences in predicted and measured results can be explained rationally.

However, one nagging question arises:

"Is any predictive model or theory relevant in the real world?"

Most predictive models ***are*** relevant in the real world. There is ***no reason*** to believe that a theory would be less relevant in a "contaminated" world than in a "sterile" world. However, one should just keep in mind that the results yielded by the model in a "contaminated" world would differ from that obtained in a "sterile" world. The predominant reason for this difference is not the "contamination" *per se*, but rather the uncertainties regarding the magnitudes of the input variable set caused by the "contamination".

How does one take these uncertainties into account?

The first paradigm shift that one has to make when answering this question is the following:

"Do not believe only one answer" and

"The real answer is somewhere to be found"

These rather tongue-in-cheek statements should be interpreted as follows:

1. the results obtained from a prediction in the real ("contaminated") world are not singular, and
2. the real result lies within the boundaries that are controlled by variations in the system's variable set induced by "contamination".

The research conducted for this study is presented in the following chapters:

- *Chapter 1 supplements the above-mentioned arguments and tries to explain the origins of error in a predictive model;*
- *Chapter 2 briefly describes and explains the electro-chemical nature of the corrosion process;*
- *Chapter 3 presents the various non-destructive surveillance techniques presently in use to quantify corrosion damage on pipelines;*
- *Chapter 4 presents the expected stresses present in underground pipelines as well as their relative magnitudes;*
- *Chapter 5 presents the static failure domain integrity solution;*
- *Chapter 6 presents the fatigue failure domain solution, and*
- *Chapter 7 integrates all the concepts that have been presented into one practical and workable guideline for predicting the remaining life of an underground pipe network that is subjected to the combined effects of external corrosion and internal pressure.*

Lastly, the work presented in this study should be seen as a decision-making tool or resource that can be used to obtain quantitative indications of the integrity of underground pipe networks.

1. MAKING PREDICTIONS: THE THREE ORIGINS OF ERROR

Understanding the way the world works means developing a realistic intuition of the way that human society obeys the mathematics of natural processes. Reality is non-linear. But most people's expectations are not. To understand the dynamics of change, you have to recognise that human society, like other complex systems in nature, is characterised by cycles and discontinuities. That means certain features of history have a tendency to repeat themselves, and the most important changes, when they occur, may be abrupt rather than gradual.

- James Dale Davidson and Lord William Rees-Mogg

1.1. Introduction

Predictions concerning the behaviour of a certain entity are usually based on the behaviour exhibited by the entity under certain previously known conditions. Thus, the prediction is simply an extrapolation of trends observed in the entity's previous behaviour. Numerous cases where predictions have turned out to be incorrect are known. This usually happens when the underlying processes that govern the entity's behaviour are not taken into account or understood correctly. Due to the complexity of these underlying processes that govern the entity's behaviour, predictions are difficult to make. A widely accepted belief exists that the amount of effort made in insuring mathematical accuracy will lead directly to the reduction of error in a predictive model. This may be true for certain predictive models, but it is certainly not the norm. A better understanding of the underlying processes of an entity will increase accuracy of prediction.

This chapter represents the author's views on the origins of error in predictive models.

1.2. What is a scientific theory?

In order to talk about the nature of the universe and to discuss questions such as whether it has a beginning or an end, you have to be clear about what a scientific theory is. I shall take the simpleminded view that a theory is just a model of the universe, or a restricted part of it, and a set of rules that relate quantities in the model to observations that we make. It exists only in our minds and does not have any other reality (whatever that might mean).

A theory is a good theory if it satisfies two requirements: It must accurately describe a large class of observations on the basis of a model that contains only a few arbitrary elements, and it must make definite predictions about the results of future observations.

- Stephen W. Hawking, *A Brief History of Time*

1.3. Why do we make predictions?

In order to judge the accuracy of a certain prediction, it is necessary to understand the process of prediction. In order to understand the process of prediction, it is necessary to understand why we need to make predictions.

The primary purpose of making predictions is to evaluate the present state of an entity and, if necessary, to adjust present actions to obtain a more desirable future state. If we know what lies in the future, it will be possible to adjust our present actions so that we may obtain a more acceptable outcome. Knowledge of what lies in the future greatly affects our actions, decisions and judgements. If one is able to predict events in the future, it will be possible to adjust one's present actions in order to maximise future gain.

1.4. Destiny

The present state of an entity is a multi-dimensional function, $f(\underline{x})$, that depends on the ***whole*** set of variables ($\underline{x} = [x_1 \quad x_2 \quad x_3 \quad \ldots \quad x_N]$), known and unknown, that influences the state of the entity. Depending on the specific entity, these variables might be anything from temperature, interest rate, and time. A change in any one of these variables will adjust the state of the entity. It is normally desirable to determine the change in the variables, $\Delta\underline{x} = [\Delta x_1 \quad \Delta x_2 \quad \Delta x_3 \quad \ldots \quad \Delta x_N]$, that is necessary in order to arrive at a specific destination or future state. Predictions are thus dependent on the ***present state*** of the entity, the desired ***destination*** and the ***system variables***. These concepts can be interpreted graphically as shown in Figure 1.1.

A natural interaction and inter-dependence exist between variables of the same and of different sets. These interactions cause the variable set to change and, ultimately, are time dependent. The entity thus has a natural tendency to change in multi-dimensional space. If there is no external adjustment of the variable set ($\underline{x(t)}$), which affects the entity state ($f(\underline{x(t)})$), the entity will naturally tend to reach a specific future state (see Figure 1.1.).

The ***destiny*** of an entity is the state the entity would reach in the absence of external adjustment in the system variables. Usually this is the state of lowest entity energy and it might be argued that the entity would have the same destiny regardless of its history (since it is the state of lowest energy). This echoes the known thermodynamic principle that a reaction path cannot be determined from the law of energy conservation. Destiny is a fixed point in multi-dimensional state. An entity can never avoid its destiny. Entities of the same class have the same destiny. The route, however, that each of these entities follow to their common destiny will be different.

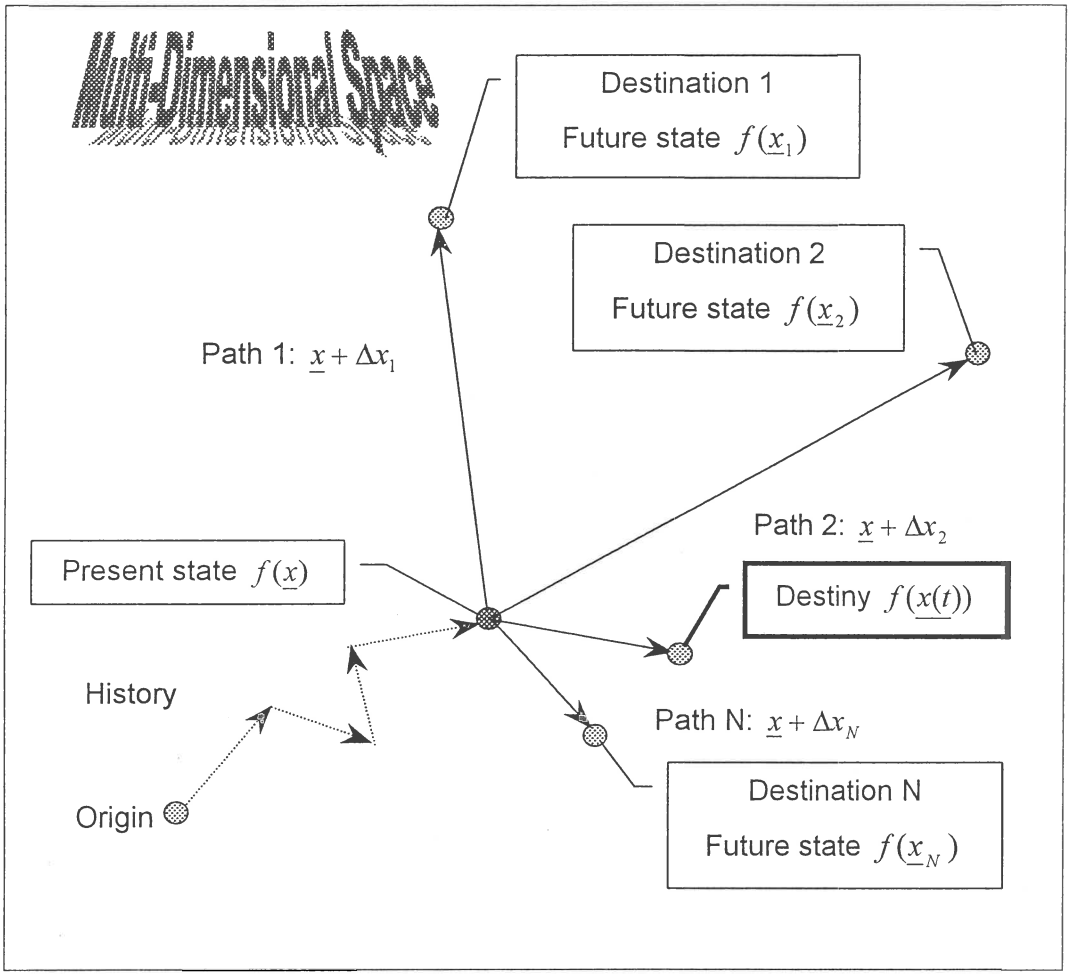

Figure 1.1. Representation of present and future entity states

1.5. The state function (*f(x)*): the first origin of error

If the entity's state function and the final state of the system variables are known, it is possible to determine the entity's destiny. In general, if the state function is known and if it is possible to measure the system variables at a specific position in space, it is possible to evaluate the state of the entity at that position in space. This can be depicted graphically as shown in Figure 1.2. Decisions can be made based on this principle. If the future state ($f(\underline{x})$) associated with a certain change in the system variables ($\Delta\underline{x}$) is unfavourable, the state can be avoided by adjusting the system variables.

The state function has as input a set of variables, it takes into account all the intricacies and dynamics of the system, and is basically a depiction of the underlying processes that govern the entity's behaviour. The state function is

partly physical and partly magical. The importance of having knowledge of the state function is clear. One can, however, argue that this function is seldom, if ever, absolutely known. The whole issue of making predictions is the approximation of the state function. The approximated state function is simply a model that describes the behaviour of the entity and it may consist of a large set of theories.

It can be assumed that the real state function is a linear superposition of two sets of functions: a set that is quantifiable and describable, and a set that is indescribable and indeterminable. Mathematically it can be described as follows:

$$f(\underline{x}) = \sum_i G_i(\underline{x}_1) + \sum_j D_j(\underline{x}_2) \qquad (1.5.1)$$

where $G_i(\underline{x}_1)$ is the quantifiable set and $D_j(\underline{x}_2)$ is the indescribable set. The quantifiable set, $G_i(\underline{x}_1)$, is the only obtainable set of functions and can be obtained from a large number of classical theories and/or numerical techniques. The indescribable set ($D_j(\underline{x}_2)$), on the other hand, will always remain unknown to the analyst. $D_j(\underline{x}_2)$ is the set of functions that describes the unpredictable part of every prediction.

The quantifiable set, $G_i(\underline{x}_1)$, depends on a different set of variables than $D_j(\underline{x}_2)$. In general the sum of the subsets of variables should be equal to the whole set of system variables:

$$\underline{x}_1 + \underline{x}_2 = \underline{x} \qquad (1.5.2)$$

The quantifiable behaviour function (i.e. the approximated state function), $F(\underline{x}_1) = \sum_i G_i(\underline{x}_1)$, is the only obtainable description of an entity's behaviour. Thus, the part of the entity's behaviour that remains unpredictable always exists. This is the first origin of error in the model that predicts the entity's behaviour. The error in the prediction of the entity's state can be defined as the difference in real state and predicted state:

$$Error = f(\underline{x}) - F(\underline{x}_1) = \sum_j D_j(\underline{x}_2) \qquad (1.5.3)$$

As the quantifiable behaviour function grows in complexity and takes more of the system variables into consideration, the error will tend to decrease:

$$\lim_{\underline{x}_1 \to \underline{x}} F(\underline{x}_1) = f(\underline{x}) \qquad (1.5.4)$$

$$\text{and } Error \to 0$$

The most important property of the approximate state function is that it has definite boundaries – there are points or regions in space where the approximate state function will fail to predict the behaviour of the entity. These concepts are illustrated graphically in Figure 1.3.

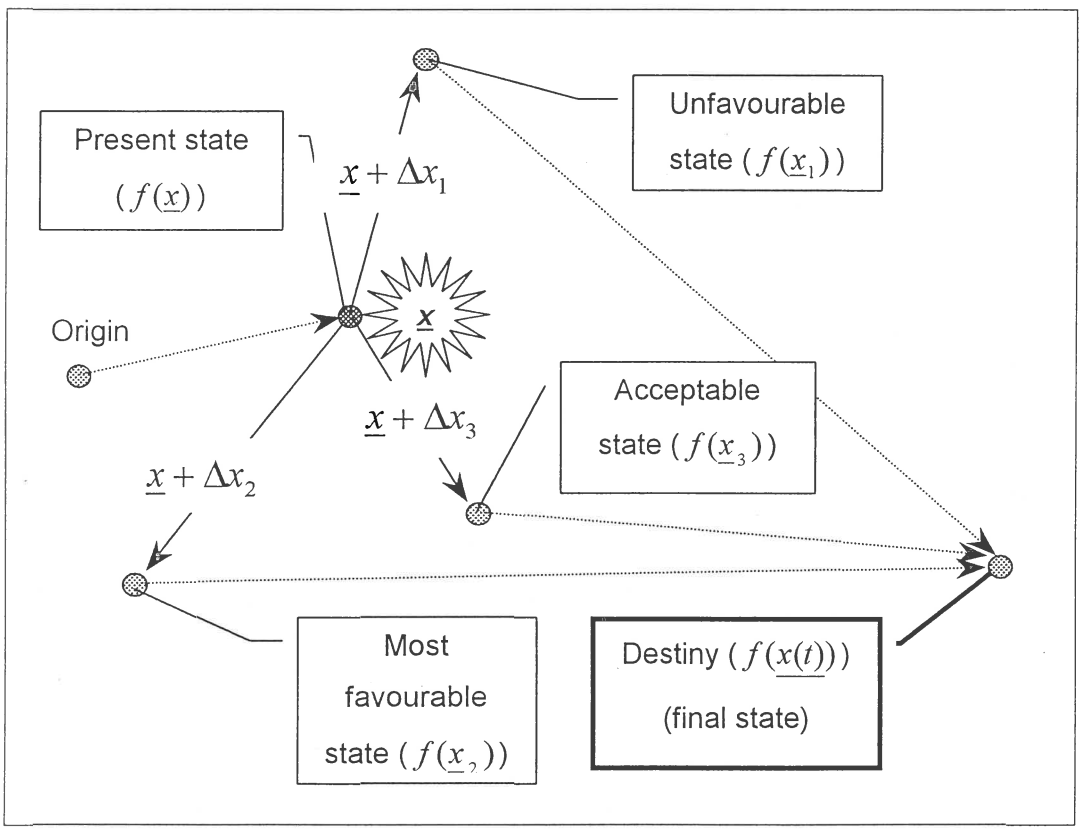

Figure 1.2. Different system variables = different entity states

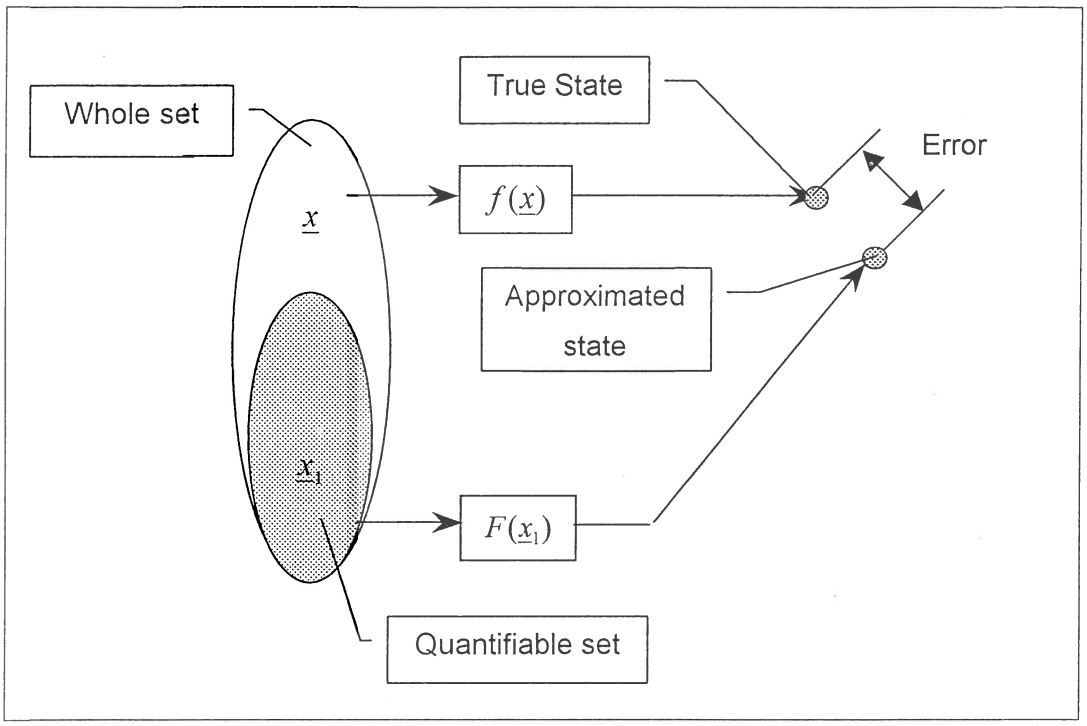

Figure 1.3. The effect of the number of variables on the predicted state

1.6. Events: the second origin of error

Events are sudden changes in the entity's state. An event cannot change the entity's destiny but it has a definite influence on the route that the entity follows to its destiny. It abruptly changes the direction of the entity's route and therefore it can be seen as a ***fixed*** discontinuity in multi-dimensional space. Events are the coming together of an amalgamation of different factors that suddenly adjust the system variable set. Common examples of events are accidents, births, deaths and all sorts of system failures. Events are "known" to the state function since it has to describe the state of the entity at that specific point in space. Events are not gradual but instantaneous. Because events are fixed in space, they may or may not be avoidable. An entity's route through space may be changed when it comes into close contact with an event. An event is thus surrounded by an "event field" that influences the route of the entity through space. These concepts are graphically depicted in Figure 1.4.

A very common application of making predictions is to determine under what conditions a certain event will take place. An example of this is a fatigue analysis where one wishes to determine whether a component will fail under a

given set of conditions (i.e. system variables such as load, geometry and material properties).

The second origin of error in a predictive model is the inability of the approximated state function ($F(\underline{x}_1)$) to predict events accurately in space. The accuracy of the predictive model may decrease even more if the approximated state function is unable to predict the effect that the "event field" has on the entity's route through space.

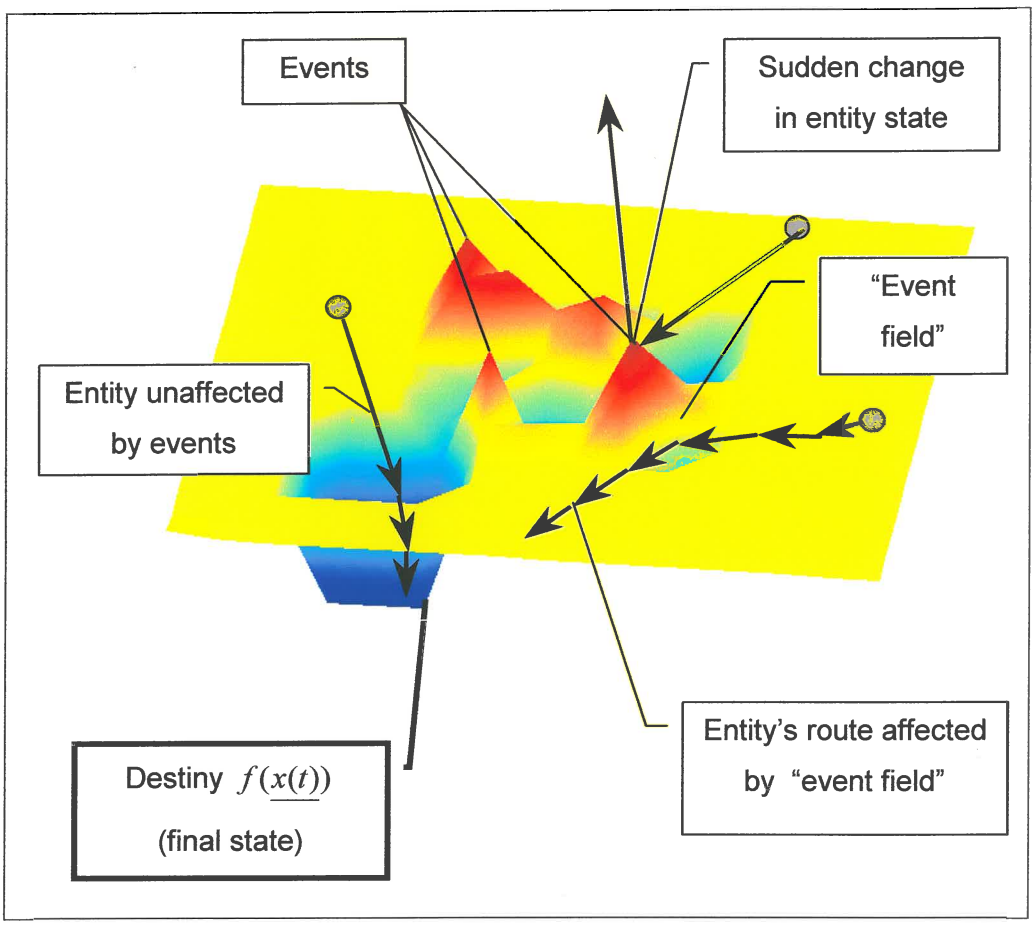

Figure 1.4. The effect of events on the entity's state

1.7. Assumptions and simplifications: the third origin of error

The approximate state-function ($F(\underline{x}_1)$) may consist of a variety of theories and laws that are needed to describe the entity's behaviour under certain conditions. The sum of all these theories and laws may be very complex in nature and the approximate state function may become tedious and expensive to evaluate. If certain tendencies in entity behaviour are observed, certain assumptions and simplifications can be made in order to make the evaluation of the approximate state function less rigorous. The third origin of error in the predictive model is the total of all errors that are made in the simplification and evaluation of the approximate state function. This error is usually of minor concern if the assumptions are believed to be valid.

An example is the simplification that $\sin(\theta) = \theta$ for small θ. This simplification is 94 % accurate for $\theta = 0.6\ rad = 34.4^{\circ}$. This is by no means a small angle but the difference between the simplified and original model is just 6 %.

1.8. Approximating the state function

The three origins of error were discussed in the previous three sections. Of these three, the main contributors to error in a predictive model were identified as 1) the human inability to describe the entity state function in totality, and 2) the inability of the approximate state function to accurately predict the effect that events have on the entity's behaviour. Both these origins of error are directly related to the ability of the analyst to identify and prioritise trends seen in the entity's real behaviour.

If, for example, the analyst was unable to detect that the stress intensity at the crack tip of a cracked specimen was dependent on the crack geometry, the approximated state-function would have been in gross error. Any other theories that would have followed on this (erroneous) approximated state-function would have "tried" to adjust the approximation in order to predict the real crack behaviour of the specimen. For this reason it is necessary to have the capability to accurately approximate the state function.

The state function can be approximated in two ways:

1. An entity can be isolated and a set of variables that is believed to be the predominant driving force behind the entity's behaviour can be identified. The variables are then "fed" to the entity and its response to the various variable magnitudes are logged. Hopefully there will be certain trends in the entity's response and extrapolations, based on these trends, can be made. These extrapolations are usually tested and, if necessary, the predictive model is adjusted and refined.

2. The problem with the above-mentioned approach is that, in some cases, it is impossible to isolate certain entities or the entity's behaviour is greatly influenced by other entities so that it becomes impossible to identify the predominant variable set. It may also happen that large changes in the predominant variable set only result in very small changes in entity behaviour (i.e. the entity is relatively insensitive to changes in the variable set). In these cases the scale of the problem does not permit an intrinsic investigation into the effect the variable set has on the entity's behaviour and a holistic approach must be taken. Certain properties of the entity are coupled to other models that describe the behaviour of certain aspects of the entity. From this holistic model it will be possible to deduce specific trends in the entity's behaviour.

1.9. Conclusion

Detailed knowledge of an entity's behaviour enables the designer/analyst to use optimisation techniques to determine the value of the variable set that will obtain the most favourable entity state. This optimisation has become more and more important due to the decreasing availability of natural resources, the onset of global trading and a society that has become more aware of product performance.

With the increase in the availability and computational ability of computers, there has been an accelerated growth in the development of numerical analysis techniques, and it has become easier to evaluate complex mathematical functions. However, events still exist that remain

unpredictable – despite the mathematics and all the complex theories that have developed over the ages, the pivotal question of how the universe came about still remains unanswered.

As an analyst, one should guard against over-emphasising the required level of accuracy of a prediction. Predictions can be very accurate but it is not always necessary to make predictions that are accurate to the thirteenth decimal. One must recognise the sources of error in the prediction, and through good sense and insight, evaluate the results. It is good practice not to make predictions about events very far ahead in time. Thus, it is possible to assess the accuracy of the prediction when the specific time comes and, if necessary, to adjust the predictive model.

In the following chapters it will be shown that the parameters/variables that influence the state of a pipeline (i.e. the corrosion rate and resulting deterioration of strength) are not constant. The extent of the corrosive attack may vary along the length of the pipeline or it may be highly localised. Due to practical constraints uncertainty will exist regarding the integrity of the pipeline and it is therefore not practical or logical to try to determine a singular and unique life expectancy of the pipeline. This chapter should, therefore, be kept in mind during the arguments presented in this research.

2. UNDERSTANDING CORROSION

The universe rewards us for understanding it and punishes us for not understanding it. When we understand the universe, our plans work and we feel good. Conversely, if we try to fly by jumping off a cliff and flapping our arms the universe will kill us.

- Jack Cohen and Ian Stewart

2.1. Introduction

Pipeline degradation caused by corrosion is by far the most prevalent reason for failure in various process piping systems. In order to determine the remaining life of an underground pipe network, it is necessary to understand the corrosion process. Corrosion may be defined as the deterioration of a material due to a reaction with its environment or the destruction of the material by means that are not simply mechanical (Fontana and Greene, 1967:2).

The corrosion rate of a pipe is influenced by a variety of factors. Some of these factors include:

1. the ambient pH;
2. the ambient salinity;
3. moisture;
4. temperature;
5. the presence of bacteria;
6. the electrical potential difference between the pipe and other structures;
7. the material composition of the pipe, and
8. the presence of preventative measures (cathodic protection and wrapping).

Corrosion is generally a slow process. In the United States, more than 329 water and gas utilities have cast iron distribution mains with continuous service records that stretch back further than 100 years. Nine have mains that are over 150 years old (Cast Iron Soil Pipe Institute, 2000). According to the *Cast Iron Soil Pipe Institute* (CISPI), over 95 % of all cast-iron pipes that have ever been installed in underground service in the United States are still in use. In the case of an underground water main buried in significantly moist soil, corrosion is a definite concern in cases where the pipe is over 30 years old. According to a survey conducted by the *Canadian National Research Council*, every year ageing pipes rupture at a rate of 35.9 breaks for every 100 kilometres of pipeline and more recently installed metallic pipes still average approximately 9.5 breaks per 100 kilometres (Chlorine Chemistry Council, 2000). It is important to note that not only metallic materials, but also non-metallic materials, are susceptible to corrosion damage.

Corrosion rates are expressed in a variety of ways, but in this document the rate of corrosion will be expressed in terms of the ***rate of penetration***, either in ***mm / year*** [***mmpy***] or ***mils / year*** [***mpy***] (1 mil = 1" / 1000). The rate of penetration expression is preferred to corrosion rates expressed in terms of weight loss since most structural strength calculations are based on component geometry and the penetration rate is directly linked to the geometry of the stress-bearing material that remains.

Although an atomic-level approach will not be used in this study, this chapter should serve as an introduction to corrosion. The content of this chapter is adapted from various texts listed in the bibliography at the end of this document.

2.2. The electrochemical nature of corrosion

The electrochemical nature of corrosion can be illustrated by the attack of hydrochloric acid on zinc. When zinc is placed in diluted hydrochloric acid, a vigorous reaction occurs: hydrogen gas evolves and the zinc dissolves, forming a solution of zinc chloride. The reaction is:

$$Zn + 2HCl \rightarrow ZnCl_2 + H_2 .$$

Noting that the chloride ion is not involved in the reaction, this equation can be simplified:

$$Zn + 2H^+ \rightarrow Zn^{2+} + H_2 .$$

Hence, zinc reacts with the hydrogen ions of the acid solution to form zinc ions and hydrogen gas. If one examines the above equation it can be seen that during the reaction zinc is oxidised to form zinc ions, and hydrogen ions are reduced to hydrogen.

The above equation can thus be divided into two reactions: the oxidation of zinc and the reduction of hydrogen ions:

OXIDATION (anodic reaction): $Zn \rightarrow Zn^{2+} + 2e$

REDUCTION (cathodic reaction): $2H^+ + 2e \rightarrow H_2$

The reactions reflected above are partial reactions and both must occur simultaneously and at the same rate on the metal surface. This leads to one of the most important basic principles of corrosion: during metallic corrosion, the rate of oxidation equals the rate of reduction (Fontana and Greene, 1967:10). If either the rate of oxidation or the rate of reduction is reduced, the overall corrosion rate will be reduced. The above example is valid for other acids too because it is only the hydrogen ion that is active in the reaction. In general, the anodic reaction in every corrosion reaction is the oxidation of metal M to its ion: $M \rightarrow M^{n+} + ne$.

Several different cathodic reactions are frequently encountered in metal corrosion. Some of these are:

Hydrogen evolution: $2H^+ + 2e \rightarrow H_2$

Oxygen reduction (in acid solutions): $O_2 + 4H^+ + 4e \rightarrow 2H_2O$

Oxygen reduction (neutral and basic): $O_2 + 2H_2O + 4e \rightarrow 4OH$

Metal ion reduction: $M^{3+} + e \rightarrow M^{2+}$

The corrosion of zinc in aerated hydrochloric acid is depicted graphically in Figure 2.1.

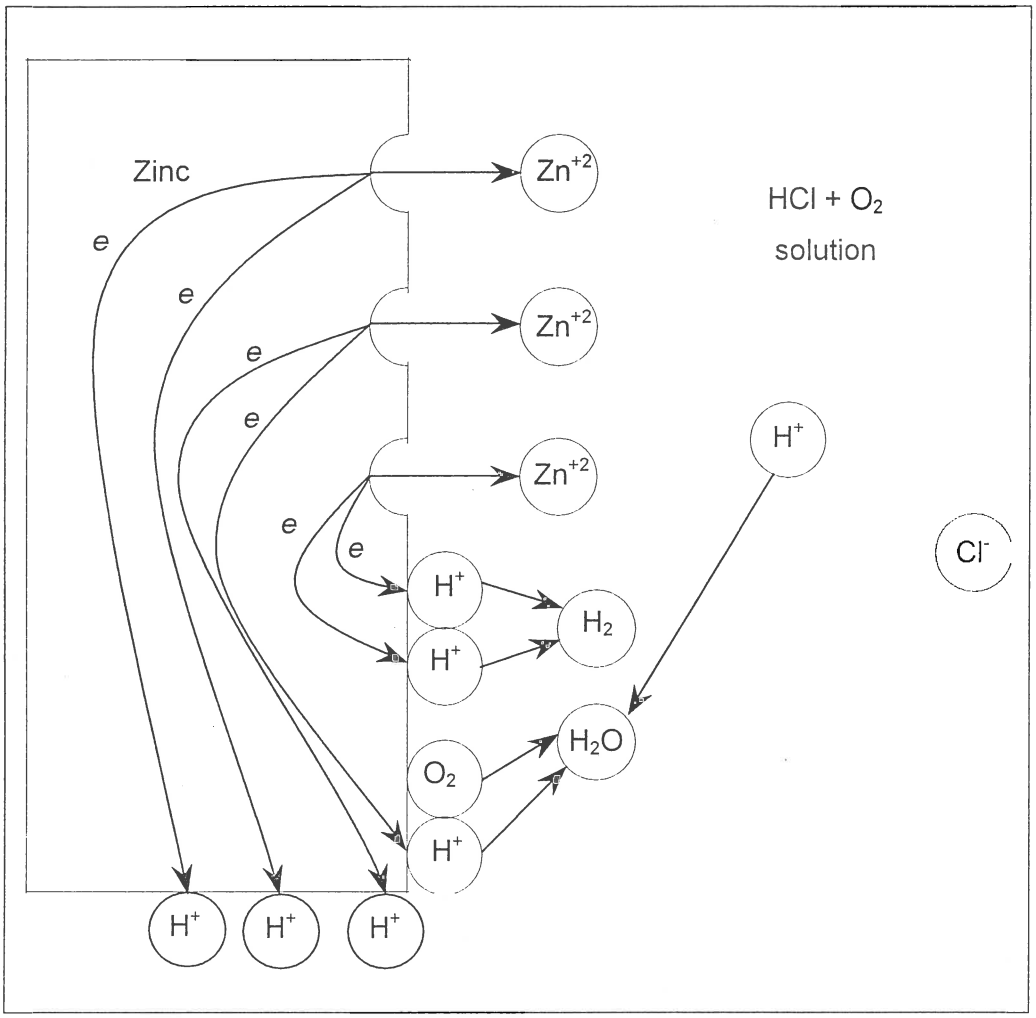

Figure 2.1. Electrochemical reactions that occur during the corrosion of zinc in an aerated hydrochloric acid

It is important to note that, since the anodic and cathodic reaction rates are mutually dependent, it is possible to control the corrosion rate by controlling either the anodic or the cathodic reaction. If the surfaces of the corroding metal were to be covered by a non-conducting material, both the anodic and cathodic reactions will be reduced and the total rate of corrosion is retarded. Also, it is clear that good conductivity must exist in both the metal and the electrolyte for corrosion to occur. Therefore, if the resistance of the electrolyte were increased, the rate of corrosion would be decreased (since it is impossible to predict where the sites of the anodic and cathodic reactions are

and it therefore makes no sense to reduce the conductivity of the metal). The fact that the hydrogen ions must diffuse to the reaction sites will also cause the reaction rate, and therefore the corrosion rate, to decrease.

2.3. Uniform attack

The most common form of corrosion is uniform attack. It is characterised by a chemical reaction that proceeds uniformly over the entire exposed surface (or over a large area) and at an almost uniform corrosion rate over the exposed area. The metal becomes thinner and eventually the remaining strength of the specimen falls below that which is required by the structure and failure occurs (i.e. the structural resistance is less than the structural load).

2.4. Galvanic or two-metal corrosion

An electrical potential difference usually exists between two dissimilar metals when they are immersed in a corrosive or conductive medium. When these metals are placed in electrical contact, this potential difference produces a flow of electrons between them. This has the effect that the corrosion rate of the less resistant metal is increased, while that of the more resistant metal is decreased. The less resistant metal becomes anodic and the more resistant metal becomes cathodic. This type of corrosion is called galvanic or two-metal corrosion.

The potential generated by a galvanic cell consisting of dissimilar metals can change over time. The potential difference generated causes a flow of current and corrosion occurs at the anodic electrode. As corrosion progresses, the products of corrosion may accumulate at either or both of the electrodes and this has a reducing effect on the corrosion rate. It is usual for the metal with the lower corrosion resistance to the given environment to become the anodic electrode (and it will therefore be the corroding electrode).

One expects accelerated corrosion attack due to galvanic effects to be greatest near the junction of the two dissimilar metals. Attack is expected to decrease as the distance between the two metals increases.

Another important aspect of galvanic corrosion is the ratio of cathodic to anodic electrode area. An unfavourable ratio is that of large cathodic and small anodic electrode areas. For a given current flow in the galvanic cell, the current density is much larger for the corroding anodic electrode than for the cathodic electrode. The higher current density in the anode has a direct accelerating effect on the corrosion rate of the anodic electrode.

As stated, galvanic corrosion is of concern where two different metals are in contact with one another in a conductive medium. A typical example of this is where a mild steel pipe is connected to a brass or copper valve. Definite inspections should be undertaken in such cases.

A number of preventative measures can be taken to combat the effect of galvanic corrosion (Fontana and Greene, 1967:37). These are to:

1. select material combinations that are as close as possible in the galvanic / EMF series;
2. avoid an unfavourable area effect (an anodic area that is smaller in comparison to the cathodic area);
3. insulate dissimilar metals if possible;
4. keep coatings in good condition (especially on the anodic area);
5. add inhibitors to decrease the aggressiveness of the conductive environment;
6. avoid threaded joints, since much of the remaining material is cut away and spilled liquid or condensed moisture can collect and remain trapped in the threaded grooves. Brazed or welded joints using an alloy more noble than at least one of the materials are preferable;
7. design for the use of readily replaceable anodic parts, or to make the anodic parts thicker for longer life, and
8. install a third metal anodic to both metals in the galvanic cell.

2.5. Crevice corrosion

Highly localised corrosion frequently occurs within crevices and other shielded areas on metal surfaces exposed to a corrosive medium. This type of corrosion is usually associated with small volumes of stagnant solution caused by holes, gaskets, lap joints, surface deposits and crevices under bolt and rivet heads. Examples of deposits that may lead to crevice corrosion are sand, dirt and products of corrosion. The deposit acts as a shield and creates a stagnant condition under it. Contact between metallic and non-metallic surfaces (such as the contact between a flange and a gasket) can lead to crevice corrosion. To function as a site of corrosion the crevice must be wide enough to allow for penetration of the corrosive medium, but narrow enough to maintain a stagnant zone. Fibrous gaskets may have a wick action and this will produce an almost permanent stagnant zone.

2.6. Pitting

Pitting is a form of extremely localised corrosive attack that results in holes in the metal surface. These holes may be small or large in diameter, but the diameter of a pit is usually much smaller than the depth of the pit. Pits are usually difficult to detect due to their small size and their relative small scale with respect to the rest of the structure. Pitting is usually difficult to predict using laboratory tests since some pits require a long initiation period before they become visible. Pits usually develop in the direction of gravity and they propagate at an increasing rate. In addition, they tend to undercut the surface as they propagate. Pitting is usually associated with stagnant conditions. Increasing the velocity of the corrosive medium often decreases the pitting attack.

If one considers the equivalent shear stress (as calculated using Mohr's circle) at the root of the pit, it can easily be shown that the pit depth is the predominant driving force behind failure at sites where pitting occurs. Consider the cylindrical pit in the pipe wall shown in Figure 2.2.

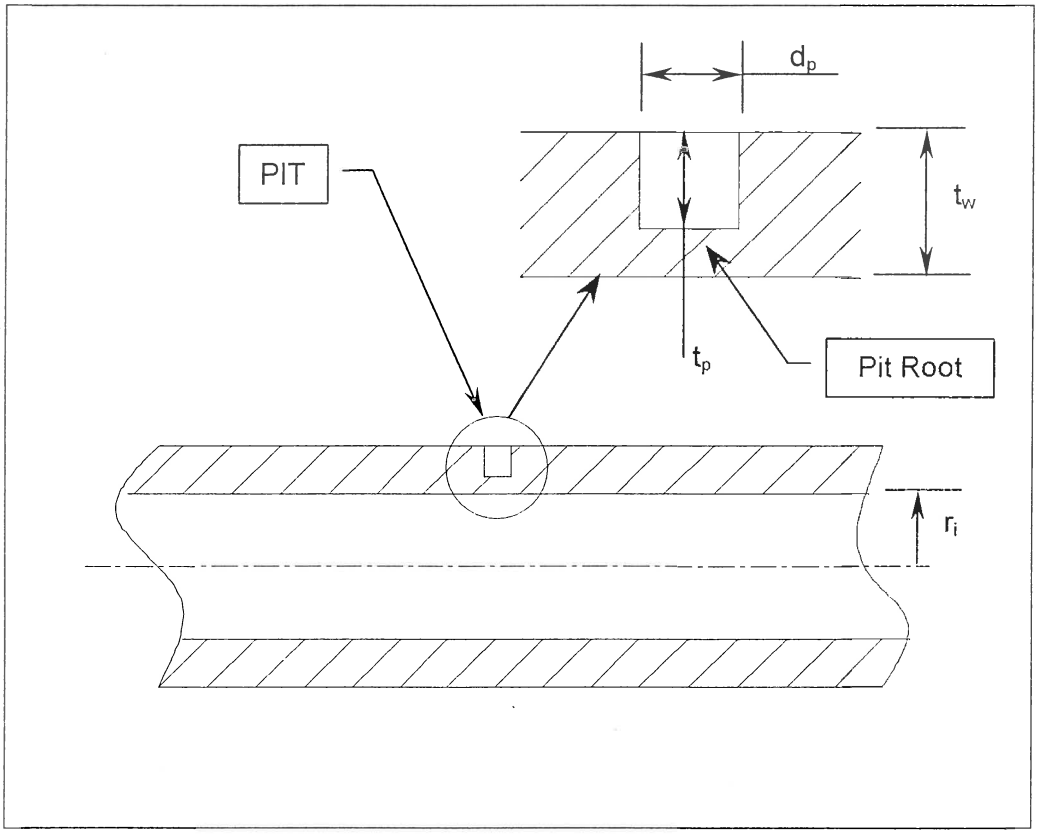

Figure 2.2. Detail of pit geometry in a pipe wall

Assume that the section of pipe is subjected to an internal pressure (p_i) of 5 MPa, has an internal radius (r_i) of 0.5 m and a wall thickness (t_w) of 21 mm. Also assume that the pit has diameter d_p and depth t_p.

An indication of the stress magnitude at the pit root can easily be approximated as follows:

1. A tensile circumferential stress exists in the pipe wall. The magnitude of the circumferential stress in the remaining material plug, at the pit root, can be approximated by reducing the wall thickness term by the pit depth:

$$\sigma_{hoop} = \frac{p_i r_i}{t_w - t_p} \qquad (2.6.1)$$

2. A shear stress exists in the pit root. This stress is caused by the effect of the internal pressure that tends to force the remaining material plug to "pop" out. The shear stress has a maximum value of

$$\tau_{\max} = \frac{3V}{2A} \qquad (2.6.2)$$

The shear force (V) is equal to

$$V = p_i(\tfrac{\pi}{4}d_p^2) \qquad (2.6.3)$$

and the area of the material in shear (A) and is equal to

$$A = \pi d_p(t_w - t_p) \qquad (2.6.4)$$

Thus, the maximum shear stress in the pit root reduces to

$$\tau_{\max} = \frac{3p_i d_p}{8(t_w - t_p)} \qquad (2.6.5)$$

3. Superimposing these stresses, using Mohr's circle, the maximum shear stress in the pit root can be calculated as:

$$\tau_{\max} = \sqrt{\left(\frac{3p_i d_p}{8(t_w - t_p)}\right)^2 + \left(\frac{p_i r_i}{2(t_w - t_p)}\right)^2} \qquad (2.6.6)$$

4. According to Tresca's failure criteria, failure will occur when the maximum shear stress in the pit root exceeds half of the yield stress of the material. Thus failure results if $\tau_{\max} \geq 0.5 \times S_y$.

Stress concentration effects caused by the pits are neglected in the analysis. The results obtained in the analysis are, however, still very indicative of the behaviour of a pitted surface. This is due to the fact that the pits are small with respect to the rest of the structure and the stress concentration caused by the pits will be negligible.

If the values of internal pressure, internal radius and wall thickness are kept constant, a three-dimensional graph of Equation 2.6.6 can be plotted to show the dependence of the maximum shear stress on pit diameter (d_p) and pit depth (t_p). This has been done and the results can be seen in Figures 2.3, 2.4 and 2.5. It is clear that the root stresses are much more dependent on the depth of the pit than on the diameter of the pit. Another interesting property of Equation 2.6.6 is that it is only when the internal radius

(r_i) tends to zero, that the maximum shear stress becomes strongly dependent on the diameter of the pit. An analysis of the first and second terms in Equation 2.6.6 reveals that the magnitude of the second term (the pit depth term) is larger than the first term (the pit diameter term) for most pipes that normally have a large diameter to thickness ratio. This explains the large dependence of the maximum shear stress on the pit depth.

Two domains of failure can be identified in Equation 2.6.6:

1. when the pipe has a large diameter to thickness ratio, and
2. when the pipe has a very small diameter to thickness ratio.

In the first domain, where the depth of the pit dominates the maximum shear stress at the pit root, the pipe will tear longitudinally. This is due to the large contribution of the circumferential normal stress to the shear stress in the root.

In the second domain, where the diameter of the pit dominates the shear stress at the pit root, failure is accompanied by a "blow-out" of the remaining material in the pit root.

One should realise that other modes of failure exist in addition to the stress relationship established in Equation 2.6.6. Another noteworthy mode of failure is that of bulging which occurs when corrosion causes the pipe wall to thin over a large patch. A significantly large patch of reduced wall thickness can behave like a locally-clamped plate that is subjected to uniform surface pressure and bending stresses that exist in the material due to bending moments induced on the plate. The author acknowledges that this is a possible mode of failure but does not feel that it needs further investigation. The principle reason for this opinion is that, since the pipe is buried, the soil pressure acting on the external pipe surface constrains the corroded patch in the outwardly radial direction, and the proposed plate behaviour might not occur.

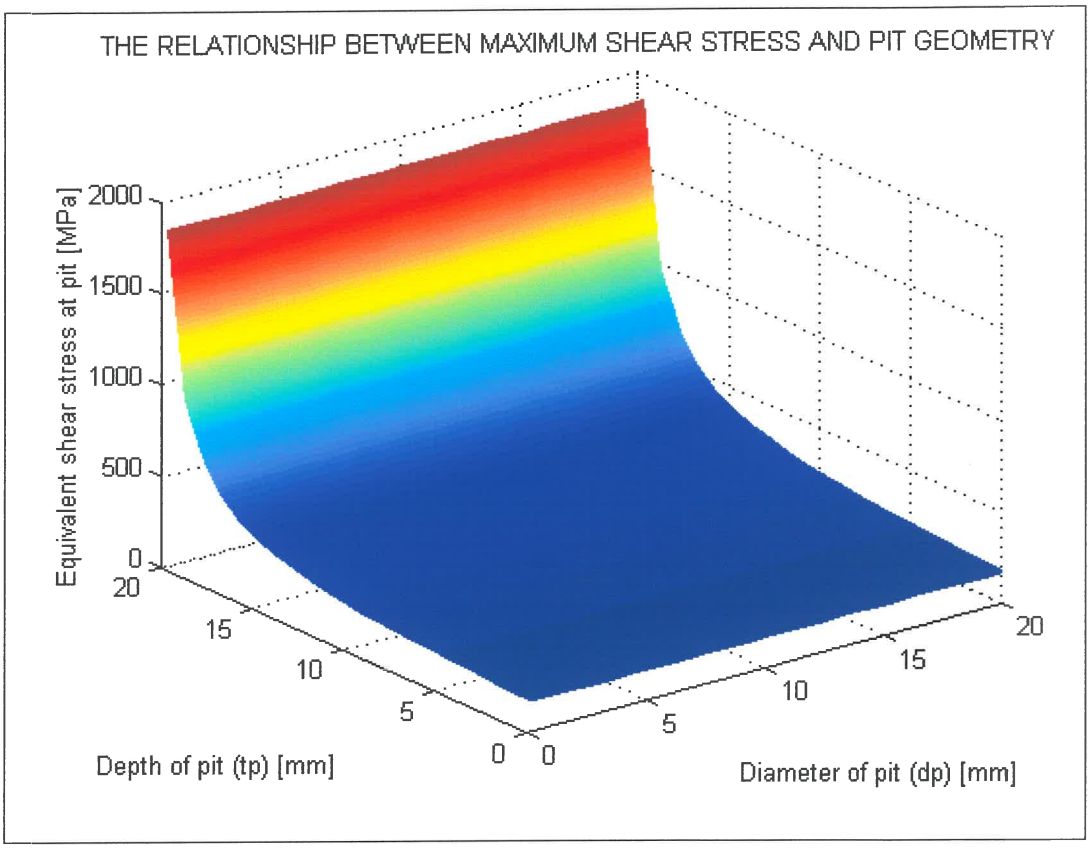

Figure 2.3. The dependence of shear stress on pit diameter and pit depth

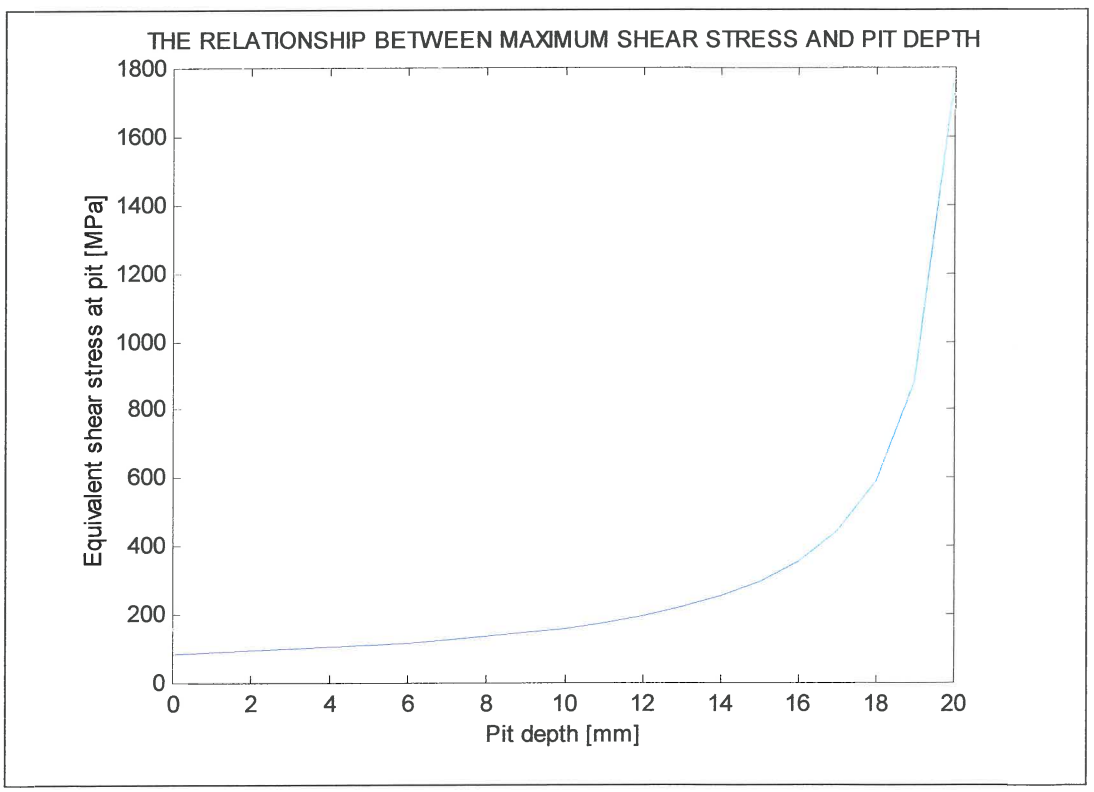

Figure 2.4. The strong dependence of shear stress on pit depth

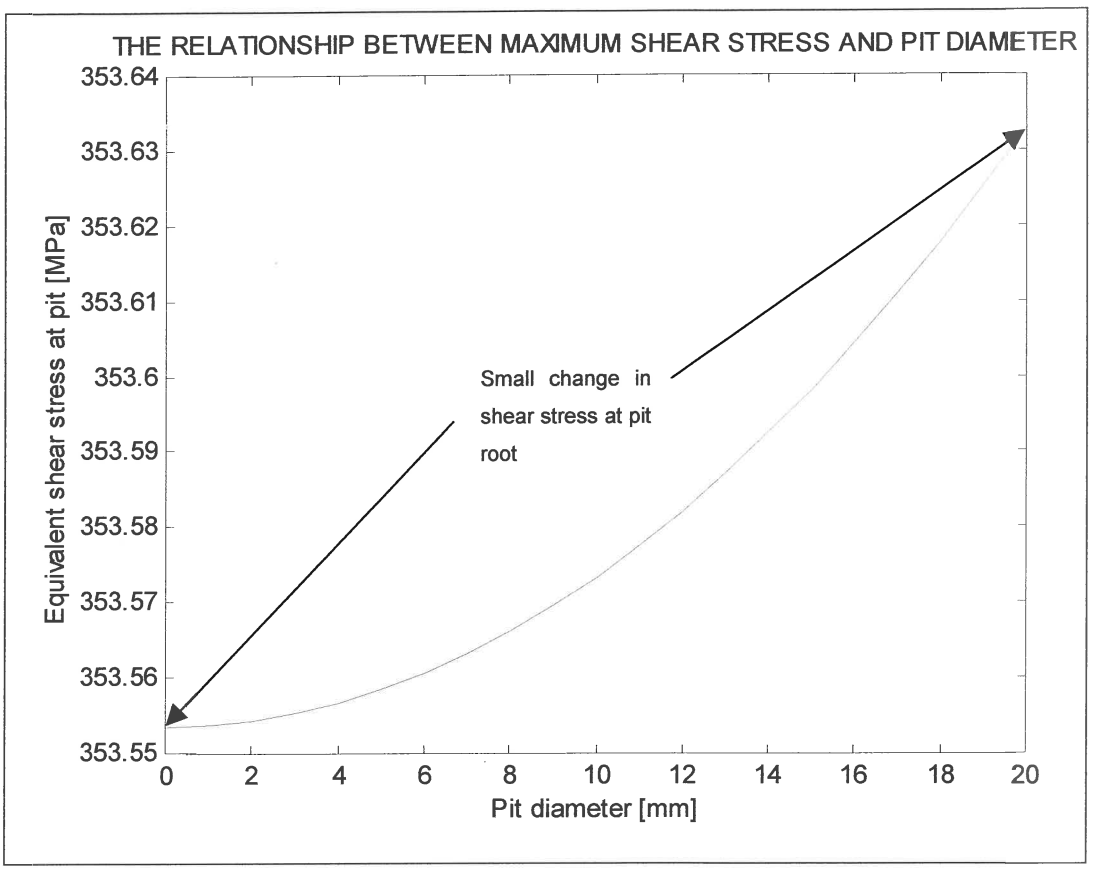

Figure 2.5. The weak dependence of shear stress on pit diameter

To evaluate the extent of pitting damage it is necessary to determine the depth of the deepest pit in the structure since failure will occur at that point. The measurement of pit depths is complicated by the fact that the number of pits in the structure is usually large and it becomes difficult to determine the depth of the deepest pit. This has resulted in the use of a statistical approach in the evaluation of pitting damage. One should also note that pit depth is a function of sample size. Standard rating charts are used to rate pits in terms of size, density and depth. One of these rating charts (as found in the ASTM 1986: G46 – 76: *Standard Practice for Examination and Evaluation of Pitting Corrosion* specification) is shown in Figure 2.6. A pit with density 1×10^4 pits/m^2, size 8 mm^2 and depth 0.4 mm, would thus be rated as A-2, B-3, C-1.

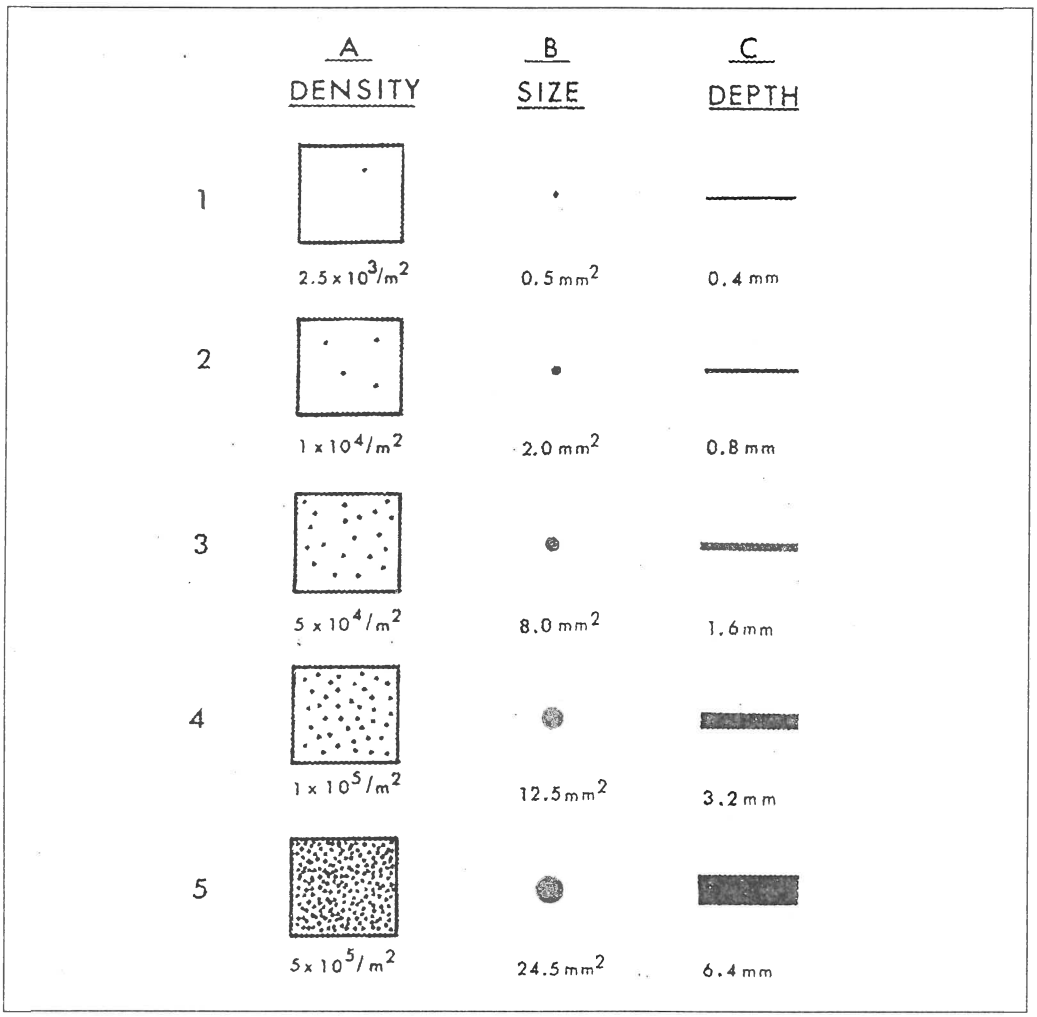

Figure 2.6. Standard rating chart for pits (ASTM 1986: G46 - 76)

Denison (Denison and Uhlig, 1948:1048) suggested that the corrosiveness of a soil towards a given material is most completely defined in terms of three constants and expressed the relationship between pit depth and specimen area using the following equation:

$$P = b_p A^a \qquad (2.6.7)$$

where P = the depth of the deepest pit in the area A, a = an exponent depending on the exposure conditions and b_p = a constant equal to the average depth of the deepest pits in unit area. Denison concluded that a minimum of four samples should be used to determine pitting damage. He also concluded, from the relation between pit depths and time shown in Figure 2.7, that the relationship between pit depth and time can be expressed by the following equation:

$$P = kT^n \qquad (2.6.8)$$

where k and n are constants derived from the physical corrosion data, and where T = time.

Typical values for n are shown for different soils in Figure 2.8 and one can see that n generally increases as the aeration of the soil decreases ($n \propto \frac{1}{aeration}$). The standard error shown in Figure 2.8 is noteworthy since it indicates that different values for n were obtained for the same soil sample. This also serves as motivation for the reliability approach that will be used later to predict the integrity of an underground pipeline.

The relationship between the maximum pit depth and exposure time is very important and forms the basis of classical corrosion theory. The constants k and n are determined from physical corrosion data (as shown in Figure 2.7) and will depend on the various parameters having an effect on the corrosiveness of the soil.

Ahammed and Melchers have used the above-mentioned relationship ($P = kT^n$) to describe uniform attack and have suggested typical values for $k \approx 0.066$ and $n \approx 0.53$ (Ahammed and Melchers, 1997:990). In this study the relationship $P = kT^n$ is also utilised to describe uniform attack.

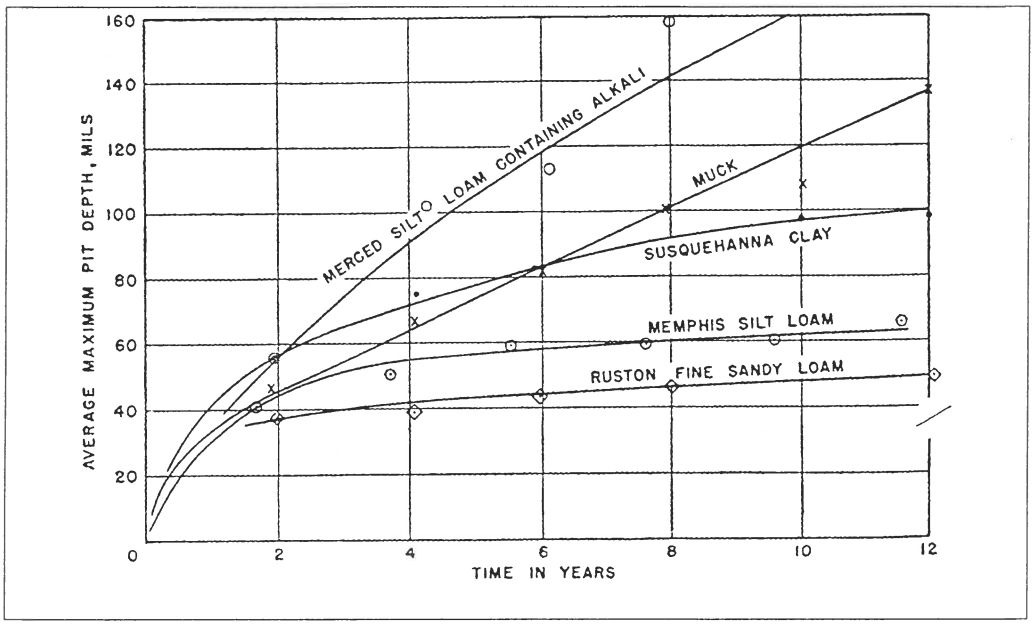

Figure 2.7. The relationship between pit depth and exposure time (Denison and Uhlig, 1948:1048)

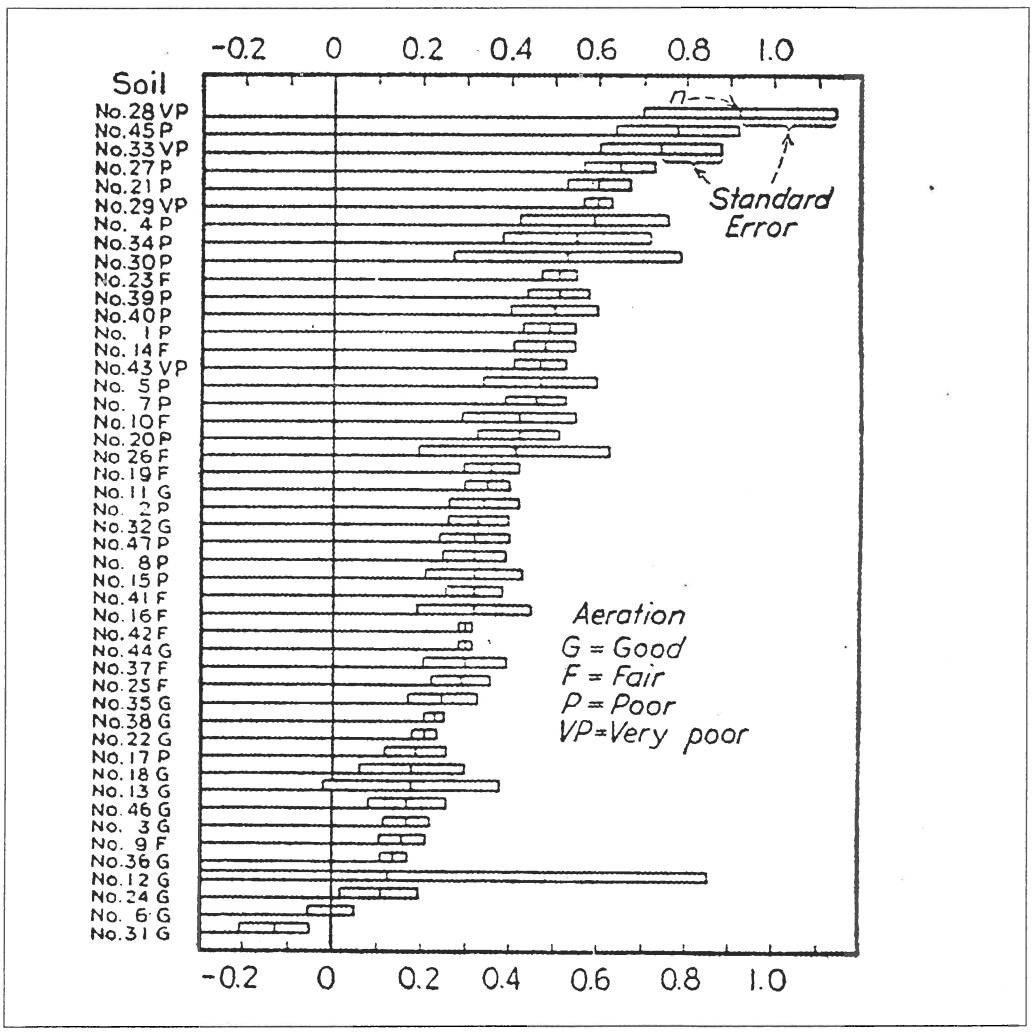

Figure 2.8. Typical values of n (Denison and Uhlig, 1948:1048)

The author has conducted a brief study on a galvanised water pipe that has been buried for 37 years at a depth of 240 mm below ground level. The details of the pipe are as follow:

1. the working pressure of the pipe is 80 kPa (i.e. a water head of 8 m);
2. the original outer diameter of the pipe was 27.3 mm;
3. the internal diameter is 21.6 mm;
4. the original wall thickness of the pipe was 2.85 mm, and
5. it was also noticed that a similar pipe, buried in similar conditions for 17 years, shows no excessive corrosion damage.

Five sections of the pipe (each approximately 200 mm in length) were inspected for corrosion damage. The products of corrosion were removed from the sections. One of the sections was turned down on a lathe until the root of the deepest pit was reached (shown in Figures 2.9 to 2.11). The deepest pits on the other four sections were carefully opened with a small grinding bit, sawed and measured. A total of eight pits were surveyed on the sections and the results are shown in Table 2.1. The remaining wall thickness of the pipe at the pit root and the pit depths are shown in Table 2.1.

Table 2.1. Measured pit depths of a pipe buried for 37 years

CORROSION DATA							No Retardation		10 Year Retardation	
	Remaining tw			Pit Depth			k	n	k	n
Pit 1	tw =	1.05	mm	1.8	mm		0.1837	0.632	2.12E-01	0.649092
Pit 2	tw =	0.6	mm	2.25	mm		0.2082	0.659	2.39E-01	0.6802
Pit 3	tw =	1.1	mm	1.75	mm		0.1808	0.627	0.20946918	0.644084
	tw =	1.4	mm	1.45	mm		0.1627	0.606	0.18812503	0.619634
	tw =	1.1	mm	1.75	mm		0.1808	0.627	0.20946918	0.644084
Pit 4	tw =	1.6	mm	1.25	mm		0.1497	0.588	0.17323861	0.599614
	tw =	1.9	mm	0.95	mm		0.1284	0.554	0.14874003	0.562608
	tw =	1.6	mm	1.25	mm		0.1497	0.588	0.17323861	0.599614
Pit 5	tw =	1.4	mm	1.45	mm		0.1627	0.606	0.18812503	0.619634
	tw =	1.4	mm	1.45	mm		0.1627	0.606	0.18812503	0.619634
	tw =	1.4	mm	1.45	mm		0.1627	0.606	0.18812503	0.619634
Pit 6	tw =	1.9	mm	0.95	mm		0.1284	0.554	0.14874003	0.562608
	tw =	2.2	mm	0.65	mm		0.1038	0.508	0.11967586	0.513431
	tw =	1.8	mm	1.05	mm		0.1358	0.566	0.15745729	0.575693
Pit 7	tw =	1.02	mm	1.83	mm		0.1854	0.634	0.21384103	0.651379
	tw =	1.4	mm	1.45	mm		0.1627	0.606	0.18812503	0.619634
	tw =	1	mm	1.85	mm		0.1865	0.635	0.21525612	0.652676
	tw =	1	mm	1.85	mm		0.1865	0.635	0.21525612	0.652676
Pit 8	tw =	1.7	mm	1.15	mm		0.1429	0.578	0.16529879	0.588549
	tw =	1.7	mm	1.15	mm		0.1429	0.578	0.16529879	0.588549
	tw =	1.3	mm	1.55	mm		0.1689	0.614	0.1952128	0.628647
	tw =	1.5	mm	1.35	mm		0.1563	0.597	0.18097396	0.609711
mean	tw =	1.41227	mm	1.4377273	mm		0.16055	0.600182	0.18558239	0.613699
standard dev		0.37693	mm	0.3769291			0.02436	0.034546	0.02792987	0.038282
COV		0.2669		0.2621701			0.15172	0.057558	0.1504985	0.062379

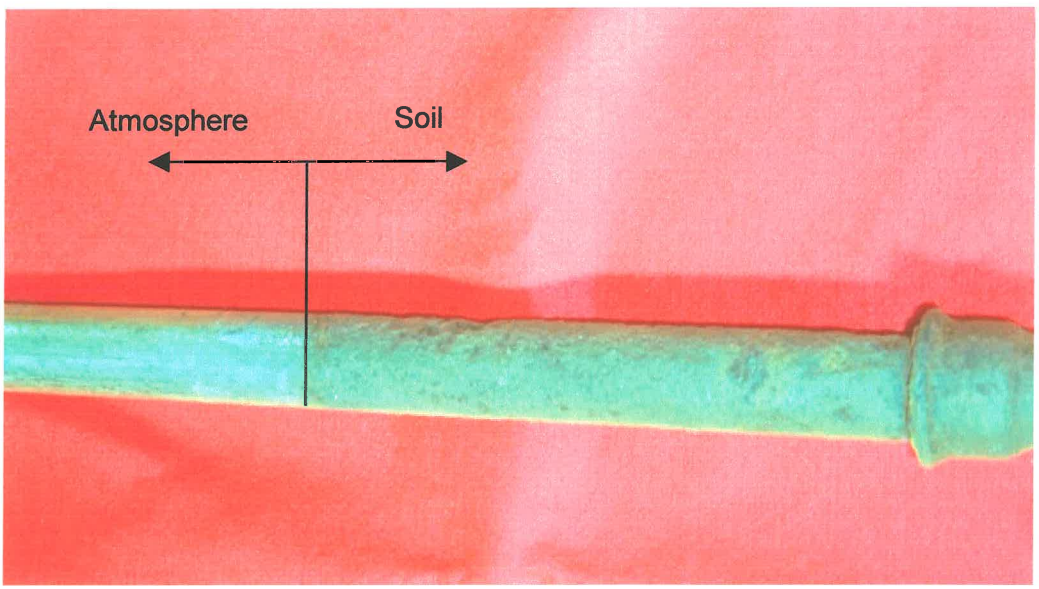

Figure 2.9. Original pipe – the boundary between soil and atmospheric attack is clear

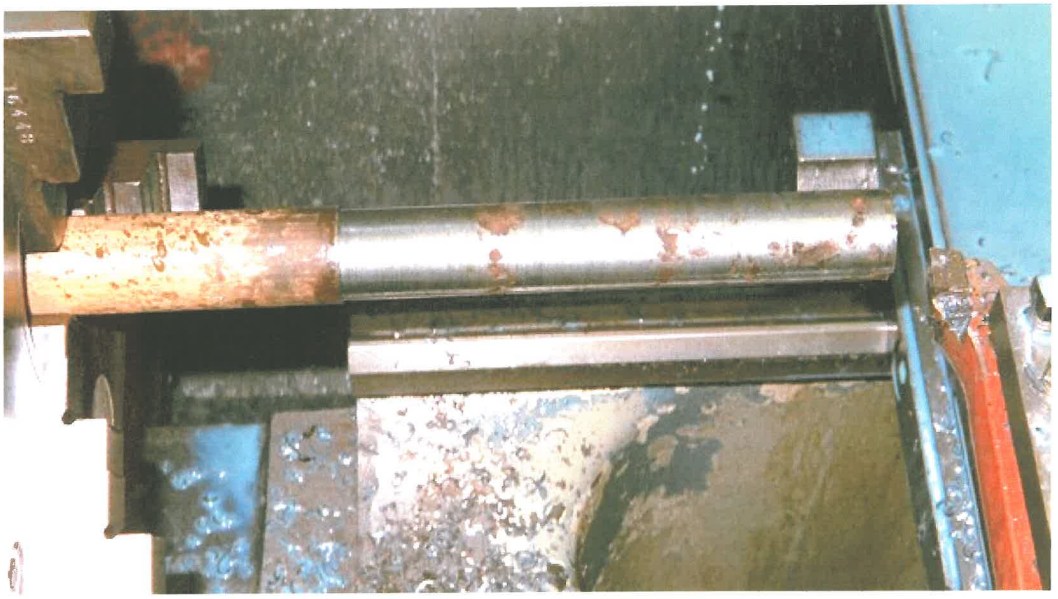

Figure 2.10. Corrosion products removed – deepest pits are visible.

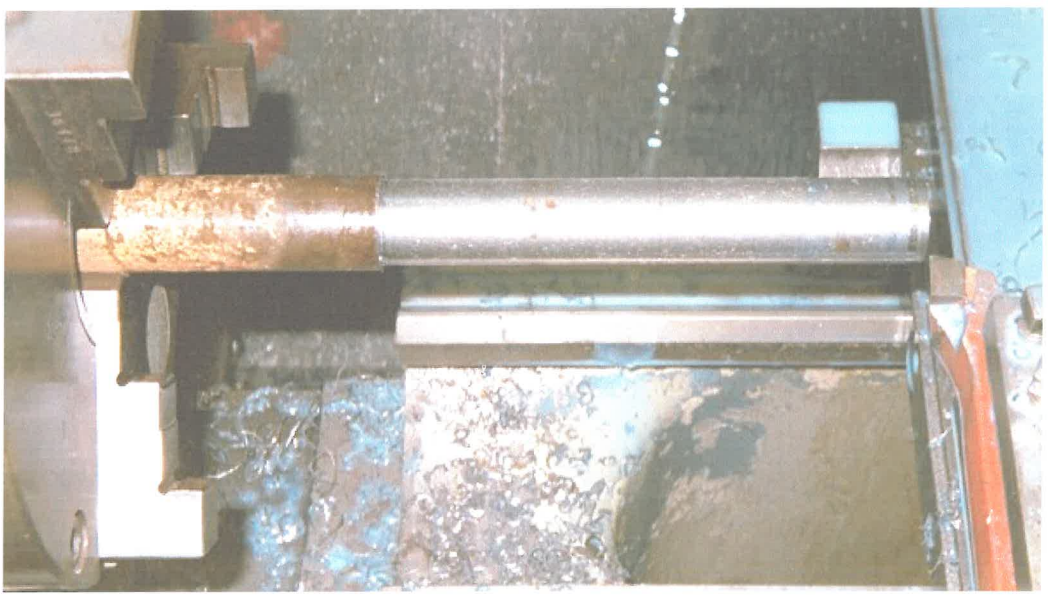

Figure 2.11. Material removed until pit roots are visible.

At least two boundary conditions are necessary in order to determine the constants k and n, in the equation $P = kT^n$. The first boundary condition is determined on the basis of fact that no pits existed on the pipe at time T = 0 (P = 0 mm). The second condition is the depth of the deepest pit at time T = 37 years (P = 2.25 mm). However, while performing the analysis, one quickly recognises that the first condition cannot, mathematically speaking, be

satisfied. The reason for this is that, at some stage or the other, in the analysis one would have to evaluate the logarithm of the deepest pit. Since the deepest pit has zero depth at the beginning, one would end up with $\ln(0)$, which of course tends to negative infinity. One way in which to remedy this trivial problem would be to specify an initial pit depth that is very close to zero and in this analysis an initial pit depth of 0.01 mm was specified for the pipe at the beginning of service. Thus one needs to solve, for each pit depth measured, two unknowns (k and n) in the equation $P = kT^n$. Two equations with two unknowns are constructed:

1. P_0 at time $T = T_0$, thus $P_0 = kT_0^n$, and
2. P_1 at time $T = T_1$, thus $P_1 = kT_1^n$.

The values for k and n determined from the corrosion data are shown in Table 2.1 and compare relatively well with those in presented in Figure 2.8. Since it was observed that a similar pipe buried in similar soil did not show excessive corrosion damage after 17 years of service, one could safely assume that no corrosion took place in the first 10 years of service (taking 10 years as a thumb-suck value). Thus, corrosion was retarded for 10 years and this should be reflected in the k and n values. The k and n values determined for the case in which corrosion was delayed are also shown in Table 2.1. These values are believed to be more correct and more indicative of the real corrosion process in this specific example. The pit depth equation for the retarded corrosion rate becomes

$$P = k(T - T_{delay})^n, T \geq T_{delay} \qquad (2.6.9)$$
$$P = 0, T \leq T_{delay}$$

where T_{delay} is the time during which no corrosion takes place. In this case $T_{delay} = 10$ years. Graphs of the various responses of the wall-thickness vs time are shown in Figure 2.12. It is clear that the k and n values that were suggested by Ahammed and Melchers (1997:990) lead to a very low corrosion rate indeed. Furthermore, since failure first occurs at the deepest pit, the necessity for using the maximum pit depth in the analysis is clear.

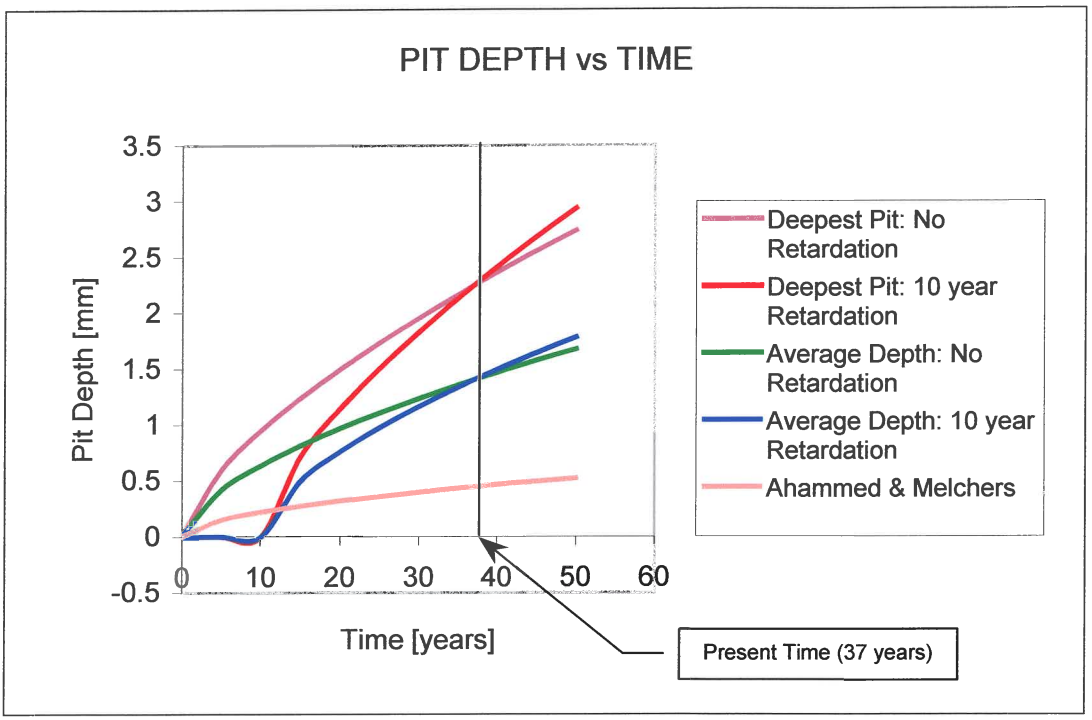

Figure 2.12. Graph showing the influence of retardation on pit depth

The following conclusions can be drawn by considering the deepest pit and average pit response shown in Figure 2.12:

- The responses of the 10 year retardation pits and the original pits (no retardation) intersect at time $T_0 = 0$ and at time $T_1 = 37$ years. Both constraints in the equation $P = kT^n$ are satisfied.
- The penetration rate is higher in the region $T \leq T_1 = 37$ for a pit that experiences no retardation than for a pit that experiences retardation.
- The penetration rate is higher in the region $T \geq T_1 = 37$ for a pit that experiences retardation than for a pit that experiences no retardation.

This is a noteworthy result since the penetration rate, although satisfying both the constraints of the equation $P = kT^n$, varies substantially for the delayed corrosion and the immediate corrosion responses.

2.7. Intergranular corrosion

Metals are crystalline in nature. The non-directional bonding of the metal atoms results in the ductile properties of metals. When a metal is cast, the atoms arrange themselves in a crystalline matrix. This ordering, however, occurs at various positions in the liquid. As these crystals meet, there is a mismatch in their boundaries (commonly known as grain boundaries). Since the most stable configuration of the metal is its particular crystal structure, the grain boundaries are regions of high energy and thus are generally more chemically active. Under certain conditions the grains are very reactive and intergranular corrosion results. The grain boundaries are attacked while there is relatively little corrosion of the grains. This causes the metal to fall apart or to lose its strength. It can be caused by impurities in the grain boundaries or by the enrichment or depletion of alloy elements in the grain boundary.

2.8. Selective leaching

Selective leaching is the removal of one element from an alloy by corrosion. A typical example of this is grey cast iron, which sometimes shows the effects of selective leaching in relatively mild environments. The surface of the cast iron has the appearance of graphite. The graphite in the iron or steel matrix is cathodic to iron and a galvanic cell is formed. The iron dissolves, leaving a porous mass of graphite and rust. No dimensional changes occur but the metal loses its strength.

2.9. Erosion corrosion

Erosion corrosion is the acceleration of the rate of corrosion of a metal due to relative movement between the metal and the corrosive medium. Metal is removed from the original surface as dissolved ions or it forms solid corrosion products that are mechanically removed from the metal surface. Typical examples of erosion corrosion are corrosive attacks on pump impellers, elbows in pipe networks and attacks on valves.

A few methods can be employed in order to minimise the extent of erosion corrosion damage (Fontana and Greene, 1967:82):

1. Use materials with a higher resistance to erosion corrosion.
2. Employ better designs. Designs that take erosion corrosion into account decrease the relative velocity between the corrosive and the metal, use turning vanes, decrease turbulence and, of course, select materials with higher resistance to damage.
3. Alter the environment. The addition of inhibitors into the process stream is not always possible and/or cost effective, but it can be exploited in certain instances.
4. Applying coatings between the metal and corrosive can produce a barrier that can be used to protect the metal.

2.10. Stress corrosion

Stress corrosion can be defined as the cracking of a structural part caused by the simultaneous effects of tensile stress and of a specific corrosive medium. During stress corrosion, the structural part is left principally unscathed over most of its surface, while fine cracks initiate and propagate through the part. This property of stress corrosion makes it very difficult to quantify structural damage by evaluating the remaining stress-bearing material only (i.e. thickness or structural dimensions). Other inspection techniques that are tailored to detect the crack depth have to be employed. The important variables that affect stress corrosion are temperature, solution composition, metal composition, stress, and metal structure. In stress corrosion analyses, the mechanical driving force is normally characterised in terms of the usual Fracture Mechanics parameters such as the crack-tip stress-intensity factor, K or ΔK. All the basic principles of classical Fracture Mechanics are valid in stress corrosion, except that the crack growth rate (da/dN) is usually accelerated in the corrosive medium. However, corrosion caused by exposure to soil is expected to be a slow process and the stress corrosion effect shall be neglected in this study. The number of variables that have an effect on the da/dN curve necessitates that physical tests be performed on the specific material under the specific service conditions in order to determine the crack response of the material. The usual approach, when designing a structure that will be exposed to a corrosive medium, is to adjust either the yield

strength or the fatigue limit of the material to take account of the effect that the corrosive medium will have on the structure.

2.11. Free energy

The change in free energy (ΔG) is a direct measure of the work capacity or maximum amount of electric energy available from a system. If the change in free energy accompanying the transition of a system from one state to the other is negative, it indicates a loss of free energy and thus the spontaneous reaction direction of the system. This is due to the fact that, in the absence of external forces acting on the system, the system will tend to transform to its lowest energy state (Chapter 1). It is important to bear in mind that the change in free energy is independent of the reaction path. It is, therefore, impossible to accurately predict the reaction rate from the change in free energy. The change in free energy only reflects the reaction path that will be taken by the system in the absence of any external forces. The change in free energy in an electrochemical reaction, where there is a transition from one state to another, can be calculated using the following equation:

$$\Delta G = -n_e F_c E_p \qquad (2.11.1)$$

where ΔG is the change in free energy, n_e is the number of electrons involved in the reaction, F_c is Faraday's constant (96.5 x 10^3 [A·s / mol]) and E_p is the cell potential.

For a specific transition from one system state to another, a positive change in free energy ($\Delta G > 0$) indicates that energy needs to be added to the system in order for the transition to take place. A negative change in free energy ($\Delta G < 0$) indicates that energy is released by the system during its transition from one state to the other. This means that a negative change in free energy indicates the spontaneous reaction direction of a system.

2.12. Electrode kinetics

Faraday's equation of general chemistry states that the amount of metal corroded uniformly from an anode in an aqueous solution during time T can be calculated by using the following equation (Smith, 1993:725):

$$w = \frac{iTM}{n_e F_c} \qquad (2.12.1)$$

where w is the weight (in grams) of metal that is corroded during time T (in [s]), i is the electrical current (in [A]) that flows between the corroding anode and reducing cathode, M ([g/mol]) is the atomic mass of the corroding metal, n_e is the number of electrons that takes part in the reaction, and F_c is Faraday's constant (96.5 x 10^3 [A·s / mol]).

Sometimes corrosion is expressed in terms of a current density (i_d [A/m^2]) which is equal to the current divided by the corroding area of the electrode. Substituting the current density, i_d, into Faraday's equation, the weight-loss expression becomes:

$$w = \frac{i_d ATM}{n_e F_c} \qquad (2.12.2)$$

where A is the corroding area of the electrode. In the case where the corroding electrode is a circular underground pipe corroding from the outside, the weight-loss expression can be manipulated to yield the penetration rate (P) as a function of time. Consider the circular pipe (shown in Figure 2.13) with length L, outer diameter d_{out}, inner diameter d_{inner}, original wall thickness t_{orig} and present wall thickness t_w.

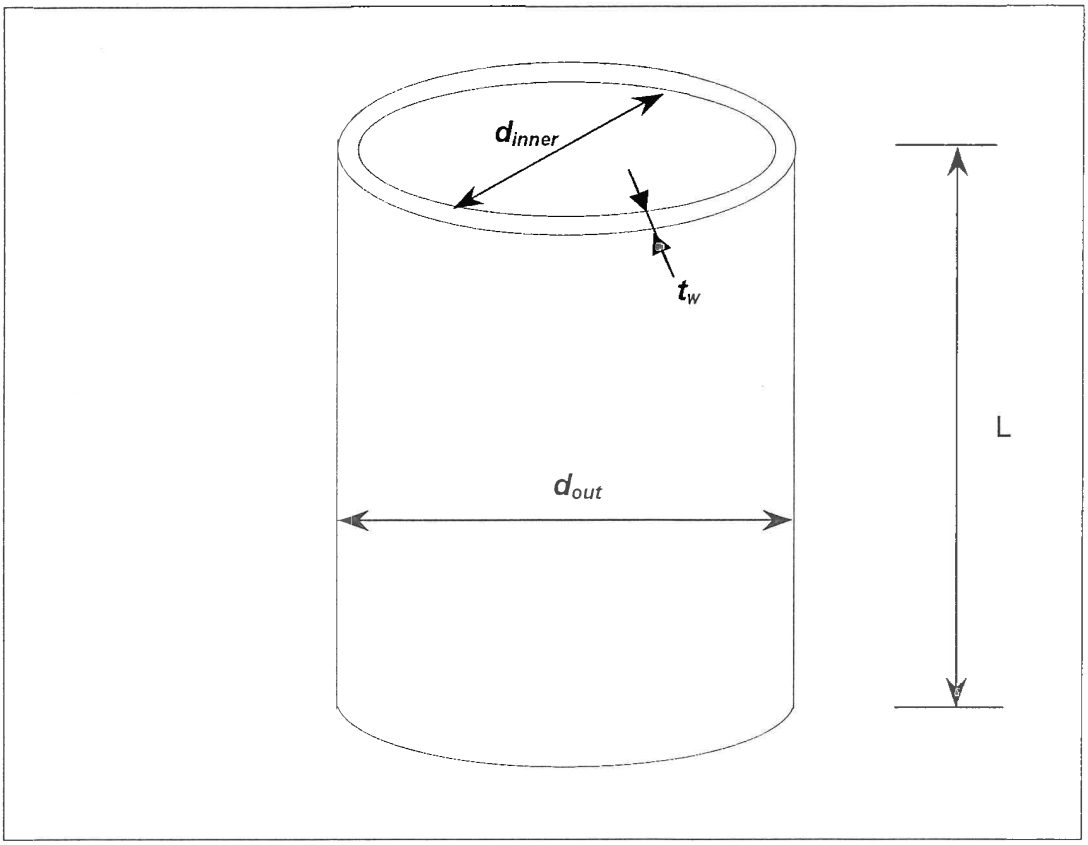

Figure 2.13. Circular pipe that is subjected to external corrosion

The corroding area of the pipe can be expressed as follows:

$$A = \pi d_{out} L \text{ and } d_{out} = d_{inner} + 2t_w \qquad (2.12.3)$$

$$\therefore A = \pi(d_{inner} + 2t_w)L \qquad (2.12.4)$$

The weight of the corroded metal is:

$$w = \rho \cdot Vol \qquad (2.12.5)$$

where ρ is the mass density of the material and Vol is the volume of the corroded material. Thus:

$$w = \rho\pi L(d_{inner} + 2t_{orig}) - \rho\pi L(d_{inner} + 2t_w) \qquad (2.12.6)$$

$$\therefore w = \rho\pi L(2t_{orig} - 2t_w)$$

$$\therefore \rho\pi L(2t_{orig} - 2t_w) = \frac{\pi i_d L(d_{inner} + 2t_w)TM}{n_e F_c} \qquad (2.12.7)$$

Rearranging and simplifying the expression yields:

$$t_w(T) = \frac{\rho \cdot t_{orig}}{\rho - \frac{i_d TM}{n_e F_c}} - \frac{i_d TM d_{inner}}{\rho n_e F_c - i_d TM} \qquad (2.12.8)$$

By substituting the penetration rate, which is defined as $P(T) = t_{orig} - t_w$, into the equation above yields the following expression for penetration rate as a function of time (T) and current density (i_d):

$$P(T) = t_{orig} - \frac{\rho \cdot t_{orig}}{\rho - \frac{i_d TM}{n_e F_c}} + \frac{i_d TM d_{inner}}{\rho n_e F_c - i_d TM} \qquad (2.12.9)$$

It is important to realise that, since the penetration rate may vary with time, the current density might not be constant over time and should, therefore, be monitored as a function of time. If one could determine the corrosion current density, it would be possible to determine the penetration rate. How one determines the corrosion current density will be discussed in the following sections.

2.13. Corrosion rate measurements – Tafel extrapolation

Up to now, the main focus has been on describing the corrosion phenomenon. The types of corrosion as well as the electrochemical nature of corrosion have been discussed. In the following chapter, methods will be discussed that can be used to determine the corrosion rate by physically measuring the remaining amount of material at the corroding electrode after a time period T. However, it will be clear that these methods are not ideal for measuring the severity of corrosion in systems subjected to relatively low rates of corrosion (as in underground pipe networks). On the other hand, these methods are well suited to give an objective indication of the integrity of the corroding electrode (i.e. the underground pipe).

Fortunately, it is possible to determine the corrosion rate of an electrode through electrochemical measurements. Two types of electrochemical corrosion-rate measurement techniques are available namely, 1) Tafel extrapolation and 2) linear polarisation (Fontana and Greene, 1967:342). In this section Tafel extrapolation is described and discussed.

The Tafel Extrapolation technique uses data obtained from either cathodic or anodic polarisation measurements.

Consider the schematic circuit diagram for conducting cathodic polarisation (shown in Figure 2.14). The metal, of which the corrosion rate needs to be determined, is named the *working electrode*. A cathodic current is supplied to the corrosion system by means of an *auxiliary electrode*. The auxiliary electrode is not allowed to participate in the corrosion reaction and should therefore be manufactured from an inert material (such as platinum). The current flowing between the working electrode and the auxiliary electrode is measured with an ammeter. The potential of the working electrode is measured with respect to a reference electrode by means of a voltmeter. The current, flowing between the auxiliary and working electrode, is increased in discrete steps by decreasing the resistance of the rheostat. The electrode potential (E_p) and current (i) are measured simultaneously for each step and are recorded.

For the generic case where metal M is immersed in an acid solution, a typical plot of the electrode potential (E_p) versus the log of the applied current ($\log(i)$) will be as shown in Figure 2.15.

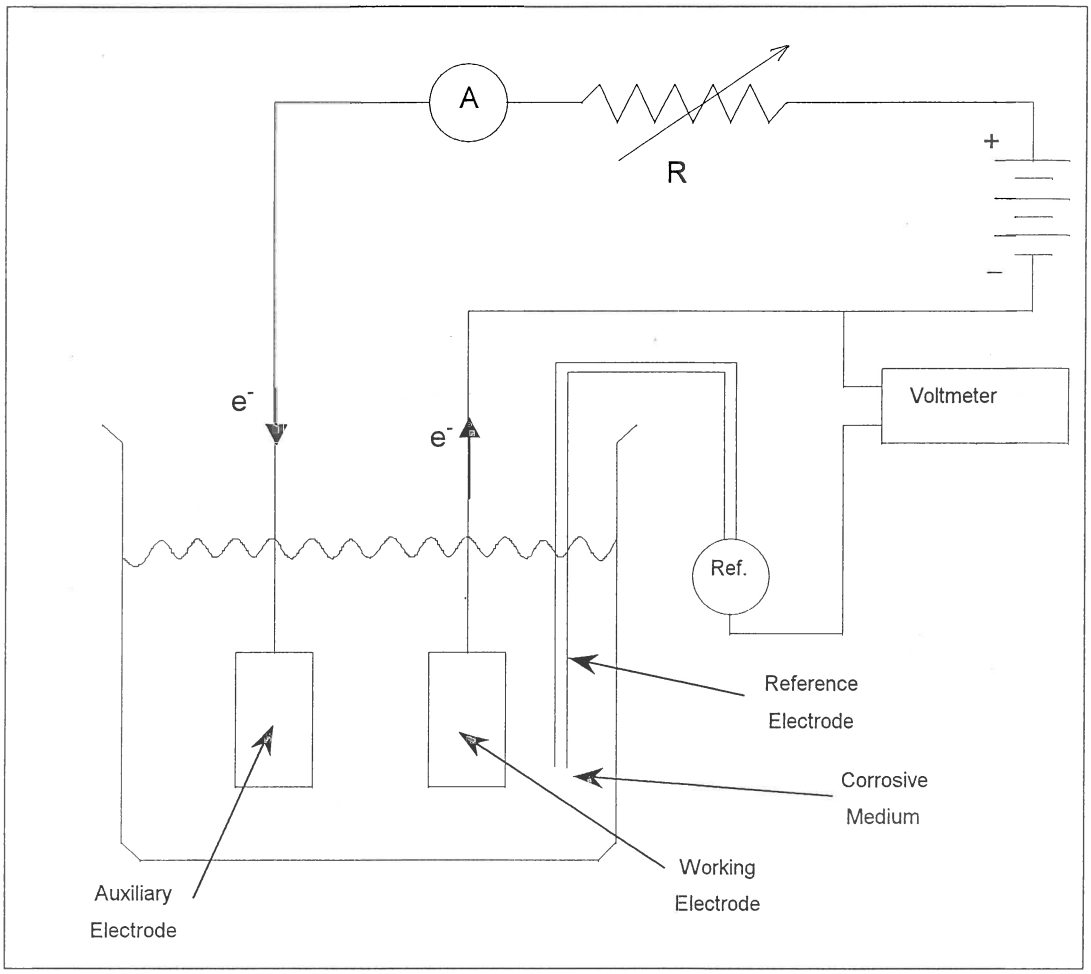

Figure 2.14. Schematic circuit diagram for conducting cathodic polarisation measurements (Fontana and Greene, 1967:342)

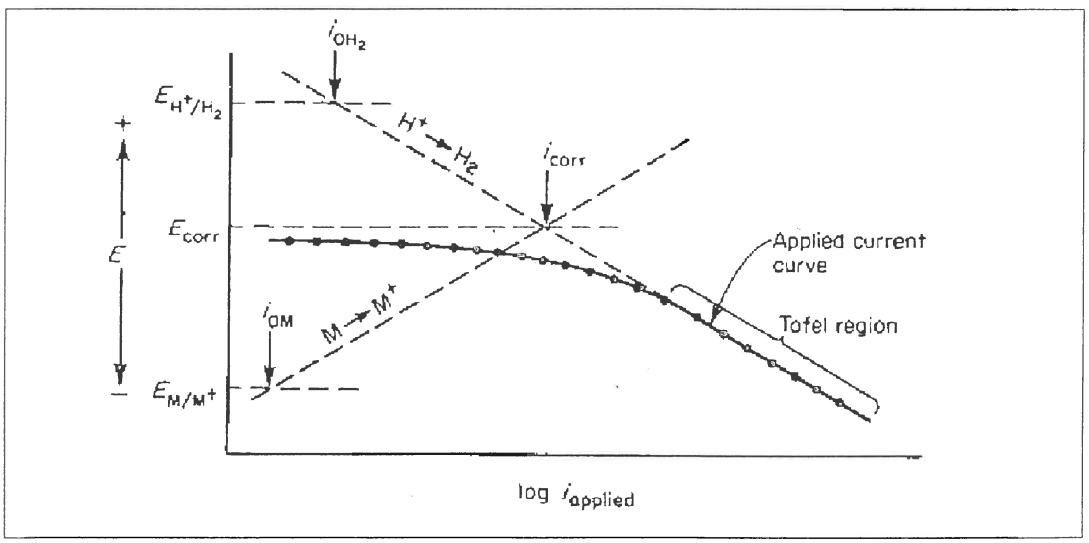

Figure 2.15. Polarisation curve of a corroding metal (Fontana and Greene, 1967:343)

Prior to current application, the voltmeter indicates the corrosion potential (E_{CORR}) of the specimen with respect to the reference electrode. The curve is non-linear at low currents, but becomes near linear at higher currents. The applied current is equal to the difference between the reduction current and the oxidation current. As the current is increased, the applied current approaches the cathodic current and this region is known as the Tafel region. The Tafel region is extrapolated to the corrosion potential in order to determine the corrosion rate from the polarisation measurements. At the corrosion potential the rate of hydrogen evolution is equal to the rate of metal dissolution and, therefore, this point corresponds to the corrosion rate of the system in terms of current density (i_{CORR}).

To determine the penetration rate as a function of time, at time T, the current density ($i_{CORR} = i_d$) is substituted into equation 2.12.9.

2.14. Conclusion

In this chapter the corrosion phenomenon was discussed. Two techniques to establish the corrosion rate were proposed:

1. the conventional weight-loss method, and
2. an electrochemical technique in the form of Tafel extrapolation.

In order to determine the remaining life of an underground pipeline it is of the utmost importance to determine the corrosion rate of the system.

In Section 2.6, it was indicated that the area of the corrosive attack (in the form of pit diameter) does not contribute greatly to the stresses in the pipe wall. However, it was indicated that the depth of the corrosive attack is the major driving force behind the stresses in the pipe wall. The penetration rate expression ($P = kT^n$) shall be used to quantify geometrical thinning due to external corrosion in the following chapters and it should be seen as an engineering relationship used to model, amongst others, pitting corrosion and uniform attack.

3. AVAILABLE TECHNOLOGIES

Here's a fact for you. In 1995, according to the Washington Post, *computer hackers successfully breached the Pentagon's security systems 161,000 times. That works out at eighteen illicit entries every hour around the clock, one every 3.2 minutes. Oh, I know what you are going to say. This sort of thing could happen to any monolithic defence establishment with the fate of the earth in its hands. After all, if you stockpile a massive nuclear arsenal, it's only natural that people are going to want to go in and have a look around, maybe see what all those buttons marked 'Detonate' and 'Code Red' mean. It's only human nature. Besides, the Pentagon has got quite enough on its plate, thank you, with trying to find its missing logs from the Gulf War. I don't know if you've read about this, but the Pentagon has mislaid – irretrievably lost, actually – all but thirty-six of the 200 pages of official records of its brief but exciting desert adventure. Half of the missing files, it appears, were wiped out when an officer at Gulf War headquarters – I wish I was making this up, but I'm not – incorrectly downloaded some games into a military computer. The other files are, well, missing. All that is known is that two sets were dispatched to Central Command in Florida, but now nobody can find them (probably those cleaning ladies again), and a third set was somehow 'lost from a safe' at a base in Maryland, which sounds eminently plausible in the circumstances. Now to be fair to the Pentagon, its mind has no doubt been distracted by the unsettling news that it has not been getting very good reports from the CIA. It has recently emerged, according to other news reports, that despite spending a decidedly whopping $2 billion a year monitoring developments in the Soviet Union, the CIA failed to foresee the break-up of the USSR – indeed, I understand, is still trying to confirm the rumour through its contacts at the McDonald's in Moscow – and understandably this has unnerved the Pentagon. I mean to say, you can't expect people to keep track of their wars if they're not getting reliable reports from the field, now can you?*

- Bill Bryson

3.1. Introduction

In the previous chapter, the basic principles of corrosion were described. Three important aspects were touched upon:

1. Corrosion only occurs when the free energy of the corroding system is reduced. From this principle, it is possible to determine the corrosion rate of either the anodic or cathodic electrode through the use of polarisation measurements and Tafel extrapolation.
2. If the corrosion rate of either the anodic or cathodic electrode is reduced, the corrosion rate of the system will be reduced.
3. When time-based corrosion data exists for a corroding system it is possible to fit a curve through the data that expresses the depth of penetration (P) as a function of time (T). A well-known and widely used relationship between depth and time has been shown to be $P = kT^n$. The constants k and n are determined from the time-based corrosion data through a least squares fit.

Different failure criteria exist for assessing the structural integrity of a structure if the stresses present in the load-bearing members are known. The most important indicators of these stresses are the amount, geometrical distribution and mechanical properties of the material from which the load-bearing members are manufactured. Corrosion alters all of the above parameters, and thus alters the stresses in the load-bearing members. Usually an increase in stress can be expected when a structure is exposed to corrosive attack.

The first two indicators, namely the amount and geometrical distribution of the load-bearing material, are the primary concern of this chapter. Methods for determining the properties of the load-bearing material that remains will be described. Methods that can be used to identify possible problematic areas in the pipe network will also be described.

A variety of non-destructive inspection techniques is available for determining the condition of a pipe network. Several anomalies can be inspected for, but

the most important of these for the prediction of the remaining life of the network is the identification of the thickness of the pipe wall (t_w). Certain of the non-destructive inspection techniques are discussed below.

3.2. Visual inspection

Visual inspection is by far the most basic and most subjective inspection technique currently in use and it is prone to inaccuracies and results may vary from technician to technician. Visual inspection is only feasible where accessibility is not a problem, and it gives no quantitative indication of the pipe condition. Visual inspection is, however, useful when identifying problem areas in the pipe network and its value should not be underestimated.

3.3. Pipeline current mapping (PCM)

Corrosion may occur where a steel pipe comes into contact with the earth or with foreign metallic structures. Gas pipes are typically buried approximately 1 m underground and are covered with a coating to prevent them from coming into direct contact with the soil or foreign metallic structures. Though the coating is tough, sharp rocks, foreign objects or earth movement can damage it. Normally the type of corrosion that results from damaged wrapping is highly localised and is severe.

The PCM technique relies on a low current, low frequency electric signal that is applied to the steel pipe. Where the pipe is in contact with a foreign metallic object or where the coating has been damaged, an electric current flows between the pipe and the earth. A hand-held receiver detects this current flow and identifies possible problem spots.

3.4. Magnetic flux leakage (MFL)

This method is very similar to the PCM method. An intelligent "pig" (shown in Figure 3.1) is inserted into the pipeline and is connected via an umbilical cord to stationary control and data acquisition systems. Coils on the "pig" induce a magnetic field in the pipe wall. Any anomalies in the wall will disturb the

magnetic flux and a rotating head on the "pig" senses this disturbance. Data recorded with this method is then interpreted and various anomalies can be identified. This method gives 100 % coverage of the interior of the pipe as well as of its wall thickness. Pipelines with a length of up to 140 km can be effectively surveyed using this method.

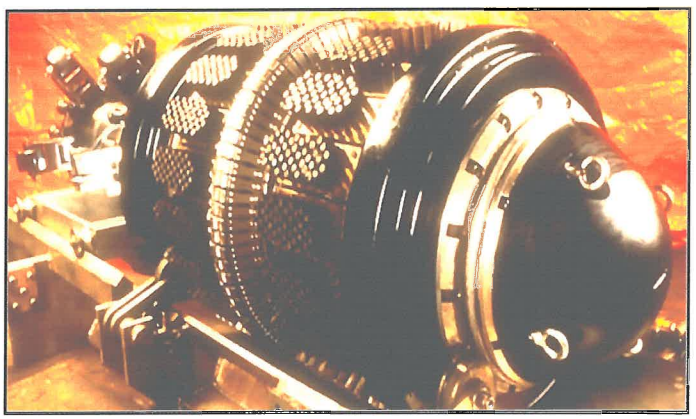

Figure 3.1. Intelligent "pig" with coils used for MFL

3.5. Manual ultrasonic spot-probing

The concept of measuring pipe interiors using sonar is simple. The travel time of a sonic pulse to a target and back can be converted into the distance to the target if the velocity of sound in the transmission medium is known. Sonic pulses are reflected from any acoustic impedance boundary. The greater the difference in the impedance of two materials, the more sonic energy will be reflected. The impedance mismatch between fluid and the rigid wall of the pipe is an excellent sonic reflector. It is thus possible to determine the wall thickness of the pipe with this method. In spot-probing, a hand-held ultrasonic device is used to determine the pipe's wall thickness at a specific place. The results obtained with this method are accurate but are highly localised and position dependent.

Process facilities contain miles of piping (the Pacific Gas and Electric Company (PG&E) operates approximately 42,000 miles of pipeline) and this method, used by itself, is not a feasible solution for determining pipe-wall thickness of large pipe networks.

3.6. Continuous ultrasonic pigging

Physically, continuous ultrasonic pigging works the same as manual ultrasonic spot-probing. The main difference is that, in a similar fashion to MFL, an intelligent "pig" (shown in Figure 3.2) is inserted into the pipeline. The "pig" is connected via an optical fibre to stationary control and data acquisition systems. A sonic pulse is transmitted from the transducer in the "pig" and is directed to the pipe wall by a rotating mirror. From the inner wall the pulse is reflected back to the rotating mirror where the same transducer detects it. With the use of this method it is possible to determine the pipe-wall thickness and inner and outer radii, and to detect internal and external material loss. This method covers the entire interior of the pipe and typical test results are shown in Figure 3.3. Pipelines with a length of up to 12 km can be effectively surveyed with this method.

Figure 3.2. Intelligent "pig" used in ultrasonic thickness tests

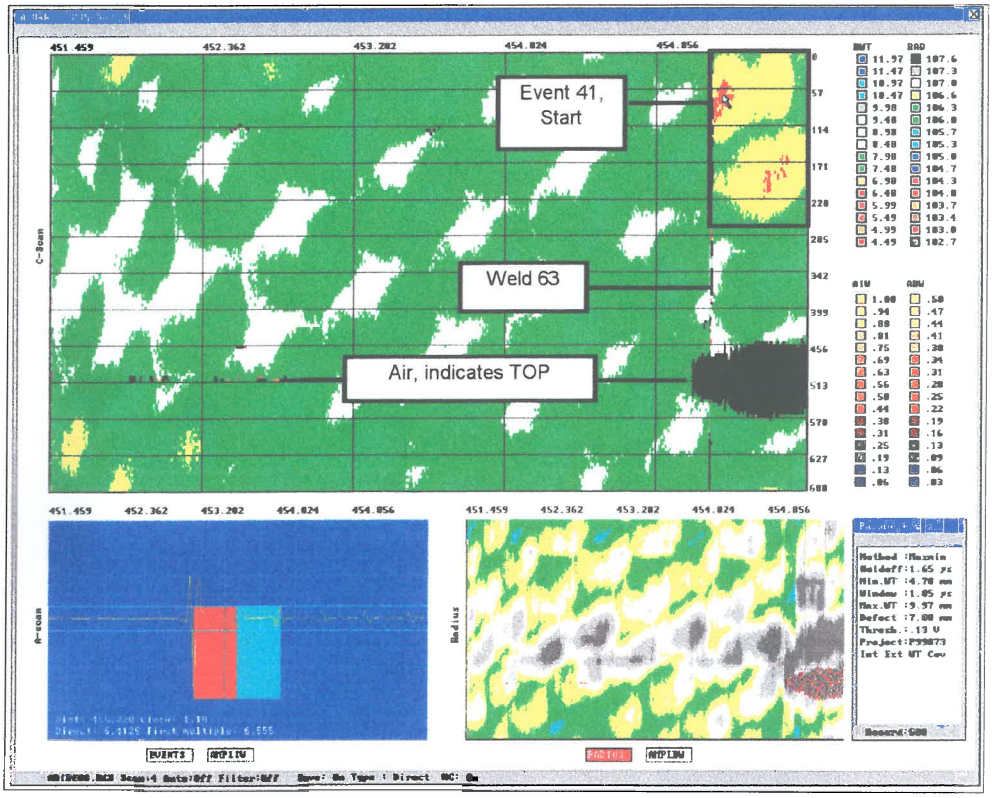

Figure 3.3. Ultrasonic test results

3.7. The corrosion severity indicator chart

Consider the general underground pipe network shown in Figure 3.4. As previously explained, the severity of the corrosion experienced by the different pipe segments in the network will depend on several factors. The information contained in the *American National Standard A21.5, American Society of Testing and Materials A674, A74 and A888,* and *American Water Works Association Specification C105* provides pipeline installation instructions and an appendix that details a 10-point scale (shown in Table 3.1) to determine whether soils are potentially corrosive. It is thus possible to identify regions of high corrosion severity to which the network is subjected. In the figure the areas enclosed by the shaded contour lines indicate these regions of varying corrosion severity. The American National Standard suggests that if the sum of the points of the test results is equal or greater than 10, the soil is potentially corrosive and some sort of preventative measure ought to be taken.

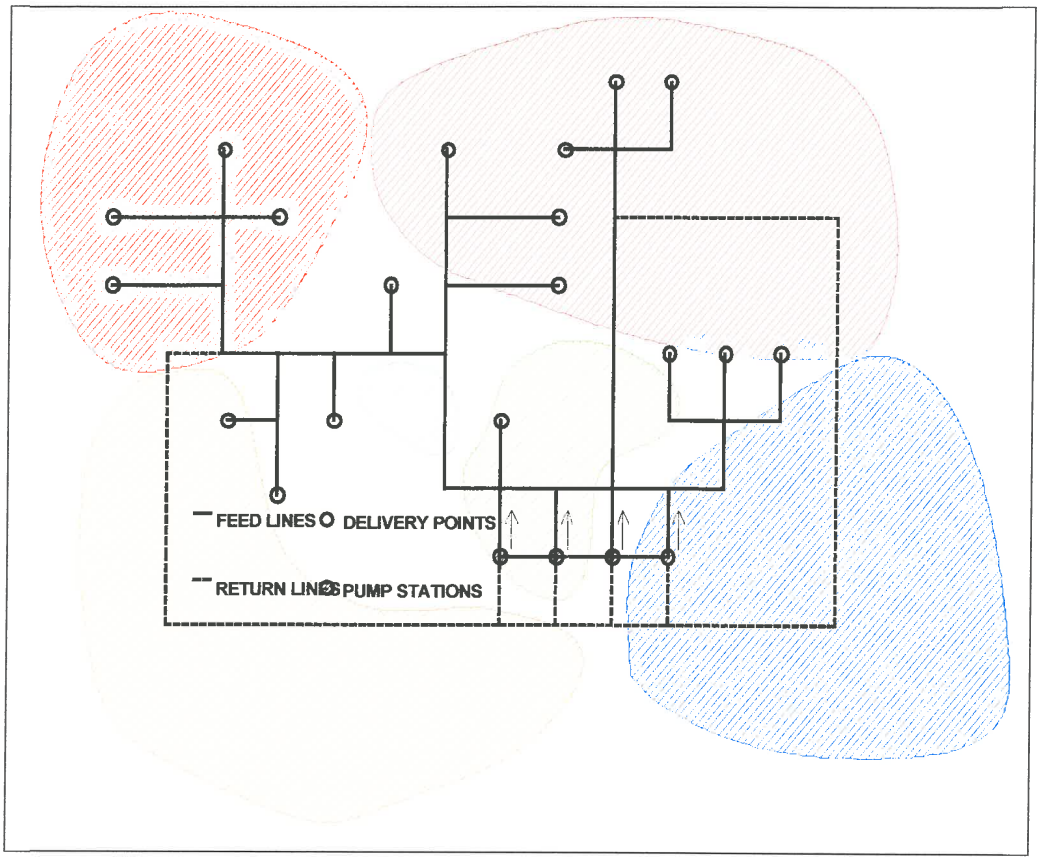

Figure 3.4. General underground pipe network

Table 3.1. Soil test evaluation chart

Soil characteristic	Points
Resistivity [ohm-cm]:	
<700	10
700-1000	8
1000-1200	5
1200-1500	2
1500-2000	1
>2000	0
pH:	
0-2	5
2-4	3
4-6.5	0
6.5-7.5	0 [A]
7.5-8.5	0
>8.5	3
Redox Potential:	
> +100 mV	0
+50 to +100 mV	3.5
0 to +50 mV	4
Negative	5
Sulphides:	
Positive	3.5
Trace	2
Negative	0
Moisture:	
Poor drainage, continuously wet	2
Fair drainage, generally moist	1
Good drainage, generally dry	0

[A] If sulphides are present and low or negative redox potential results are obtained, 3 points shall be given for this range.

3.8. Soil evaluation

The soil surrounding the pipe studied in Section 2.6 was evaluated according to the soil test evaluation chart (Table 3.1).

The test results are as follows:

Test item	Result	Points
Resistivity	1600 ohm-cm	1
pH	7.2	0
Redox potential	95 mV	3.5
Sulphides	Negative	0
Moisture	Generally dry	0
Total		**4.5**

It can be seen that the sum of the points is smaller than 10, and according to the soil test evaluation chart (Table 3.1) the soil is therefore not potentially corrosive. This is reflected in the good general condition of the pipeline and in the fact that other pipes in the region, buried in similar soil, do not show excessive corrosion damage after 17 years of service.

3.9. Conclusion

In this chapter, some of the testing techniques currently in use for determining the condition of an underground pipe network were briefly touched upon. Both MFL and Continuous Ultrasonic "Pigging" give 100 % coverage of the pipe, can detect several anomalies, are useful for inspecting long sections of pipe and are believed to be approximately 90 % accurate. The PCM technique finds application in pipe networks where the pipe is protected against damage by some sort of protective coating. Positions where the coating is damaged are prone to highly localised corrosive attack. The PCM technique can be used to indicate these areas. Manual ultrasonic spot-probing renders accurate wall thickness results but depends highly on the testing position. The corrosion severity chart can be used to indicate areas of possible concern.

One fundamental question remains unanswered:

"Which method should be used under which conditions?"

It can be argued that the method that renders the most information about the condition of the pipe should be used (thus favouring MFL and Continuous Ultrasonic "Pigging"). The problem, however, is that these methods have a definite cost premium and it may even be possible that these methods cannot be effectively employed over the whole network.

With manual spot-probing it is possible to determine the wall thickness at a few prescribed positions only.

The bottom line is that, no matter what inspection technique one uses, there will always be uncertainty associated with the values of the remaining wall thickness of the pipe. It may be possible that the deepest pit in the pipe was measured, but the analyst will never know. Since this uncertainty can not be overcome, it should, in some way or the other, feature in the analysis of the integrity of the pipe network. This can be done by using statistical models to describe the series of wall thickness measured and the way in which the integrity of the pipe network is influenced.

The best we can do is to use the methods optimally to minimise risk and these methods will be described in the following chapters.

4. PIPE STRESSES

4.1. Introduction

Corrosion plays a detrimental part in the structural performance of the pipeline, and it must be realised that the stresses present in the wall of the pipe will cause final failure. Failure will occur when the structural resistance of the pipe is smaller than the applied structural load.

In Section 2.6 it was indicated that the stresses at the pit root are highly dependent on the depth of the pit, but almost totally insensitive to the diameter of the pit and in addition to the stress relationship established in Equation 2.6.6, one should realise that other modes of failure do exist. Another noteworthy reason for pipeline failure is that of bulging which occurs when corrosion causes the pipe wall to thin over a large patch. A significantly large patch of reduced wall thickness behaves like a locally-clamped plate that is subjected to uniform surface pressure, and bending stresses occur in the material due to bending moments induced on the plate. The author acknowledges that this is a possible reason for failures but does not feel that it needs further investigation. The principle reason for this opinion is that, since the pipe is buried, the soil pressure acting on the external pipe surface would constrain the corroded patch in the outwardly radial direction and that the proposed plate behaviour might not occur.

In this chapter, stresses present in the pipe wall due to the following loads are discussed:

1. internal pressure;
2. soil loads;
3. traffic loads, and
4. stresses due to temperature differentials and to longitudinal bending.

The purpose of this chapter is not only to quantify the stresses present in the pipe wall as a result of the above-mentioned loads, but also to indicate the magnitude of each load as well as the relative contribution of each load to the equivalent Von Mises stress.

4.2. Circumferential stresses

4.2.1. Internal pressure

The circumferential stress in the pipe wall can be determined by approximating the pipe as a thin-walled cylindrical pressure vessel

$$\sigma_{c1} = \frac{pr}{t} \qquad (4.2.1)$$

where p is the internal pressure, r is the internal pipe radius and t is the wall thickness of the pipe.

4.2.2. Soil loads

Ahammed and Melchers (1997:990) suggest that the following relationship exists between circumferential stress and soil loads:

$$\sigma_{c2} = \frac{6k_m C_d \gamma B_d^2 Etr}{Et^3 + 24k_d pr^3} \qquad (4.2.2)$$

where k_m (= 0.235) is a bending moment coefficient, C_d (= 1.32) is an earth pressure coefficient, B_d is the width of the ditch at the top of the pipe, E is Young's modulus of the pipe material, k_d (= 0.108) is a deflection coefficient and γ (= 18.9 x 10^{-6} N/mm) is the unit weight of soil.

4.2.3. Traffic loads

Ahammed and Melchers (1997:990) also suggest that the following relationship exists between circumferential stress and traffic loads:

$$\sigma_{c3} = \frac{6k_m I_c C_t FEtr}{L_e(Et^3 + 24k_d pr^3)} \qquad (4.2.3)$$

where I_c (= 1.25) is an impact factor, C_t (= 0.12) is a surface-load coefficient, L_e is the equivalent length of the pipe that is subjected to the traffic load and F is the surface wheel-load.

4.3. Longitudinal stresses

4.3.1. The Poisson effect

Since the pipe is constrained in its longitudinal direction, a longitudinal stress will be present due to internal pressure (the Poisson effect)

$$\sigma_{l1} = \frac{\nu pr}{t} \tag{4.3.1}$$

where ν is Poisson's ratio of the pipe material.

4.3.2. Temperature differential

If a temperature differential (defined as the difference between operating temperature and installation temperature) were present, the longitudinal stress would be

$$\sigma_{l2} = \alpha E(\Delta\theta) \tag{4.3.2}$$

where α is the thermal expansion coefficient of the material and $\Delta\theta$ is the temperature differential.

4.3.3. Longitudinal curvature

The longitudinal stress due to longitudinal bending is

$$\sigma_{l3} = Er\chi \tag{4.3.3}$$

where χ is the longitudinal curvature.

4.4. Relative contribution of the respective loads to the Von Mises stress

Consider a pipeline with the properties listed in Table 4.1.

Table 4.1. Mean values of variables.

Symbol	Description	Mean
L_e	Pipe effective length	1000 mm
B_d	Width of ditch	760 mm
C_d	Calculation coefficient	1.32
C_t	Surface-load coefficient	0.12
E	Young's modulus	201 000 MPa
F	Wheel load of traffic	150 000 N
I_c	Impact factor	1.25
k_d	Deflection coefficient	0.108
k_m	Bending moment coefficient	0.235
p	Internal pressure	5 MPa
r	Pipe radius	225 mm
t	Pipe-wall thickness	7 mm
α	Thermal expansion coefficient	$11.7 \times 10^{-6}/^{o}C$
γ	Unit weight of soil	18.9×10^{-6}N/mm
χ	Longitudinal curvature	-1×10^{-6}rad/mm
ν	Poisson's ratio	0.3
$\Delta\theta$	Temperature differential	$10^{o}C$

The stresses in the pipe wall can be determined as:

1. The circumferential stress due to internal pressure is calculated at 160.7 MPa;
2. The circumferential stress due to soil load is calculated at 29.7 MPa;
3. The circumferential stress due to traffic loads is calculated at 46.4 MPa;
4. The total circumferential stress is, therefore, **236.8 MPa**;
5. The longitudinal stress due to Poisson's effect is calculated at 48.2 MPa;
6. The longitudinal stress due to temperature differential is calculated at 23.52 MPa;
7. The longitudinal stress due to longitudinal bending is calculated at -45.23 MPa;
8. The total longitudinal stress is therefore **26.49 MPa**.

The equivalent (tensile) stress can be determined by using the Von Mises failure criterion:

$$\sigma_{eq}^2 = (\sigma_c^2 - \sigma_c \sigma_l + \sigma_l^2) \qquad (4.4.1)$$

and is found to be equal to **224.73 MPa**. The relative contributions of the respective loads are listed in Table 4.2.

Table 4.2. Relative contribution of respective loads.

Load	Relative contribution
Internal pressure	61 %
Soil loads	11.2 %
Traffic loads	17.6 %
Poisson's effect	18.3 %
Temperature differential	8.9 %
Longitudinal bending	-17.2 %

4.5. Conclusion

It is clear that internal pressure and Poisson's effect are the two greatest contributors to equivalent stress. In Section 6.6 it will be indicated that one can reduce the complexity of the analysis by incorporating just the internal pressure load and the load due to Poisson's effect without significantly decreasing the accuracy of the prediction (see Section 1.7).

As stated previously, in addition to the stress equations presented in Sections 4.2 and 4.3, one should realise that other modes of failure exist. Another noteworthy failure mode is that of bulging which occurs when corrosion causes the pipe wall to thin over a large patch. A significantly large patch of reduced wall thickness can behave as a locally-clamped plate which is subjected to uniform surface pressure and bending stresses would exist in the material due to bending moments induced on the plate. The author acknowledges that this is a possible failure mode but does not feel that it needs further investigation. The principle reason for this opinion is that, since the pipe is buried, the soil pressure acting on the external pipe surface constrains the corroded patch in the outwardly radial direction and that the proposed plate behaviour would not occur.

The stress equations presented in Sections 4.2 and 4.3 will be adjusted in the following chapters to indicate their dependence on time due to the time-based nature of corrosion ($P = kT^n$).

5. MONTE CARLO SIMULATION OF A PIPELINE SUBJECTED TO EXTERNAL CORROSION AND NEAR-CONSTANT INTERNAL PRESSURE (STATIC ANALYSIS)

High-speed computers have facilitated many billions of times more computations in the past decade than were undertaken in all the previous history of the world. This leap in computation has allowed us for the first time to fathom some of the universal characteristics of complexity. What computers show is that complex systems can be built and understood only from the bottom up. Multiplying prime numbers is simple. But disaggregating complexity by trying to decompose the product of large prime numbers is all but impossible.

- James Dale Davidson and Lord William Rees-Mogg

5.1. Introduction

Physically pipe networks may be very large and it is therefore not unusual to find that the corrosion rate varies over length. Furthermore, it may be impossible to determine the extent of corrosive attack over the whole length of the pipe network. Due to the methods used in determining the extent of corrosive attack, a probability exists, statistically, that an anomaly in the pipe wall will remain undetected. In the following sections it will be shown that the remaining life of a pipeline is dependent on approximately 20 variables of which only 2 are used to describe the rate of corrosion (k and n). It is very possible that the variable set may differ at various positions on the pipe. Thus, some uncertainty exists regarding the variable set and it would be foolish to try and ignore this fact. The relative magnitudes of these uncertainties should thus be used in any calculations made regarding the integrity of the pipe network. This chapter is entirely based on an article by Ahammed and Melchers (1997:990) *Probabilistic analysis of underground pipelines subjected to combined stresses and corrosion*. In this chapter, however, use will be made of the Monte Carlo simulation technique instead of the First-Order, Second-Moment theory used by Ahammed and Melchers. The reason for this is the relative ease with which it can be employed and the author believes

that, with high-speed computing more freely available nowadays, Monte Carlo simulations have become cheaper to perform.

5.2. Basic statistics

The magnitudes of the individual variable (x_i) in the variable set ($\underline{x}$) may differ from position to position or from sample to sample and is not fixed. One way to deal with these variations in variable magnitudes is through statistical methods. A variety of statistical models exist, but the best known is probably the Normal Distribution Function. The frequency with which an event happens (in our case this is the frequency with which the magnitude of the individual variable differs from a certain value) can be described by the following distribution function:

$$f(x) = \frac{1}{\sigma_{stat}\sqrt{2\pi}} e^{-(x-\mu)^2/2\sigma_{stat}^2} \qquad (5.2.1)$$

where σ_{stat} is known as the standard deviation and μ is known as the sample mean.

$$\mu = \frac{\sum_{i=1}^{n} x_i}{n} \qquad (5.2.2)$$

$$\sigma_{stat} = \left[\frac{1}{n-1}\sum_{i=1}^{n}(x_i - \mu)^2\right]^{1/2} \qquad (5.2.3)$$

The standard deviation is an indication of the spread of the data. Another identity, known as the coefficient of variation (COV), can be defined as:

$$COV = \frac{\sigma_{stat}}{\mu} \qquad (5.2.4)$$

It is possible to describe the distribution function completely if any two of three quantities in Equations 5.2.2 to 5.2.4 are known. A special case of the distribution function, where $\sigma_{stat} = 1$ and $\mu = 0$, is shown in Figure 5.1.

The probability (P_f) of an event happening before a specified value (x) is defined as:

$$P_f = \int_{-\infty}^{x} f(x)dx = \int_{-\infty}^{x} \frac{1}{\sigma_{stat}\sqrt{2\pi}} e^{-(x-\mu)^2/2\sigma_{stat}^2} dx \qquad (5.2.5)$$

The cumulative probability of the distribution function with zero mean and unit standard deviation is shown in Figure 5.2.

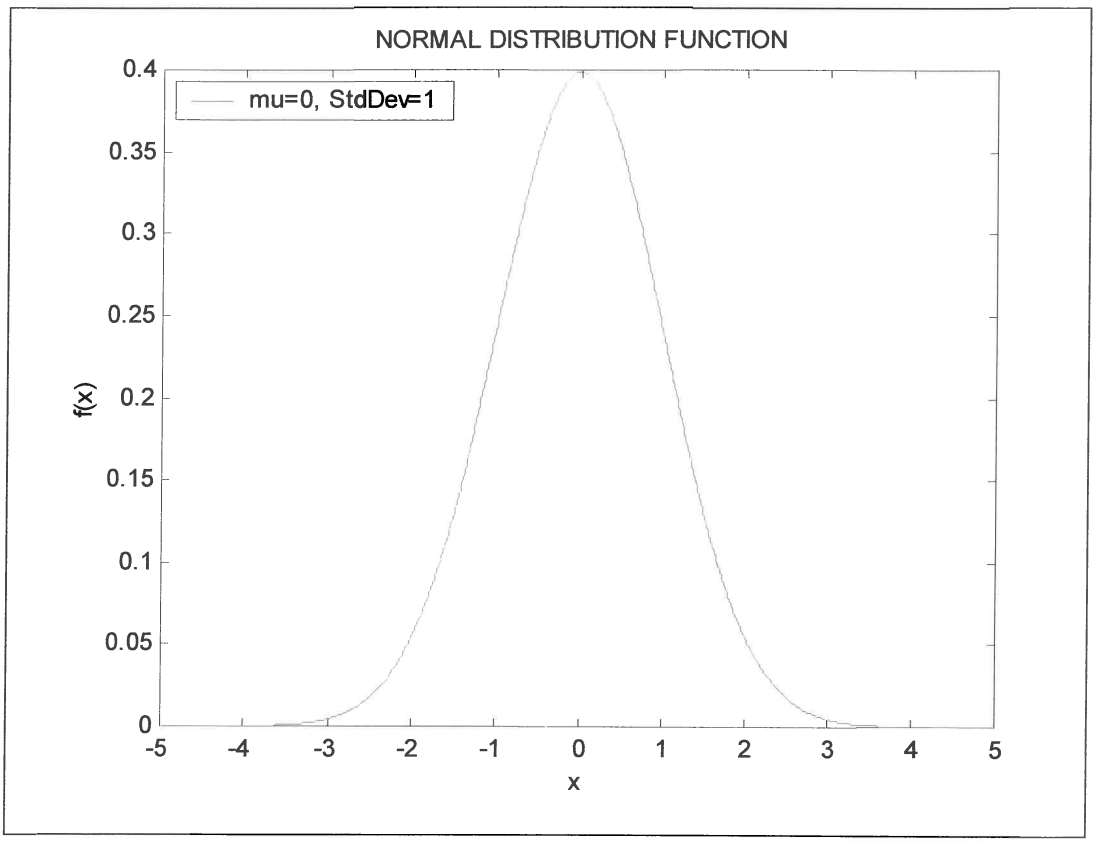

Figure 5.1. Normal distribution function

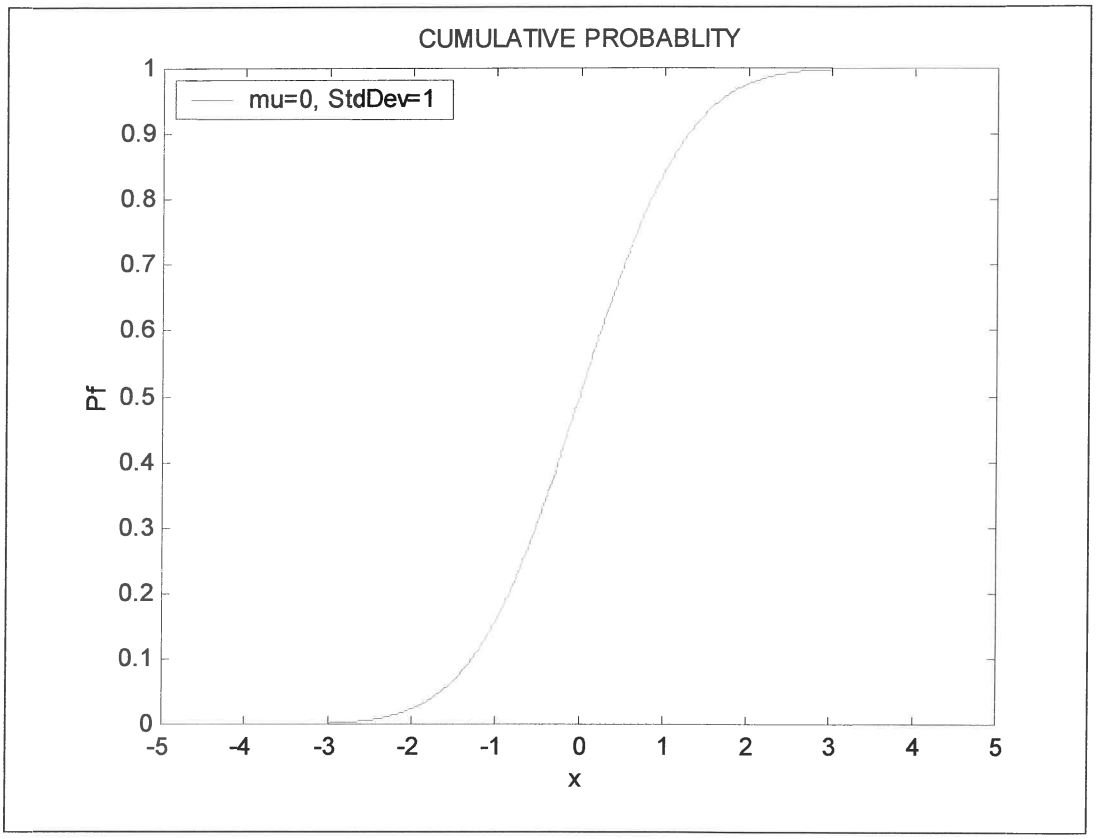

Figure 5.2. Cumulative probability function

5.3. The limit state function

In order to conduct the previously proposed reliability solution, one needs to construct a *limit state function*. This function describes regions, in multi-dimensional variable space, where the state of the pipe is deemed to be safe or unsafe.

Consider a pipe that is subjected to the following loads:

1. internal pressure;
2. soil loads;
3. traffic loads, and
4. stresses due to a temperature differential.

As presented in Chapter 4, the stresses in a section of pipe can be described as follows:

5.3.1. Circumferential stresses

The circumferential stress in the pipe wall can be written as a function of time through the use of the following equations:

$$\sigma_{c1} = \frac{pr}{t - kT^n} \tag{5.3.1}$$

$$\sigma_{c2} = \frac{6k_m C_d \gamma B_d^2 E(t - kT^n)r}{E(t - kT^n)^3 + 24k_d pr^3} \tag{5.3.2}$$

$$\sigma_{c3} = \frac{6k_m I_c C_t FE(t - kT^n)r}{L_e(E(t - kT^n)^3 + 24k_d pr^3)} \tag{5.3.3}$$

$$\sigma_c = \sigma_{c1} + \sigma_{c2} + \sigma_{c3} \tag{5.3.4}$$

where T is the time (in years) and k and n are the corrosion constants determined from the time-based corrosion data.

5.3.2. Longitudinal stresses

The longitudinal stress in the pipe wall can be written as a function of time through the use of the following equations:

$$\sigma_{l1} = \frac{\nu pr}{t - kT^n} \tag{5.3.5}$$

$$\sigma_{l2} = \alpha E(\Delta\theta) \tag{5.3.6}$$

$$\sigma_{l3} = Er\chi \tag{5.3.7}$$

$$\sigma_l = \sigma_{l1} + \sigma_{l2} + \sigma_{l3} \qquad (5.3.8)$$

The Von Mises failure criterion, which is a strain-energy criterion, states that failure will occur if $S_y^2 \leq \sigma_c^2 - \sigma_c\sigma_l + \sigma_l^2$, where S_y is the yield strength of the pipe material. Rearranging the Von Mises equation, the limit state function can be obtained as:

$$z = f(T) = S_y^2 - (\sigma_c^2 - \sigma_c\sigma_l + \sigma_l^2) \qquad (5.3.9)$$

Ultimately the limit state function (z) is time dependent, and represents a failure region if $z \leq 0$ and a safe region if $z > 0$. Typical mean values and coefficients of variation for the variables in Equation 5.3.9 are shown in Table 5.1 (Ahammed and Melchers, 1997:990).

Table 5.1. Variables, mean values and COVs

Symbol	Description	Mean	COV
L_e	Pipe effective length	1000 mm	0.1
B_d	Width of ditch	760 mm	0.1
C_d	Calculation coefficient	1.32	0.2
C_t	Surface-load coefficient	0.12	0.15
E	Young's modulus	201 000 MPa	0.033
F	Wheel load of traffic	150 000 N	0.1
I_c	Impact factor	1.25	0.2
k	Multiplying constant	0.066	0.56
k_d	Deflection coefficient	0.108	0.15
k_m	Bending moment coefficient	0.235	0.15
n	Exponential constant	0.53	0.26
p	Internal pressure	5 MPa	0.1
r	Pipe radius	225 mm	0.04
S_y	Material yield stress	400 MPa	0.05
t	Pipe-wall thickness	7 mm	0.06
α	Thermal expansion coefficient	$11.7 \times 10^{-6}/^{o}C$	0.1
γ	Unit weight of soil	18.9×10^{-6}N/mm	0.1
χ	Longitudinal curvature	-1×10^{-6}rad/mm	0.1
ν	Poisson's ratio	0.3	0.023
$\Delta\theta$	Temperature differential	$10^{o}C$	0.15

5.4. Monte Carlo simulation principles

The Monte Carlo simulation technique involves the random sampling of the system variables in order to artificially simulate a large number of "experiments" or scenarios and to observe the results. In the most basic approach one must:

1. determine a random sampling point, $\underline{x_i} = [x_{1i} \quad x_{2i} \quad x_{3i} \quad \ldots \quad x_{ni}]$;
2. evaluate the limit state function (z) at the sampling point ($\underline{x_i}$). If $z \leq 0$ then failure has occurred, and
3. repeat steps 1 and 2 N times. The probability of failure can then be evaluated as follows:

$$P_f = \frac{n(z \leq 0)}{N} \tag{5.4.1}$$

where N is the number of trials and $n(z \leq 0)$ is the number of times failure was detected.

5.5. Determining the sampling point

The random sampling point, $\underline{x_i} = [x_{1i} \quad x_{2i} \quad x_{3i} \quad \ldots \quad x_{ni}]$, is usually determined with the aid of a random number generator. A number is generated with an arbitrary value between 0 and 1, which is numerically equivalent to a certain probability. The procedure for determining the sampling point is more formally discussed below.

1. For a specific variable, x_1, generate a random variable (u_1);
2. by using Equations 5.2.1 and 5.2.5, with zero mean and unit standard deviation, determine x_{1i}, and
3. calculate the sample value, r_1, with the following relationship: $x_{1i} = \frac{r_1 - \mu_{x1}}{\sigma_{x1}}$, where σ_{x1} and μ_{x1} are the standard deviation and mean value of variable x_1.

This procedure is followed for all the variables and the limit state function is then evaluated at the random sampling point.

5.6. Generic example

The information in Table 5.1, together with Equation 5.3.9, was used to perform simulations in order to determine the probability of pipe failure. Various trials were conducted and the results are discussed in this section. The procedure followed in the simulation is described below and the program code is shown in the Appendices.

1. Define the mean values (μ) of the system variables (Table 5.1);
2. define the COVs of the system variables (Table 5.1);
3. calculate the standard deviations (σ_{stat}) of the system variables ($\sigma_{stat} = \mu \times COV$);
4. define time step T that corresponds to a specific elapsed life time of the section of pipe;
5. generate a set of random numbers ($\underline{u}$);
6. determine the value of x (either from a table of the standard Normal Distribution Function or by using Equations 5.2.1 and 5.2.5);
7. calculate the sample point $r = x \cdot \sigma_{stat} + \mu$;
8. evaluate the limit state function (z) at the sampling point (r) and at time T;
9. if $z \leq 0$, then Indicator := Indicator + 1, and
10. repeat steps 5 to 9 N times, until the probability of failure has stabilised.

The results obtained from the simulations are shown in Figures 5.3 to 5.5. In Figure 5.3 the corrosion rate is shown as a function of time and it is clear that after 200 years a corrosive penetration of approximately 1.1 mm can be expected. Figure 5.4 shows the probability of pipe failure versus elapsed time. Figure 5.5 shows the effect of the number of trials on the probability of failure (the simulation was conducted on an elapsed life of 300 years). It is clear that the probability of failure has stabilised after approximately 20,000 trials. It also shows that the result of any Monte Carlo simulation is highly dependent on the number of trials ("experiments") conducted.

Furthermore, it is clear that the probability of pipe failure is fairly small for the first 50 years of service and after 250 years the probability of failure increases to 6 %. The probability of failure is fairly small and can be attributed to the fact that the corrosive penetration is very slow and might not be representative of any real corrosive damage. The model that was used is only valid for near-constant internal pressure and is therefore not valid for systems subjected to varying internal pressure. However, the statistical approach that was used enables the analyst to couple the reliability of the pipe with the depth of the corrosive attack. Alternatively, if the remaining wall thickness of the pipe is known (through surveillance as described in Chapter 3), it is possible to determine the reliability (or probability of failure) of the pipe – this is the beauty of the approach.

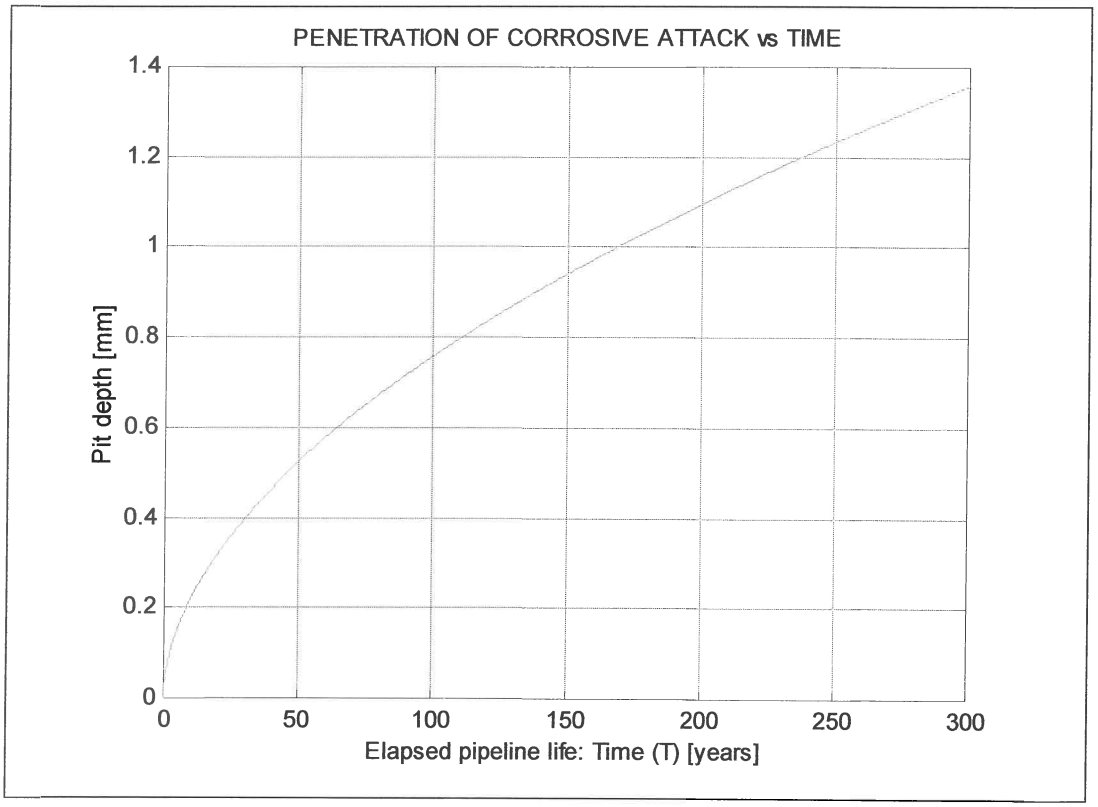

Figure 5.3. Corrosion rate versus time

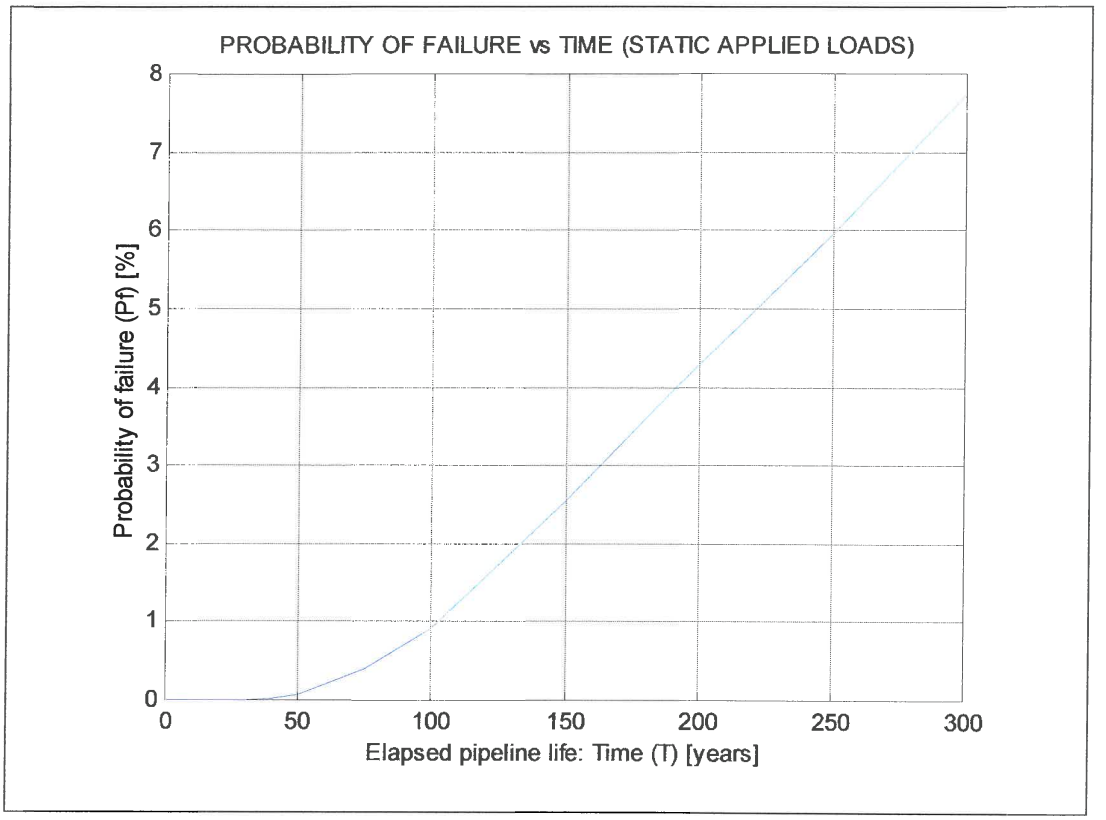

Figure 5.4. Probability of failure versus elapsed pipeline life

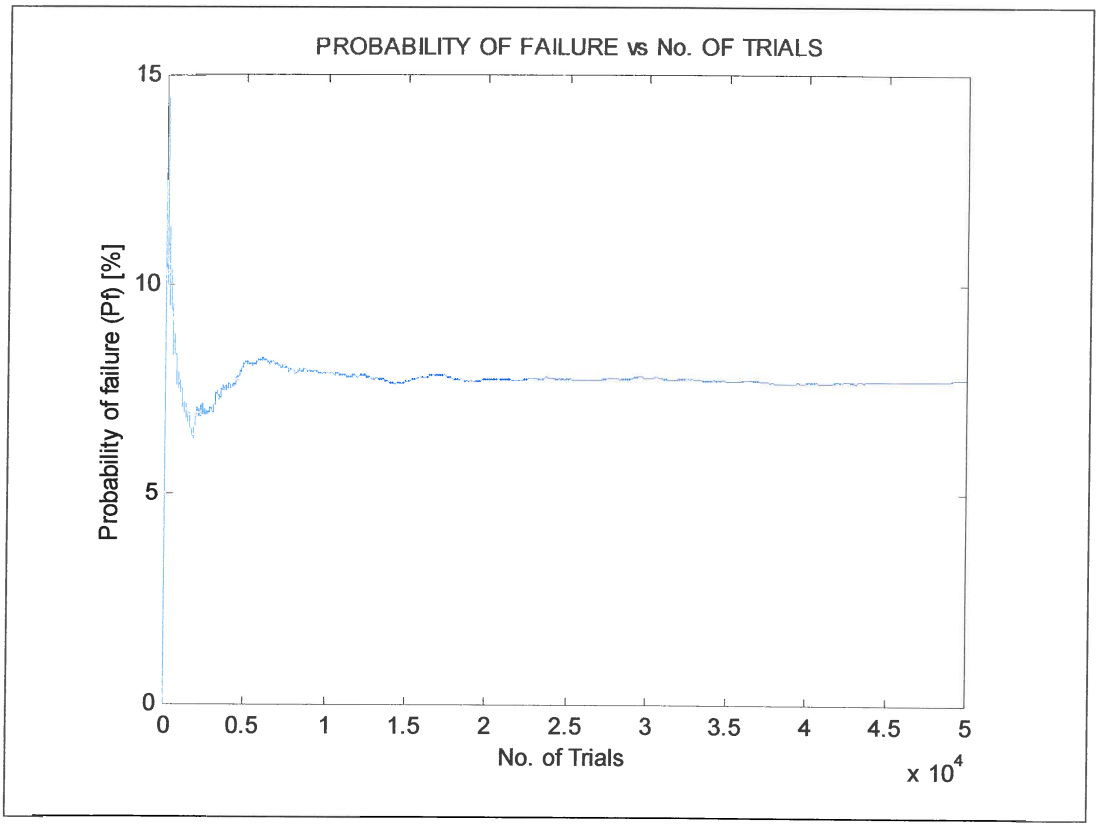

Figure 5.5. Dependence of probability of failure on the number of trials

5.7. Conclusion

By constructing a function representative of the behaviour of a section of a pipe, which is subjected to the combined effects of mechanical loads and corrosion, it is possible to investigate the probability of failure through statistical modelling and simulation. As can be expected, due to the relatively low corrosion rate, the probability of failure is relatively low. It is not inconceivable that the internal pressure may be cyclical and the model falls short in this aspect. The combined effects of fatigue and corrosion will be investigated in the following chapter.

The model proposed in this chapter is modular: the system variables (such as corrosion rate and internal pressure) can be measured or determined for various sections of pipe and then be "fed" to the model. The integrity of other components (such as tees and elbows) can be predicted by changing the limit state function and by following the same principles. Furthermore it was indicated that the success of the simulation is highly dependent on the number of trials that are conducted during the simulation.

More elegant techniques (such as the first-order, second-moment theory) are available for determining the reliability of structural members, but the Monte Carlo method proves to be very robust and extremely easy to employ in systems with complex limit state functions.

6. MONTE CARLO SIMULATION OF A PIPELINE SUBJECTED TO EXTERNAL CORROSION AND VARYING INTERNAL PRESSURE (FATIGUE ANALYSIS)

It is undesirable to believe a proposition when there is no ground whatever for supposing it true.

- Bertrand Russell

6.1. Introduction

In Chapter 5, a model was proposed to determine the probability of failure of a pipeline. Since the system variables may vary over the length of the pipeline, it might not be possible to determine them accurately and singularly. This is the predominant reason for following a statistical approach. Any deviation in the magnitudes of the variables may have an effect on the expected life of the pipeline, and should therefore be mirrored in the predictive model.

However, the proposed model has one fundamental shortcoming: it is only valid for cases where the internal pressure remains nearly constant. Although the variations in internal pressure have been statistically modelled through its mean value and coefficient of variation, the model is not indicative of the real phenomenon of fatigue. It is not inconceivable that the pipe will only be subjected to nearly constant internal pressures at certain positions in the network, but it is definitely not the case for all pipes in the network. In this chapter, a model is proposed that is more indicative of the fatigue process that takes place in the sections of pipe subjected to varying internal pressure. The model will be illustrated by a generic, illustrative example.

It is a well-known fact that the stress history of a cyclically stressed component has a definite influence on fatigue life. The strain-life equations will be used and the hysteresis behaviour of the pipe material will be modelled. Due to the decrease in wall thickness, the stresses in the pipe wall will increase with time. Therefore the strains in the pipe wall will also increase, and just before failure, the fatigue process will be governed by the plastic strain present in the pipe wall. The model will, therefore, also be valid when the pipe is subjected to

very high internal pressures. The strain-life method is probably easier to incorporate in the model and more accurate to use than a cycle counting technique that combines with the stress-life method.

6.2. Basic strain-life principles

Consider a specimen subjected to a varying tensile load (as shown in Figure 6.1). The tensile stress at section A-A can be calculated by dividing the force by the cross-sectional area at A-A (as shown in Figure 6.1).

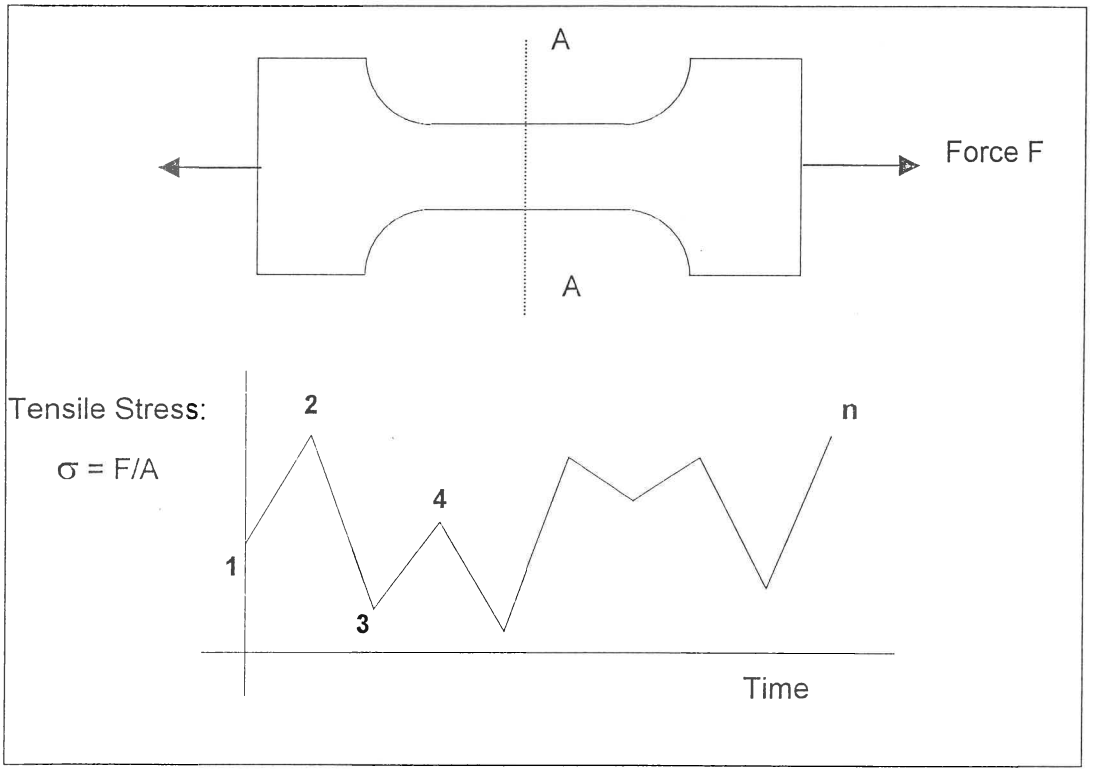

Figure 6.1. Specimen subjected to varying stress

The process between 1 and 2 is known as a reversal. Thus, one cycle consists of two reversals: there are n reversals and $n/2$ cycles in one load block. The length of the load block should be specified in units of time and the load block itself should be representative of the typical stresses encountered in the service life of the specimen.

For the following discussion consider reversal i to i+1:

1. The stress range ($\Delta\sigma$) is defined as $\Delta\sigma = |\sigma_{i+1} - \sigma_i|$.

2. The stress amplitude (σ_a) is defined as $\sigma_a = \frac{|\sigma_{i+1} - \sigma_i|}{2}$.

3. The mean stress (σ_m) is defined as $\sigma_m = \frac{\sigma_{i+1} + \sigma_i}{2}$.

4. The stress ratio (R) is defined as $R = \frac{\sigma_{\min}}{\sigma_{\max}}$.

5. The amplitude ratio (A_r) is defined as $A_r = \frac{\sigma_a}{\sigma_m}$.

6. The strain range ($\Delta\varepsilon$) can be determined from the general hysteresis curve equation

$$\Delta\varepsilon = \frac{\Delta\sigma}{E} + 2\left(\frac{\Delta\sigma}{2K'}\right)^{1/n'} \qquad (6.2.1)$$

where E = the modulus of elasticity of the material, K' = the cyclic strength coefficient of the material and n' = the strain-hardening exponent of the material.

7. The number of reversals that can be expected before failure ($2N_f$) can be obtained by solving the strain-life equation

$$\frac{\Delta\varepsilon}{2} = \frac{\sigma_f'}{E}(2N_f)^b + \varepsilon_f'(2N_f)^c \qquad (6.2.2)$$

where σ_f' = the fatigue strength coefficient, ε_f' = the fatigue ductility coefficient, b = the fatigue strength exponent and c = the fatigue ductility exponent.

8. According to Morrow, the effect that mean stress has on the fatigue life, can be accounted for by modifying the elastic term in the strain-life equation

$$\frac{\Delta\varepsilon}{2} = \frac{\sigma_f' - \sigma_m}{E}(2N_f)^b + \varepsilon_f'(2N_f)^c \qquad (6.2.3)$$

where σ_m = mean stress in reversal *i* to *i+1*.

9. The fatigue damage caused in reversal *i* to *i+1* can be calculated as:

$$D_i = \frac{1}{2N_f} \qquad (6.2.4)$$

This process can be followed for all the reversals in the load block and the fatigue damage can be summated:

$$D_{total} = \sum D_i = \sum\left(\frac{1}{2N_f}\right)_i \qquad (6.2.5)$$

According to Miner, failure will occur when the total damage $D_{total} = 1$. The number of blocks that can be expected before failure can thus be calculated as follows:

$$No.Blocks = \frac{1}{D_{total}} = \frac{1}{\sum\left(\frac{1}{2N_f}\right)_i} \qquad (6.2.6)$$

It should be noted that the fatigue strength coefficient (σ_f') is closely related to the ultimate tensile strength of the material, and when the stress in the material exceeds this value, structural failure has occurred. The hysteresis response of the material is modelled by the strain-life method, and it is therefore not necessary to use cycle-counting techniques before the analysis is started. As a result, this method also lends itself to real-time fatigue analyses – the stress signal can be "played" to the model and analysed, thus cutting down on pre-processing time.

6.3. Application of strain-life principles

In Chapter 2 a brief study, conducted by the author, was discussed. It was pointed out that it might be possible that the corrosion process does not start immediately, but that it may be delayed by a certain initiation period. For a 10 year delay period, the model describing the depth of corrosive penetration versus time was proposed as:

$$P = k(T-10)^n, T > 10 \qquad (6.3.1)$$
$$= 0, T < 10$$

The values for k and n were determined to be 0.23909 and 0.6802 respectively. A plot showing the pit depth (P) against time (T) is given in Figure 6.2.

Consider a pipe that has an internal radius $r = 500\,\text{mm}$, original wall-thickness $t_w = 7\,\text{mm}$ and which is subjected to the varying internal pressure signal (P) shown in Figure 6.3. The mean value of the internal pressure is 5.126 MPa.

Also assume that the pipe is subjected to the following loads:

1. internal pressure;
2. soil loads, and
3. stresses due to a temperature differential.

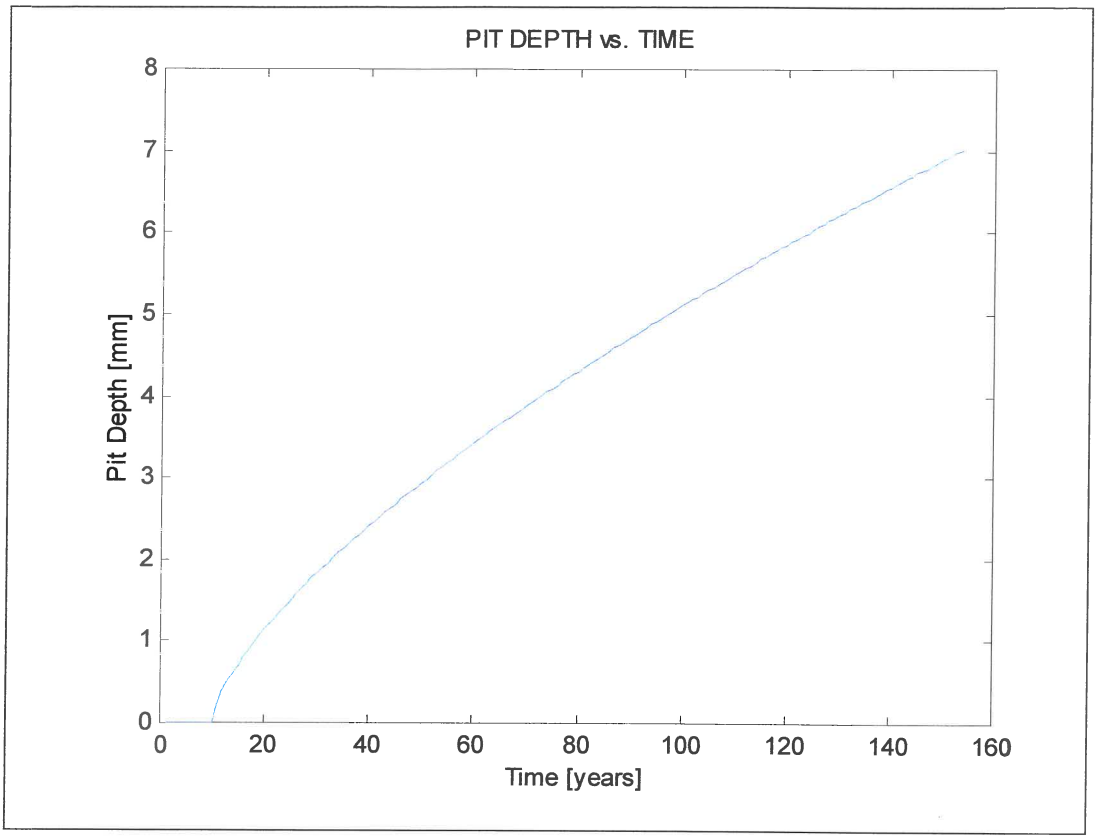

Figure 6.2. Graph showing pit depth versus time with a delay period of 10 years

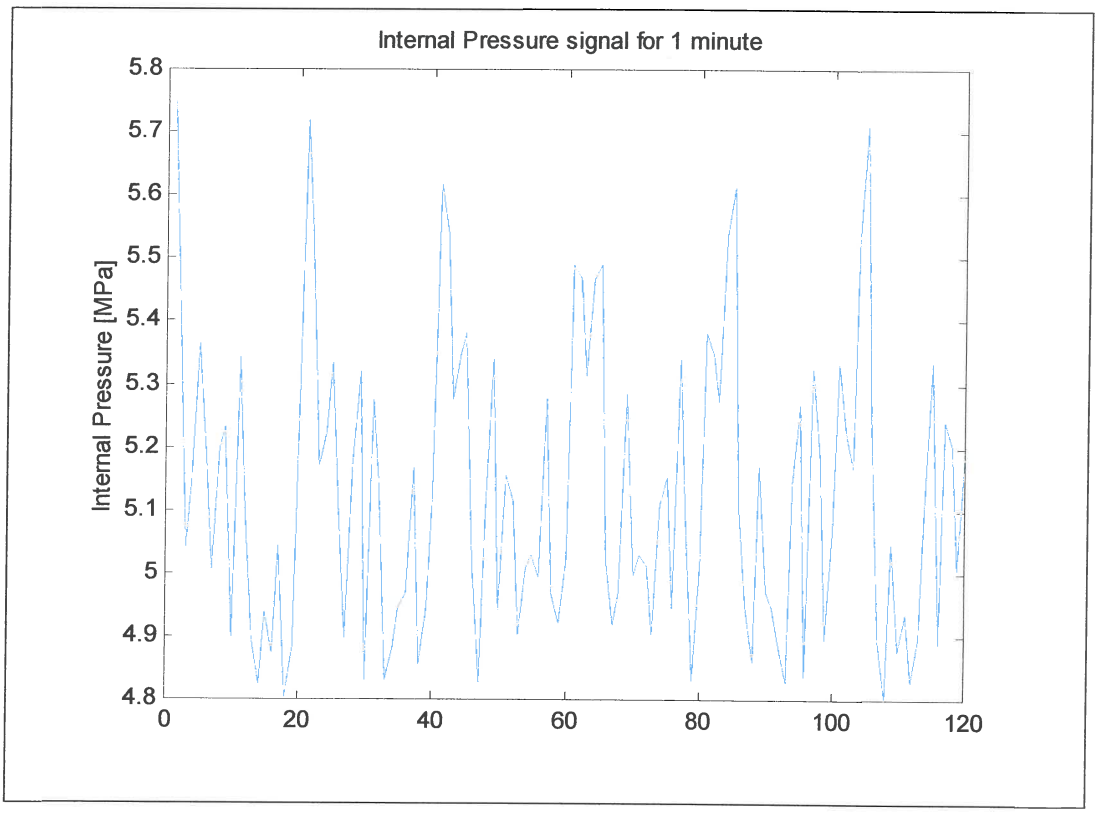

Figure 6.3. Varying internal pressure (recorded over 1 minute and reduced)

As discussed in previous chapters, the stresses in the pipe can be determined as follows:

6.3.1. Circumferential stresses

The circumferential stress in the pipe wall can be written as a function of time through the use of the following equations:

$$\sigma_{c1} = \frac{pr}{t - k(T-10)^n} \tag{6.3.2}$$

$$\sigma_{c2} = \frac{6k_m C_d \gamma B_d^2 E(t - k(T-10)^n)r}{E(t - k(T-10)^n)^3 + 24k_d pr^3} \tag{6.3.3}$$

$$\sigma_c = \sigma_{c1} + \sigma_{c2} \tag{6.3.4}$$

6.3.2. Longitudinal stresses

The longitudinal stress in the pipe wall can be written as a function of time through the use of the following equations:

$$\sigma_{l1} = \frac{vpr}{t - k(T-10)^n} \tag{6.3.5}$$

$$\sigma_{l2} = Er\chi \tag{6.3.6}$$

$$\sigma_l = \sigma_{l1} + \sigma_{l2} \tag{6.3.7}$$

The numerical values of the variables used in this example are shown in Table 6.1.

One should immediately recognise that this is a multi-axial fatigue problem. However, since the total longitudinal stress is an in-phase function of the total circumferential stress, it is possible to determine an equivalent stress through the use of the Von Mises failure criteria. This equivalent (tensile) stress can then be used in the strain-life equations to determine the life of the pipe. Of course, one could use more specialised theories (such as Sines' model) to account for the multi-axial fatigue behaviour of the pipe. However, the author is of opinion that the Von Mises approach (which is a recognised approach for in-phase, multi-axial fatigue problems) would be adequate since it will be indicated in following sections that the multi-axial fatigue problem can be greatly reduced.

The equivalent stress (σ_{eq}) can be determined by means of the following equation:

$$\sigma_{eq}^2 = \sigma_c^2 - \sigma_c\sigma_l + \sigma_l^2 \qquad (6.3.8)$$

Again it is clear that the stresses in the pipe wall are time dependent. Due to the time-dependent decrease in wall thickness, the stresses will increase as a function of time. Therefore, the damage caused by one load block will also increase with time.

Table 6.1. Variables, mean values and COVs

Symbol	Description	Mean	COV
r	Pipe radius	500 mm	0.04
t	Pipe-wall thickness	7 mm	0.06
k_m	Bending moment coefficient	0.235	0.15
C_d	Calculation coefficient	1.32	0.2
γ	Unit weight of soil	18.9×10^{-6} N/mm	0.1
B_d	Width of ditch	760 mm	0.1
E	Young's modulus	201 000 MPa	0.033
k_d	Deflection coefficient	0.108	0.15
ν	Poisson's ratio	0.3	0.023
α	Thermal expansion coefficient	11.7×10^{-6} / °C	0.1
$\Delta\theta$	Temperature differential	10°C	0.15
χ	Longitudinal curvature	-1×10^{-6} rad/mm	0.1
K'	Cyclic-strength coefficient	1337 MPa	0.03
n'	Cycling strain-hardening exponent	0.226	0.03
σ_f'	Fatigue-strength coefficient	1117 MPa	0.03
b	Fatigue-strength exponent	-0.11	0.03
ε_f'	Fatigue-ductility coefficient	0.338	0.03
c	Fatigue-ductility exponent	-0.48	0.03
k	Multiplying constant	0.23909	0.150499
n	Exponential constant	0.6802	0.062379

The structural damage suffered in the history of the pipe should also be accounted for in the determination of life expectancy.

Corrosion caused by soil exposure is generally a slow process and in the following model it is assumed that the wall thickness remains constant for one year. At the end of each year the wall thickness is reduced, and the damage caused by one load block is recalculated. Since the load block is

representative of one minute in the pipe's life, the damage caused in one year will be equal to:

$$D/year = 60 \times 24 \times 365.25 \times D_{total} = 525960 \times D_{total} \qquad (6.3.9)$$

The algorithm of the fatigue model is as follows:

Specify a starting time of interest (T).

1. At time T, calculate the equivalent stress (σ_{eq}) for each reversal in the internal pressure signal (P) by using Equations 6.3.2 to 6.3.8.
2. Calculate the damage caused by one load block (D_{total}) with Equation 6.2.5.
3. Calculate the damage caused in one year ($D/year$) with Equation 6.3.9.
4. Increase the time of interest ($T := T + \Delta T$).
5. Repeat steps 2 to 5 until the damage caused in the specific year is greater than one.

The output of the algorithm is shown in Figure 6.4 and shows the damage that is caused in one year of the pipeline's life versus the lifetime of the pipeline.

In order to determine the expected life of the pipe, it is necessary to calculate the cumulative damage caused by the load block. The cumulative damage can be obtained by integrating the function $D/year$ (shown in Figure 6.4). The cumulative damage at time T is, therefore:

$$D_{CUM}(T) = \int_0^T (\mathrm{D} / \mathrm{year}) dT \qquad (6.3.10)$$

A graph showing the cumulative damage (D_{CUM}) as a function of time is shown in Figure 6.5 and it can be seen that the cumulative damage is equal to unity (refering to Miner's damage summation rule) after approximately 80,

continuously operational, years. Therefore it can be stated that the pipe has a life expectancy life of 80 years.

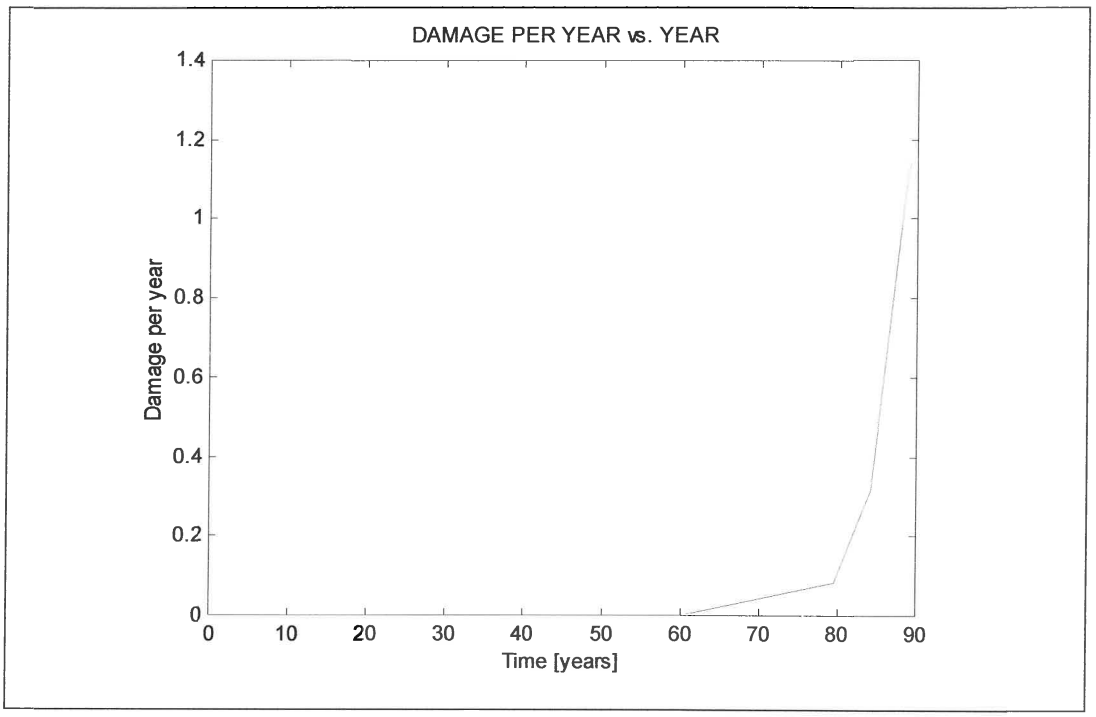

Figure 6.4. Output of fatigue algorithm showing $D/year$ vs year

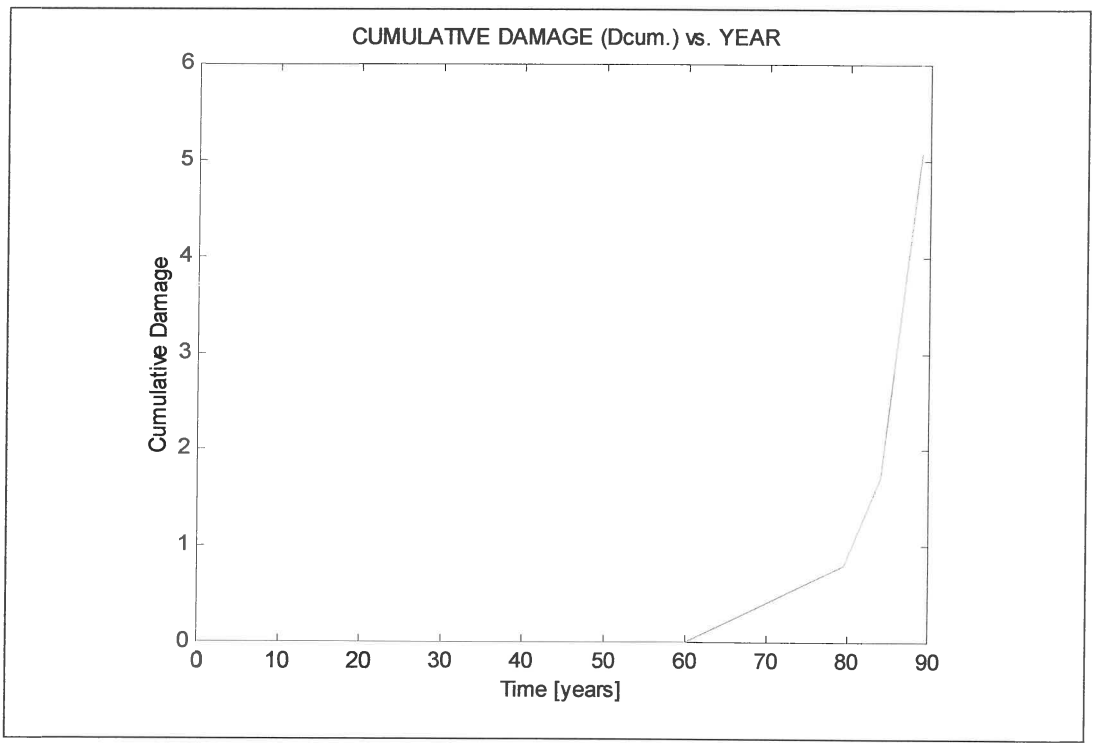

Figure 6.5. Cumulative damage as a function of time

The remaining life that can be expected at time T can be calculated with:

$$Life = F(T, \underline{x}) = \frac{1}{D_{CUM.}(T)} \qquad (6.3.11)$$

A graph showing the remaining expected life, $F(T, \underline{x})$,as a function of time is shown in Figure 6.6.

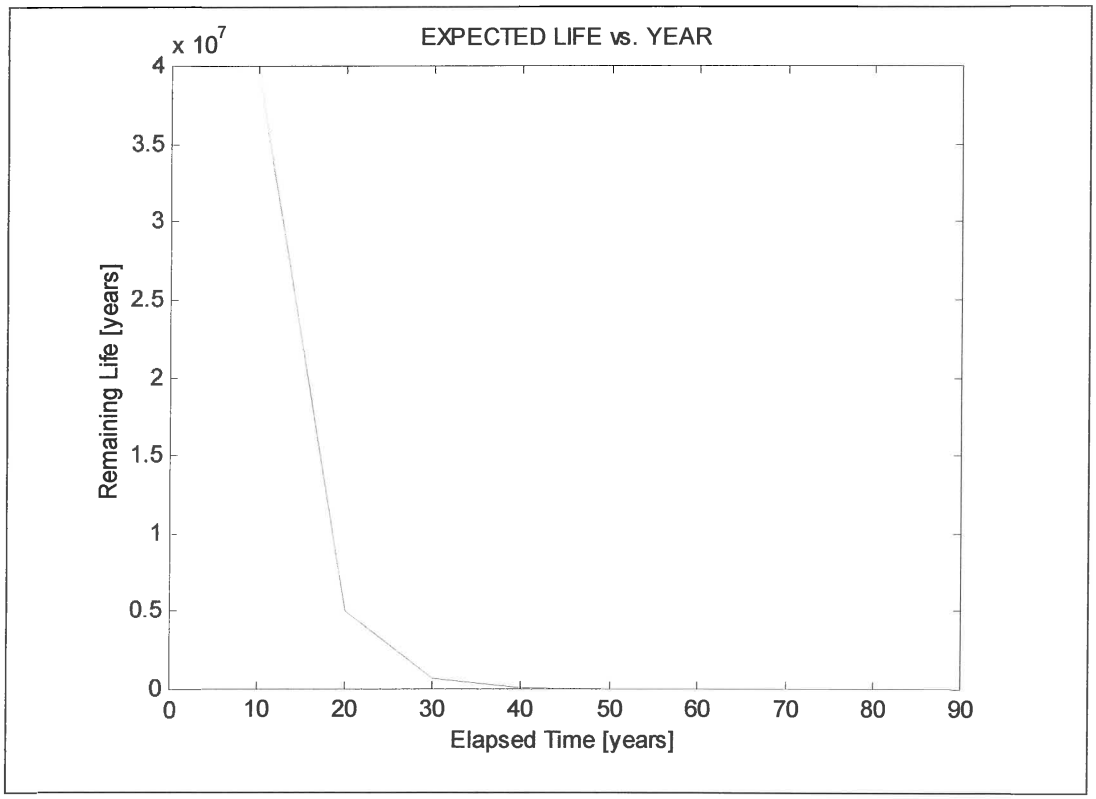

Figure 6.6. Expected remaining life as a function of time

From Figures 6.5 and 6.6 it is clear that failure occurs after 79.6796 years (≈ 80 years). This is the total life expectancy for the specific section of pipe in the network. The depth of corrosive penetration after approximately 80 years is about 4.3 mm. Conversely, it can be stated that failure would be of definite concern if an anomaly with a depth of 4.3 mm (or more) were detected at any position on the pipe. It can also be said that the critical wall thickness of the pipe is 7 mm – 4.3 mm = 2.7 mm.

6.4. Important properties of the fatigue model

The following important aspects of the fatigue model can be identified:

1. The equivalent- and mean stress signals are shown in Figures 6.7 and 6.8. It is clear that the stress levels increase with time (as can be expected).

   The dependence of the stress ratio, $R = \frac{\sigma_{\min}}{\sigma_{\max}}$, and amplitude ratio, $A_r = \frac{\sigma_a}{\sigma_m}$, on time (i.e. wall thickness) are shown in Figures 6.9 and 6.10.

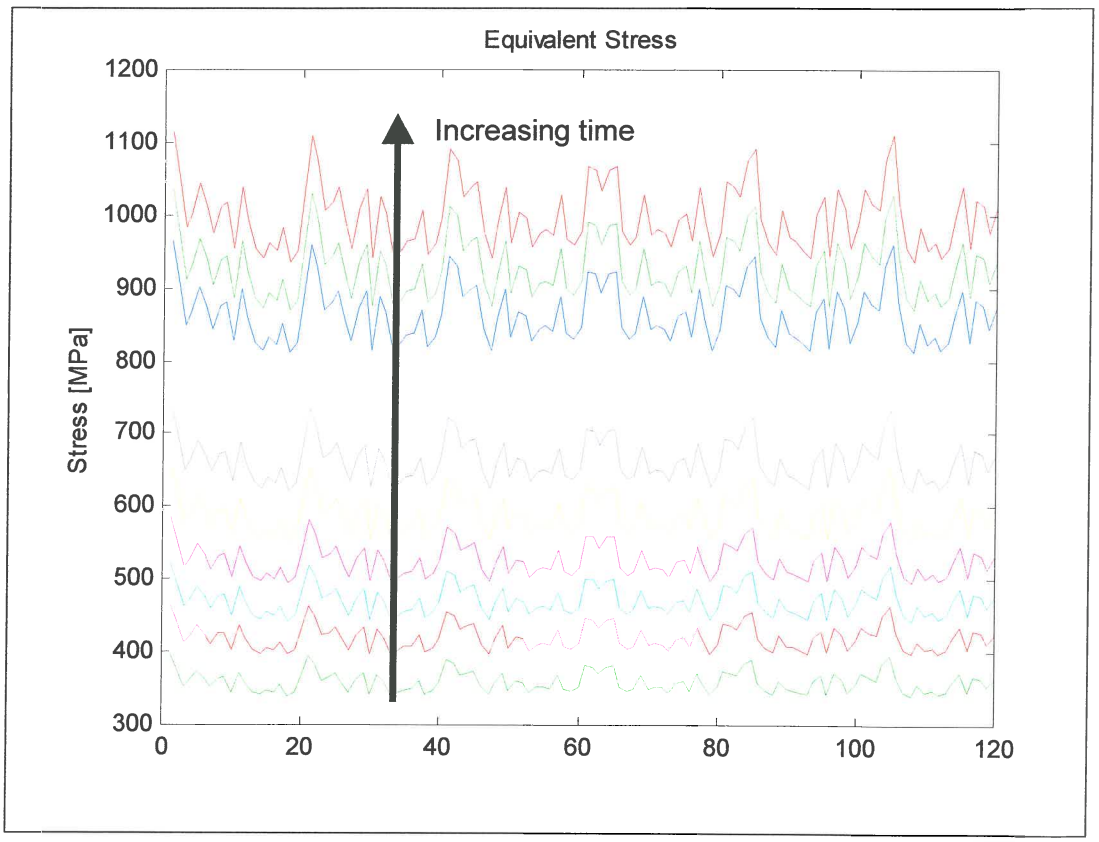

Figure 6.7. Equivalent stress ($\sigma_{eq.}$) versus time

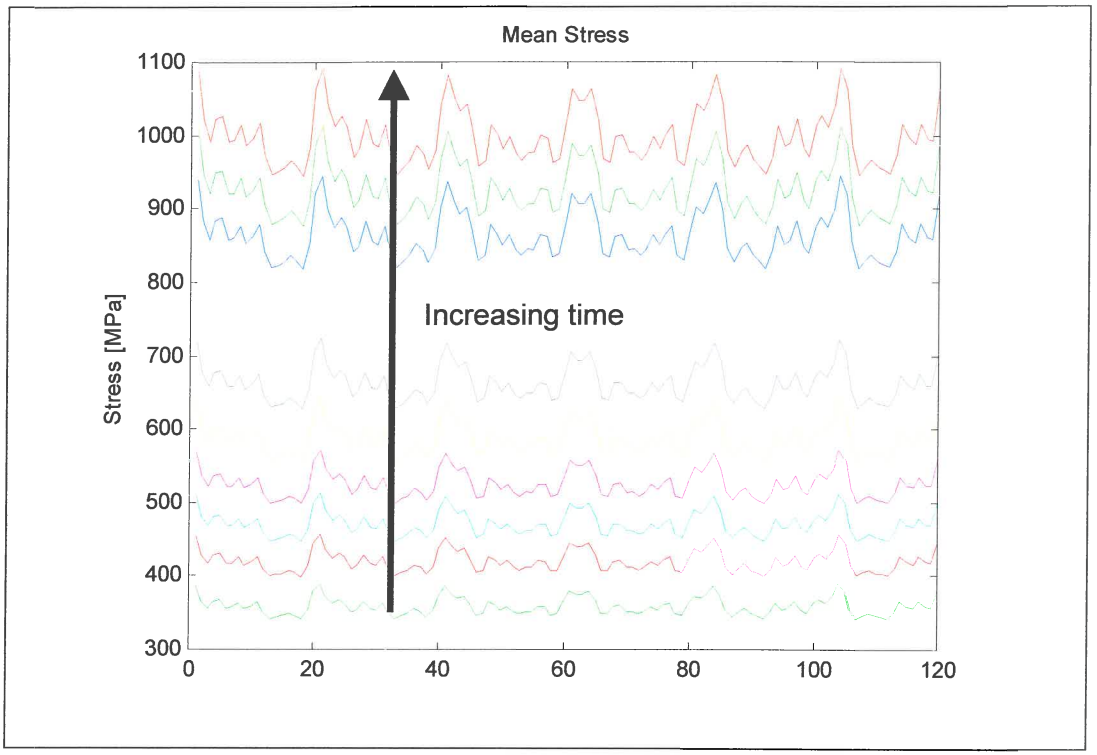

Figure 6.8. Mean stress (σ_m) versus time

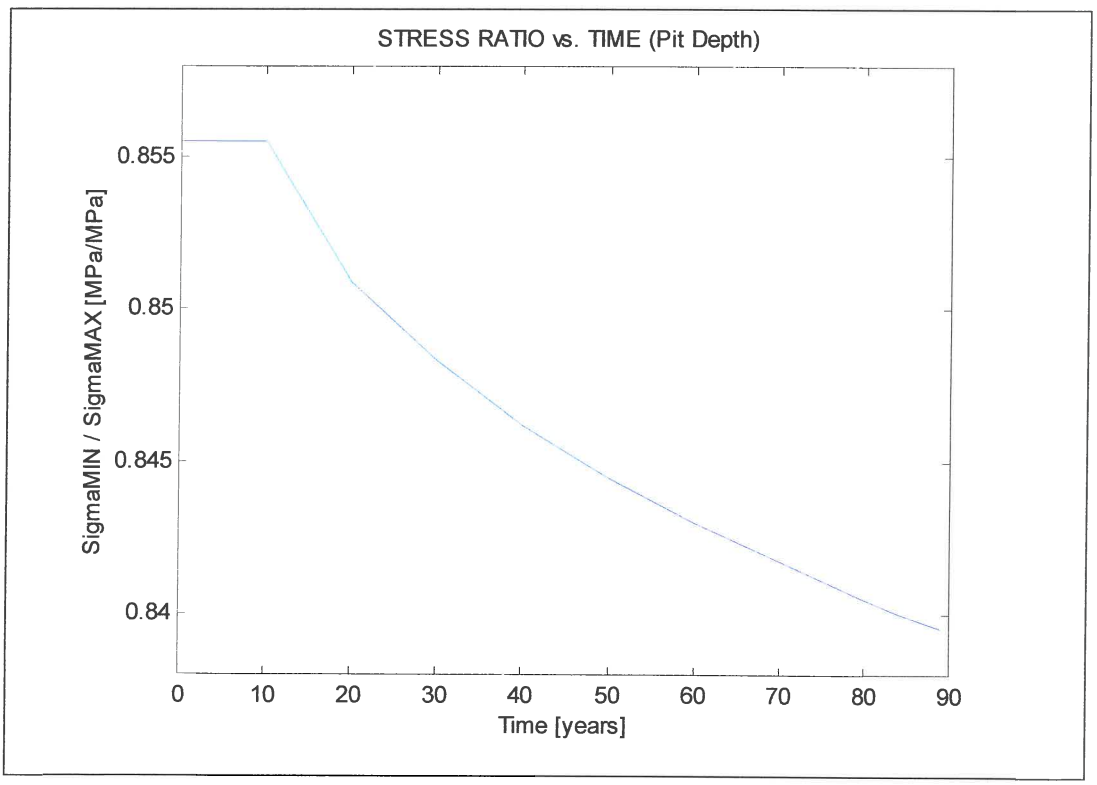

Figure 6.9. Dependence of stress ratio (R) on time

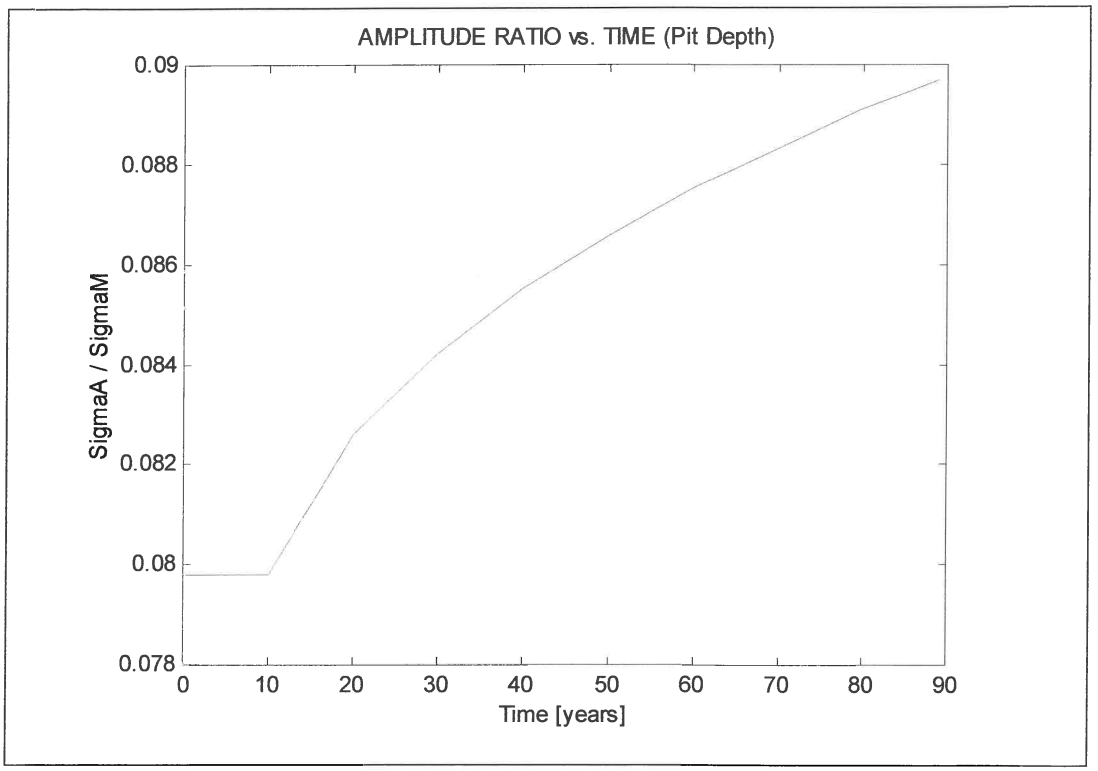

Figure 6.10. Dependence of amplitude ratio (A_r) on time

2. In order to demonstrate the dependence of expected life on internal pressure, the internal pressure (showed in Figure 6.3) was multiplied by an amplitude-modifying constant C. The internal pressure was adjusted as follows: $P' = C \times P$. The value of C was varied in steps of 0.25 between 0.5 and 2.25 and the expected life was calculated. The results are shown in Figure 6.11. It is clear that, for $C \leq 0.75$, the expected life of the pipe remains constant. In this region, the stresses are too low to cause any real fatigue damage and the life expectancy of the pipe is dominated by corrosion. In the region where $C \geq 2$, the stresses are extremely large and the life is dominated by low-cycle fatigue. The expected life is almost linear in the region $0.75 \leq C \leq 2$.

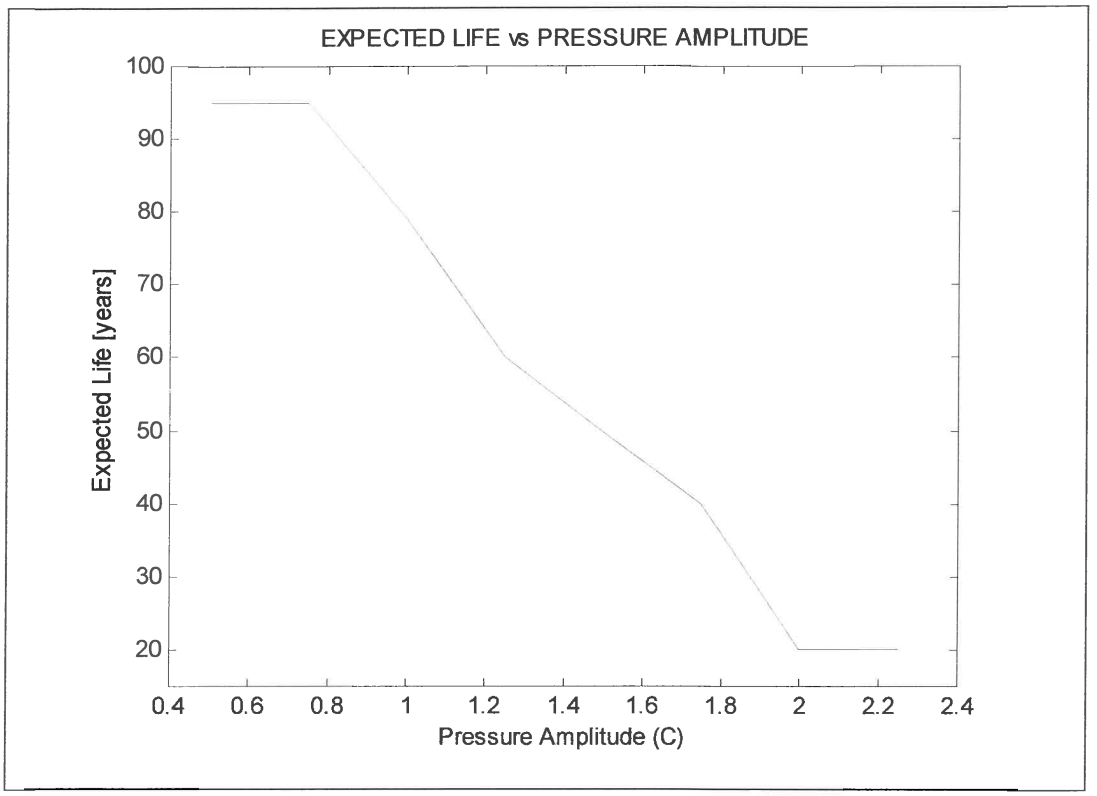

Figure 6.11. The influence of internal pressure on expected life

3. An important quantity regarding a function's sensitivity to its variables is the function's gradient vector. The gradient of a function (in this case $Life = F(T, \underline{x})$, where T = time and $\underline{x}$ = system variables) can be defined as:

$$J = \left[\frac{\partial F(T,\underline{x})}{\partial x_1} \quad \frac{\partial F(T,\underline{x})}{\partial x_2} \quad \frac{\partial F(T,\underline{x})}{\partial x_3} \quad \ldots\ldots \quad \frac{\partial F(T,\underline{x})}{\partial x_n} \right]^T \qquad (6.4.1)$$

Due to the life function's numerical nature, the gradient is determined by means of forward divided differences. The i^{th} entry in the gradient vector can be determined through:

$$J(i) = \frac{F(T,[x_1 \quad \ldots\ldots \quad x_i + \delta \quad \ldots\ldots x_n]) - F(T,\underline{x})}{\delta} \qquad (6.4.2)$$

The value of δ is taken at 1×10^{-4} of the magnitude of the specific variable. The entries of the gradient vector are listed in Table 6.2.

Table 6.2. Entries of the Gradient vector

Symbol	Description	Gradient entry
$\frac{\partial F(T,\underline{x})}{\partial r}$	Pipe radius	-1.5685 x 10^{3}
$\frac{\partial F(T,\underline{x})}{\partial t}$	Pipe-wall thickness	-1.1203 x 10^{5}
$\frac{\partial F(T,\underline{x})}{\partial k_m}$	Bending moment coefficient	-3.3372 x 10^{6}
$\frac{\partial F(T,\underline{x})}{\partial C_d}$	Calculation coefficient	-5.9411 x 10^{5}
$\frac{\partial F(T,\underline{x})}{\partial \gamma}$	Unit weight of soil	-4.1494 x 10^{10}
$\frac{\partial F(T,\underline{x})}{\partial B_d}$	Width of ditch	-1.0319 x 10^{3}
$\frac{\partial F(T,\underline{x})}{\partial E}$	Young's modulus	-3.9016
$\frac{\partial F(T,\underline{x})}{\partial k_d}$	Deflection coefficient	-7.2614 x 10^{6}
$\frac{\partial F(T,\underline{x})}{\partial \nu}$	Poisson's ratio	-2.6141 x 10^{6}
$\frac{\partial F(T,\underline{x})}{\partial \alpha}$	Thermal expansion coefficient	-6.7028 x 10^{10}
$\frac{\partial F(T,\underline{x})}{\partial \Delta\theta}$	Temperature differential	-7.8423 x 10^{4}
$\frac{\partial F(T,\underline{x})}{\partial \chi}$	Longitudinal curvature	7.8423 x 10^{11}
$\frac{\partial F(T,\underline{x})}{\partial K'}$	Cyclic-strength coefficient	-5.8656 x 10^{2}
$\frac{\partial F(T,\underline{x})}{\partial n'}$	Cycling strain-hardening exponent	-3.4700 x 10^{6}
$\frac{\partial F(T,\underline{x})}{\partial \sigma_f'}$	Fatigue-strength coefficient	-7.0206 x 10^{2}

Table 6.2. Entries of the Gradient vector (Continued)

$\frac{\partial F(T,\underline{x})}{\partial b}$	Fatigue-strength exponent	7.1295 x 10^6
$\frac{\partial F(T,\underline{x})}{\partial \varepsilon_f{}'}$	Fatigue-ductility coefficient	-2.3202 x 10^6
$\frac{\partial F(T,\underline{x})}{\partial c}$	Fatigue-ductility exponent	1.6338 x 10^6
$\frac{\partial F(T,\underline{x})}{\partial k}$	Multiplying constant	-3.2800 x 10^6
$\frac{\partial F(T,\underline{x})}{\partial n}$	Exponential constant	-1.1529 x 10^6

Table 6.2 indicates that the expected life of the pipe is fairly sensitive to variations in most of the variables. However, surprisingly, it is almost totally insensitive to changes in the modulus of elasticity (E). One reason for this phenomenon is the fact that large strains are present in the pipe material at final failure. These strains are a superposition of elastic and plastic strain components. Since the elastic strain is only a small part of the total strain at failure, the stress in the material is therefore driven by the plastic strains in the material. The modulus of elasticity describes the slope of the stress-strain curve in the elastic region only. Therefore, it can be argued that, at final failure, the life function becomes insensitive to changes in the modulus of elasticity. This also indicates the necessity of using a fatigue model that is valid at high strain values (i.e. the strain-life method).

6.5. Determining the probability of failure through simulation

Until now, time has been spent on the development of a model that predicts the life expectancy of a pipe that is subjected to the combined effects of fatigue and external corrosion. However, as argued previously, any variation in the system variables will have an effect on the expected life of the pipe. These variations are statistically described through the mean values and coefficients of variation of the variables (as given in Table 6.1). The coefficients of variation were obtained from various texts or were based on experience.

It may be very difficult to construct a limit state function for the fatigue problem. Instead, the variables can be adjusted in a similar fashion to that used in a Monte Carlo simulation. For each trial, the expected life is predicted and recorded. The data obtained through the simulation is then used to construct a statistical distribution function, and the probability density function can be obtained. In Figure 6.12, the cumulative damage functions ($D_{CUM}(T)$) are shown for 150 trials conducted. Figure 6.13 shows the life expectancy of the pipe determined during the trials. A histogram of the expected life of the pipeline is shown in Figure 6.14. A Weibull distribution function has been constructed from the pipeline's expected life data and is shown in Figure 6.15. The cumulative distribution function (which indicates the probability of pipe failure) is obtained by integrating the distribution function and can be seen in Figure 6.16.

It can be seen that the probability of failure is 20 % for an expected life of 50 years. Conversely it can be said that an 80 % probability exists that the pipe will not fail within 50 years of service. The pipe is deemed to be 80 % reliable after 50 years of service.

Similarly, the maximum corrosive penetration that can be allowed (so that the reliability never falls below 80 %) can be determined from Figure 6.2 to be approximately 3 mm. The minimum wall thickness that can maintain a reliability of 80 % is, therefore, 4 mm.

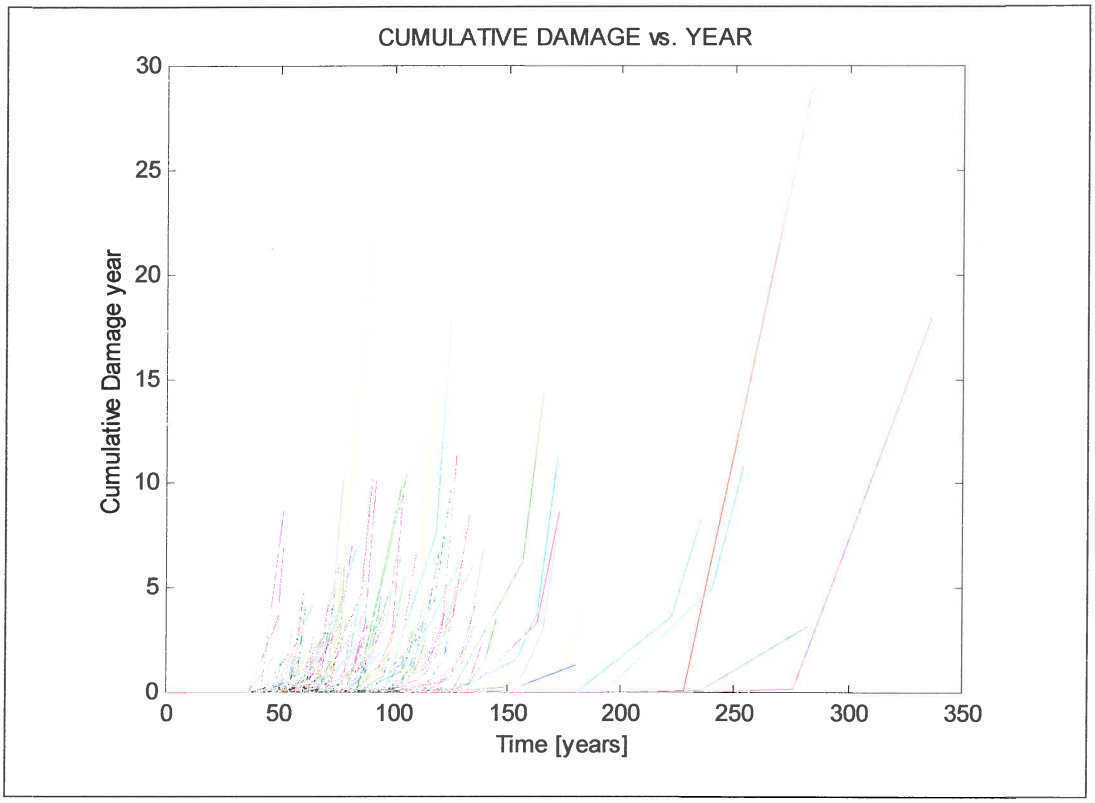

Figure 6.12. Cumulative damage functions for 150 trials

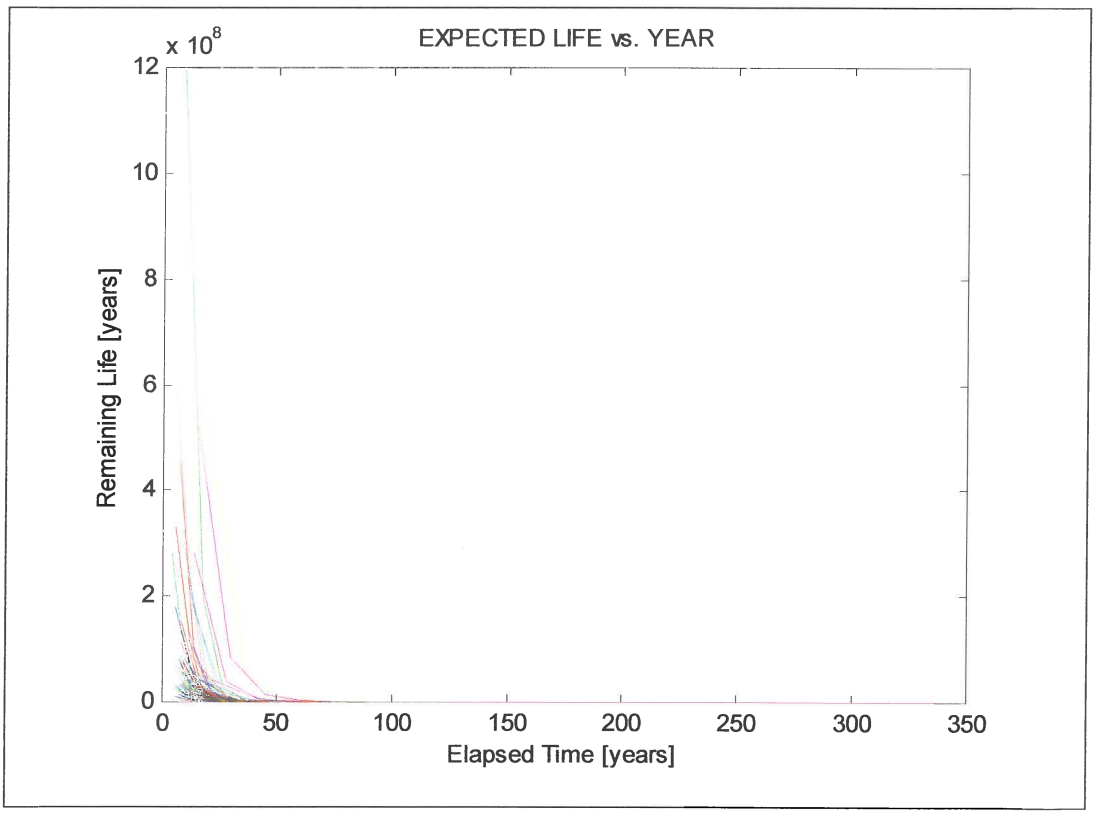

Figure 6.13. Expected life for 150 trials

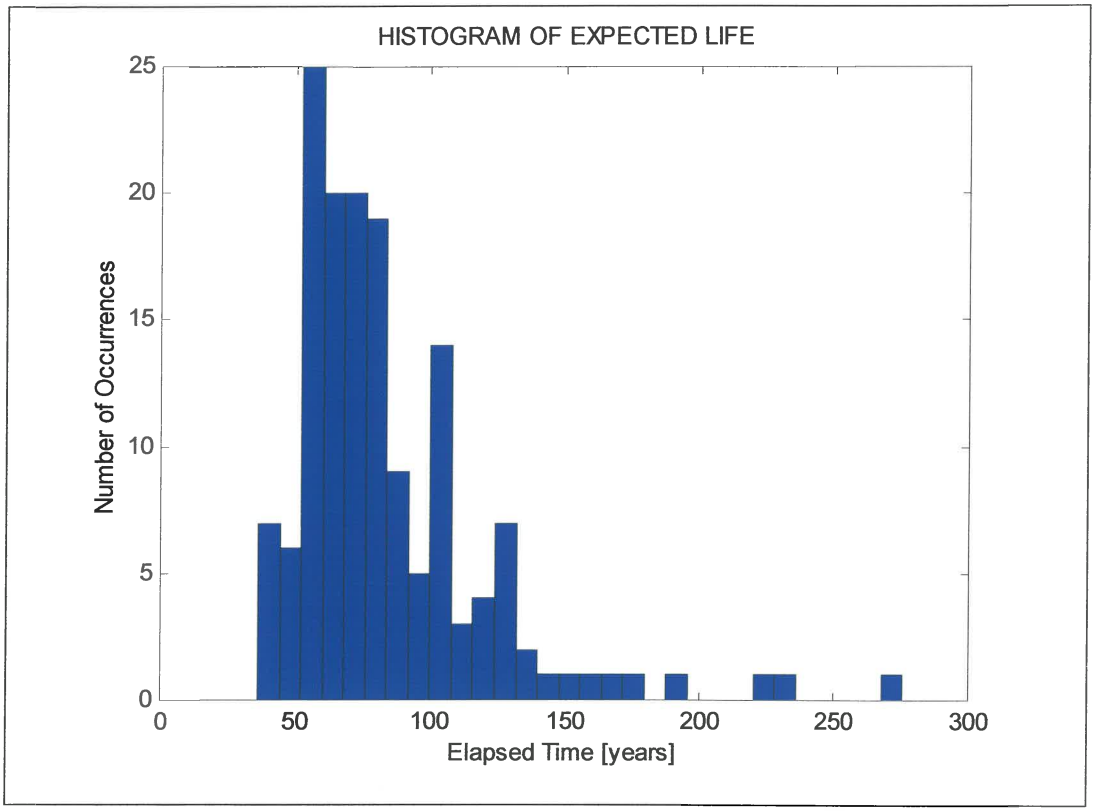

Figure 6.14. Histogram of expected life data

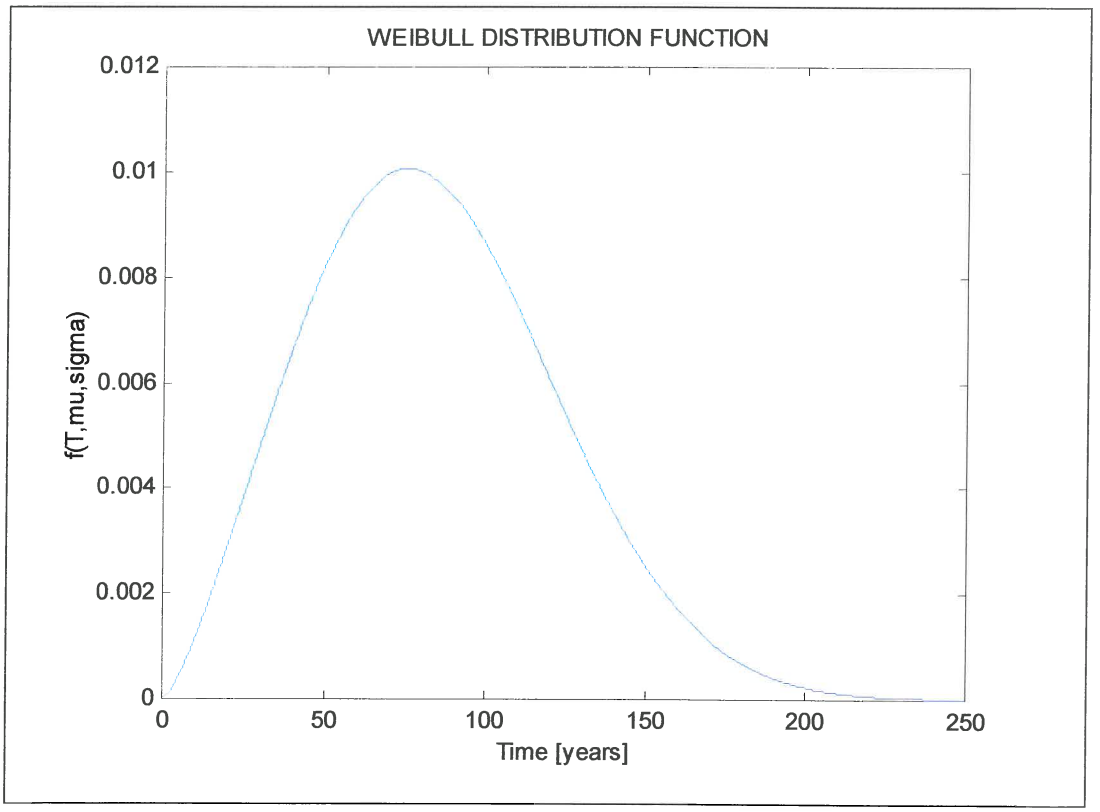

Figure 6.15. Weibull distribution of expected life data

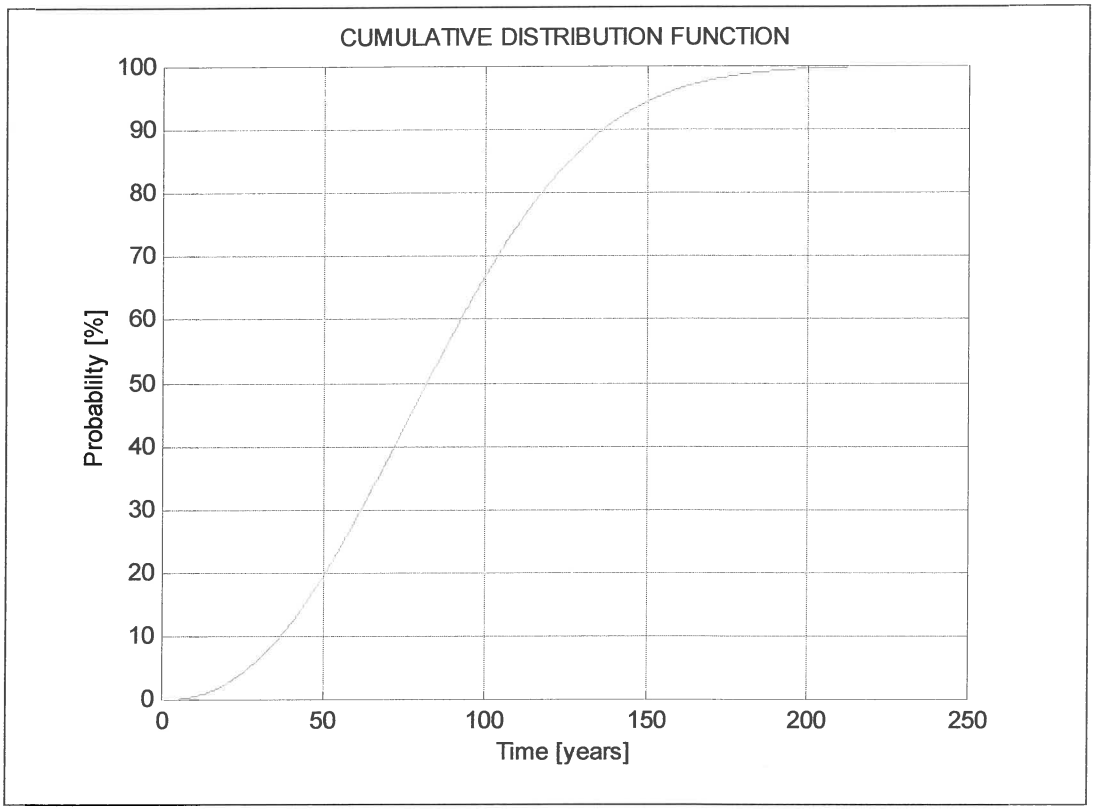

Figure 6.16. Cumulative distribution function

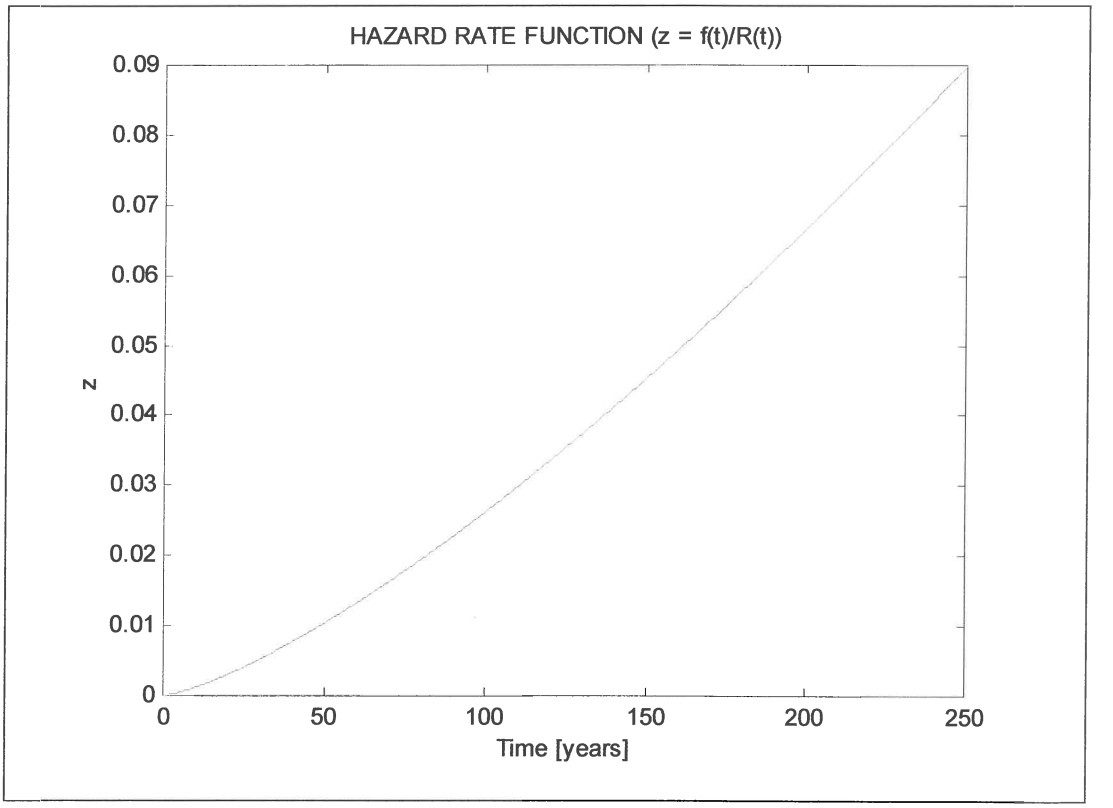

Figure 6.17. Hazard rate function of pipe versus elapsed life

The hazard rate function, which is defined as the distribution function divided by the reliability function,

$$z_H(T) = \frac{f(T)}{1 - \int_{-\infty}^{T} f(T)dT},$$

is shown in Figure 6.17. The hazard rate function is also known as the momentary probability of failure and it gives the probability of pipe failure at a certain age, given that it has survived up to that age. It is a measure of the risk of failure of the pipe at a specific age. Since it is clear from Figure 6.17 that the hazard rate increases with time until pipe failure, use-based preventative maintenance will certainly be a maintenance option (Coetzee, 1997:62). This implies that the maintenance plan put in place for the pipe should have the following qualities:

- the maintenance plan must take the life history and expected future use of the pipeline into account (i.e. is "use based"), and
- the maintenance plan must take a preventative standpoint with respect to failure. This means that failures need to be prevented. Furthermore, this implies that corrective maintenance (i.e. maintenance only in the case of failure) would not suffice.

6.6. Reducing the complexity of the stress equations

The relative contributions of the loads were discussed in Section 4.4. It was indicated that internal pressure accounts for 61 % of the total stress in the pipe wall and that the Poisson effect accounts for 18.3 % of the total stress in the pipe wall.

In this section the probability of failure is determined in a similar manner to that employed in Section 6.5. However, the stresses used in this simulation are reduced to the following:

6.6.1. Circumferential stresses

$$\sigma_{c1} = \frac{pr}{t - k(T-10)^n} \qquad (6.6.1)$$

6.6.2. Longitudinal stresses

$$\sigma_{l1} = \frac{vpr}{t - k(T-10)^n} \qquad (6.6.2)$$

The equivalent Von Mises stress is equal to:

$$\sigma_{eq}^2 = \sigma_{c1}^2 - \sigma_{c1}\sigma_{l1} + \sigma_{l1}^2 \qquad (6.6.3)$$

The results obtained through simulation are shown in Figures 6.18 to 6.23. It is clear that the histogram of the reduced-stress simulation (Figure 6.20) differs from that of the original (unreduced) simulation (Figure 6.14). However, the differences are so small that there is hardly any difference between the Weibull distribution functions of the two simulations (Figures 6.15 and 6.21). Consequently, the probability of failure and the hazard rate functions are almost exactly the same for the two simulations (Figures 6.16 and 6.17, and Figures 6.22 and 6.23).

This is a peculiar result since one would expect that the probability of failure would be lower for a component that is subjected to lower stresses. This is true. However, the result merely implies that the resolution of the mathematics used to describe the probability of failure is not high enough to mirror the principle that a component that is subjected to lower stresses would have a lower probability of failure.

On the other hand, it can be seen that the reduced-stress model errs on the side of caution. Therefore, it would be safe to use the reduced-stress model and would be advantageous in the following respect:

The number of variables and coefficients to be determined is reduced and the time spent on pre-processing can be cut down. This has a direct influence on the costs involved in the analysis.

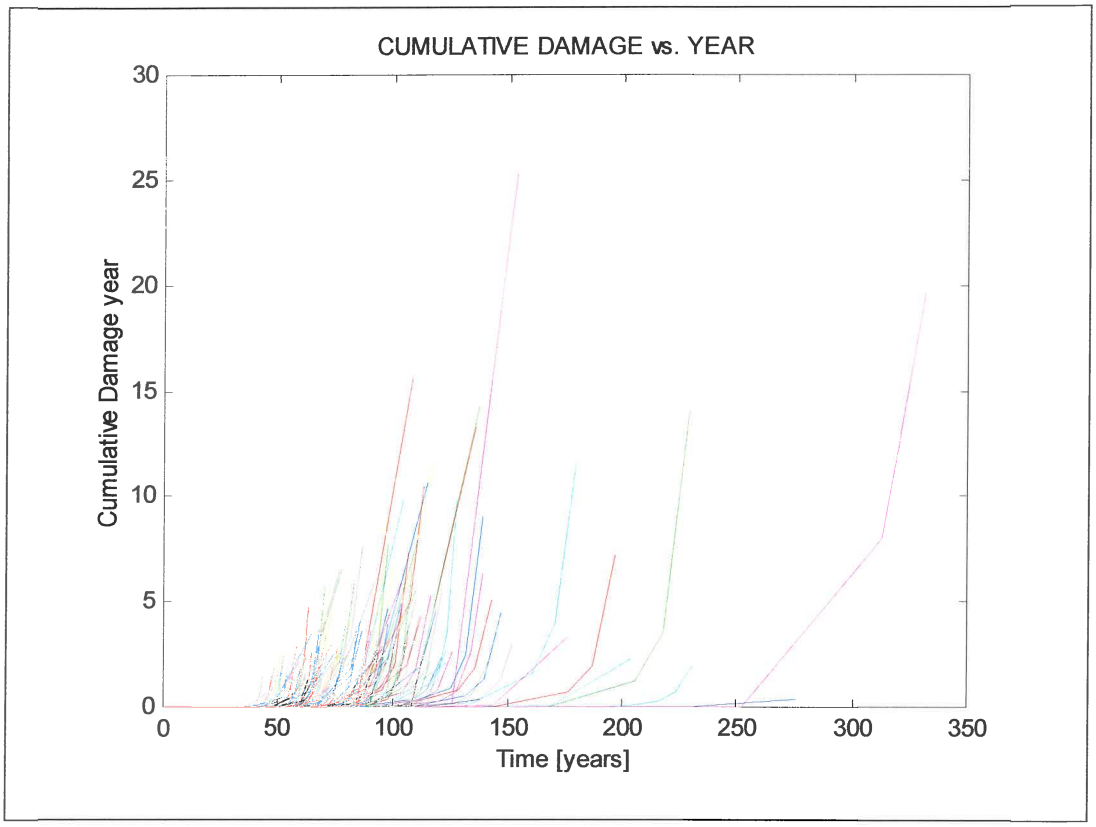

Figure 6.18. Cumulative damage functions for 150 trials

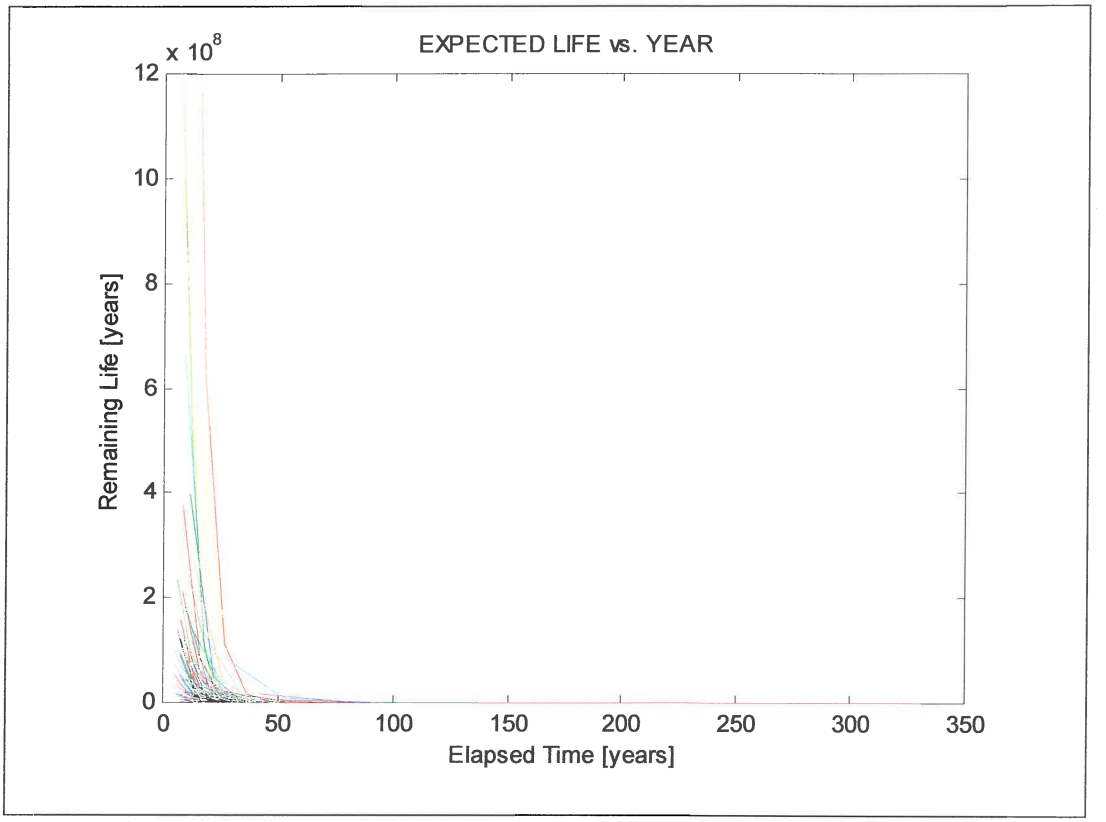

Figure 6.19. Expected life for 150 trials

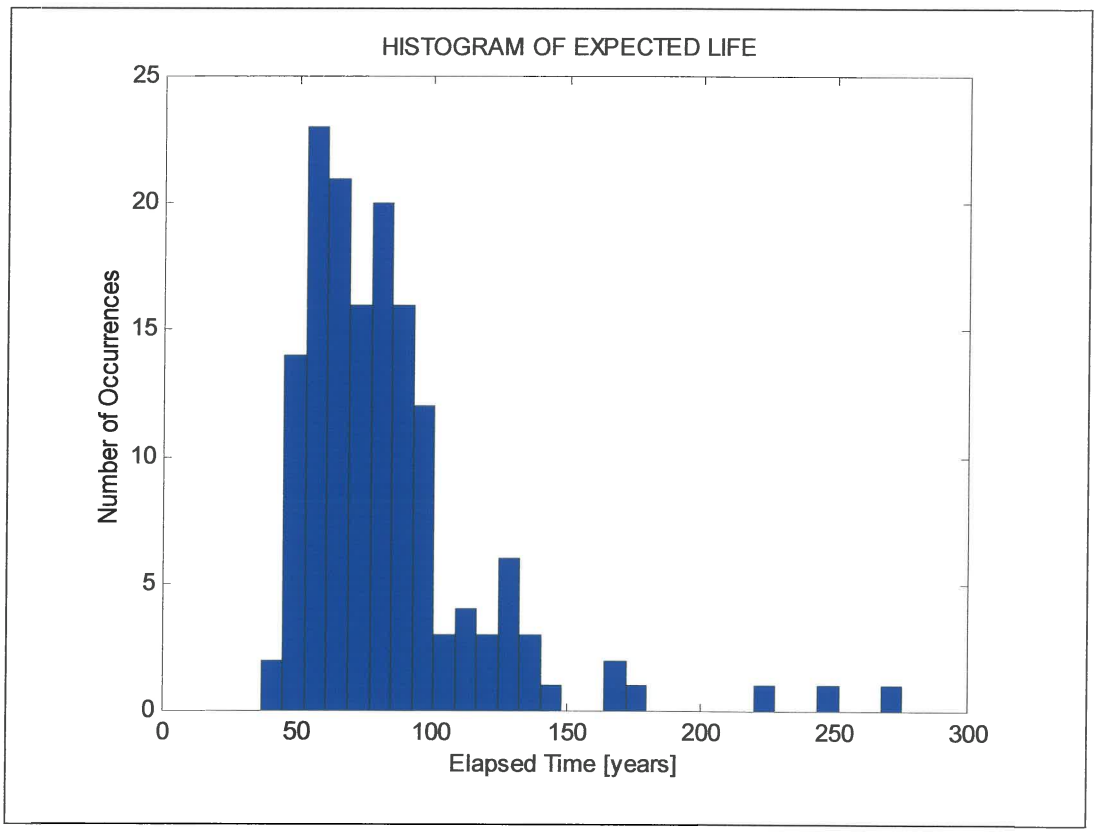

Figure 6.20. Histogram of expected life data

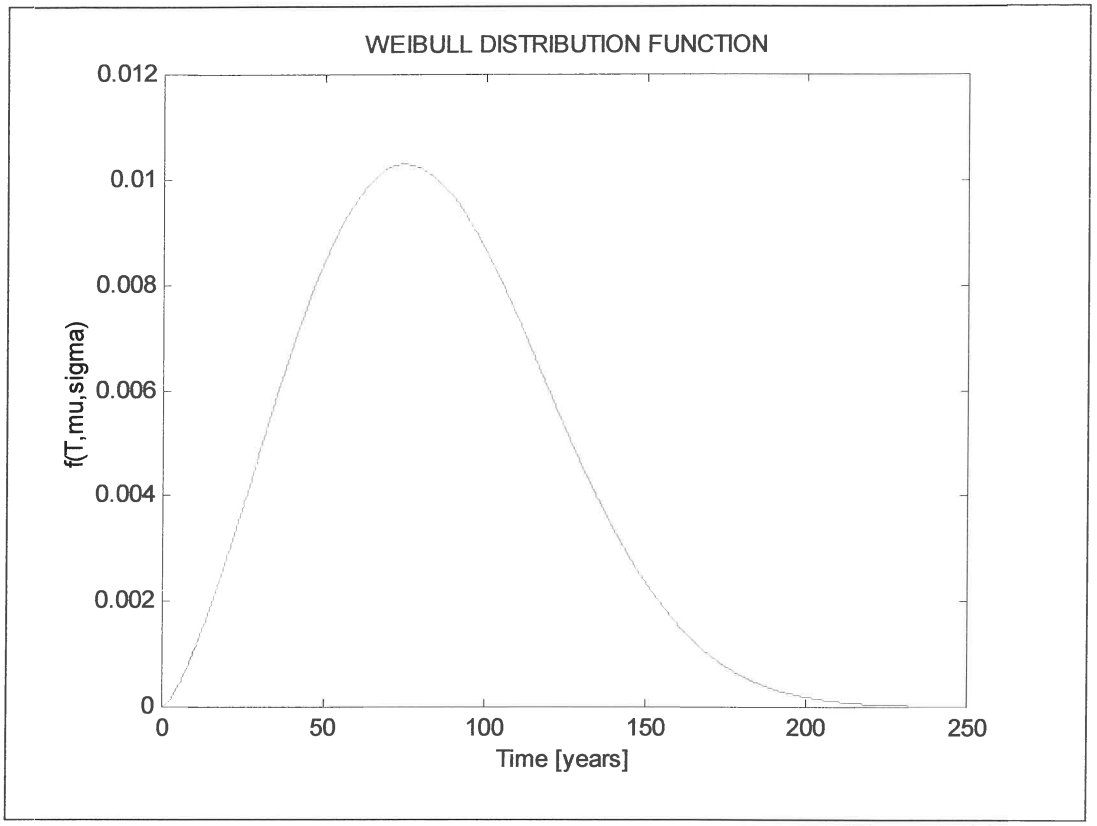

Figure 6.21. Weibull distribution of expected life data

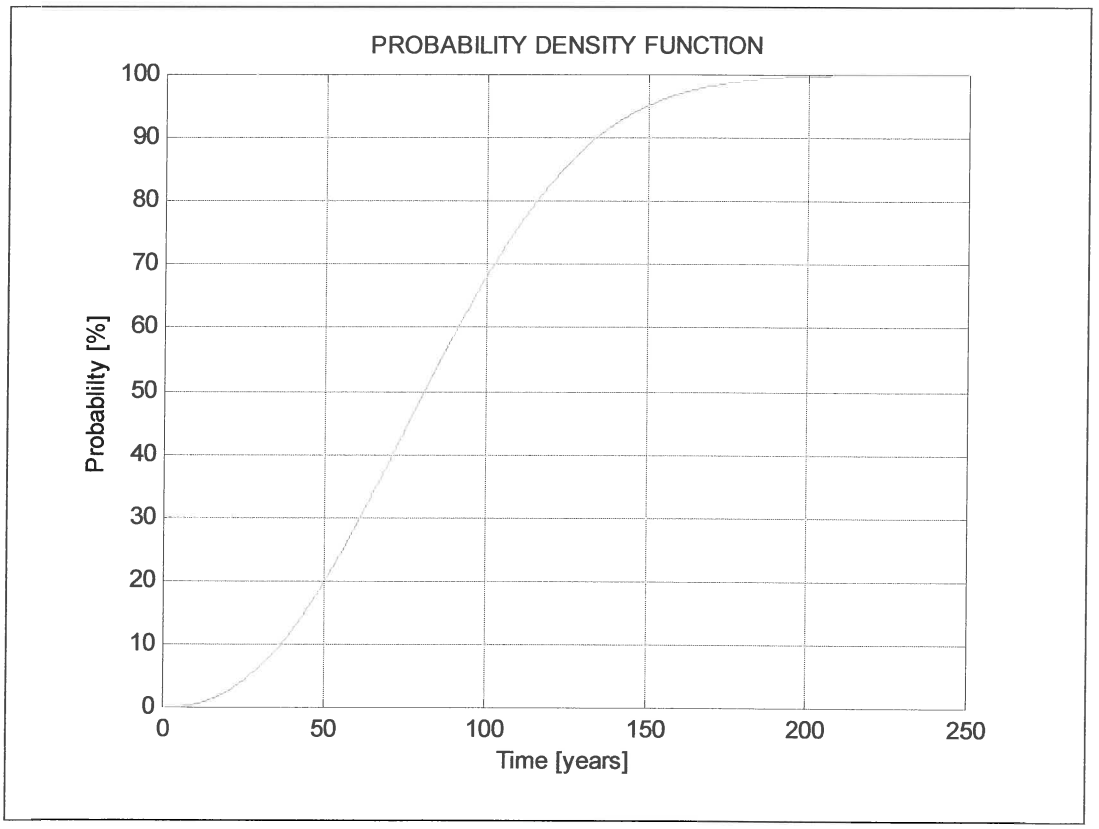

Figure 6.22. Cumulative distribution function

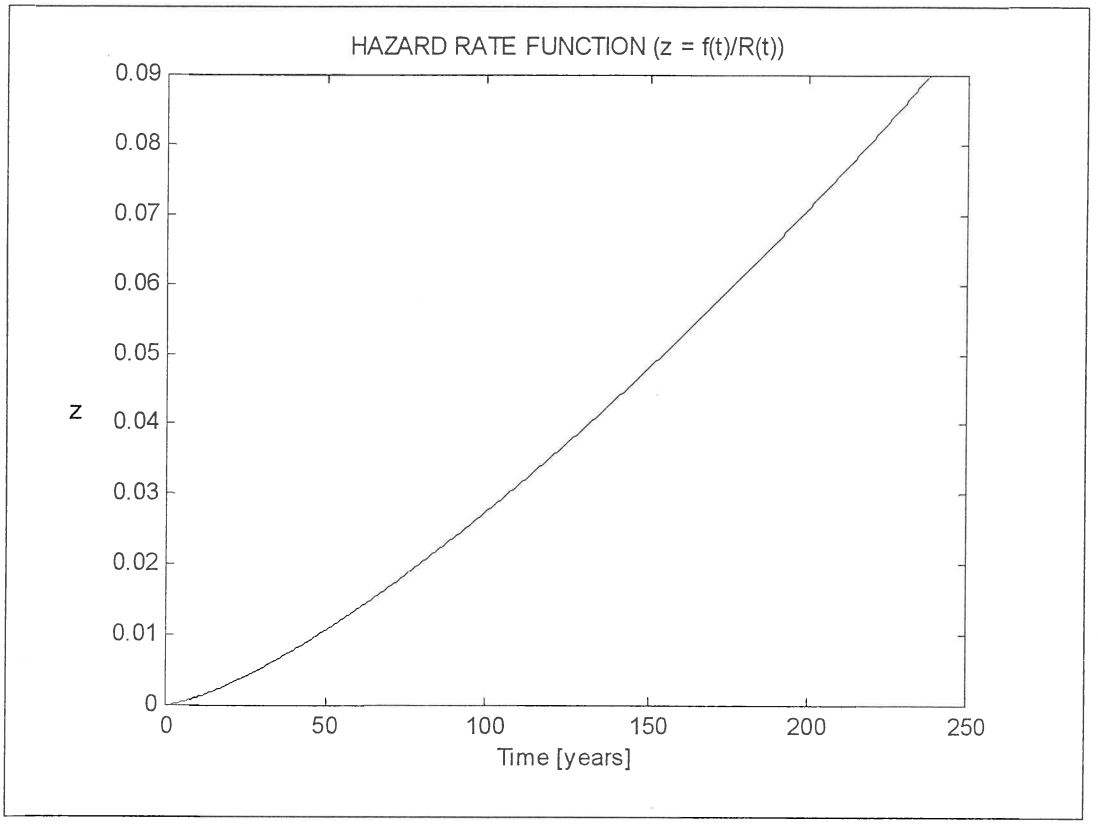

Figure 6.23. Hazard rate function of pipe versus elapsed life

6.7. Conclusion

In this chapter, the pipe stresses were expressed as functions of time. Through the use of the Von Mises failure criteria, the equivalent tensile stress in the pipe wall was determined. By using a strain-based fatigue model, the expected life of a generic pipe, which is subjected to the combined effects of external corrosion and material fatigue, was determined.

The corrosion model allowed for a delay period in which no corrosion occurred. The sensitivity of the expected life function to changes in the system variables was determined through the evaluation of the gradient vector of the expected life function ($Life = F(T, \underline{x})$). The necessity of using a strain-based fatigue model was indicated.

Monte Carlo simulation principles were employed to model the statistical variations in the system variables. The result of the simulation was a failure probability that is time dependent. Since the wall thickness of the pipe is also time dependent, a direct, non-linear, relationship between the probability of pipe failure and wall thickness exists. Thus, for a specific pipe reliability, the critical wall thickness (and of course the expected pipe life) is fixed.

The expected life function ($F(T,\underline{x})$) is primarily a function of the remaining stress-bearing material and the model proposed in this chapter could easily be extended to account for the effects of internal corrosion. The internal corrosive penetration can be modelled through the following equation:

$$P_i = k_i T^{n_i} \qquad (6.7.1)$$

where k_i and n_i are the corrosion parameters that describes the internal corrosive penetration. The stress equations in Section 6.3 can be adjusted by incorporating Equation 5.6.1. As an example, the first component of the circumferential stress could be written as:

$$\sigma_{C1} = \frac{P(r + k_i T^{n_i})}{t - (k(T-10)^n + k_i T^{n_i})} \qquad (6.7.2)$$

7. INTEGRATION OF CONCEPTS IN ORDER TO DETERMINE THE REMAINING LIFE OF AN UNDERGROUND PIPE NETWORK

7.1. Introduction

Until now, the main focus has been on the development of a mathematical model that is able to predict the reliability of a section of a pipeline that is subjected to the combined effects of internal pressure and external corrosion. By altering the relevant stress equations in the predictive model, the reliability of other piping components that exists in the network (such as bends and T-junctions) can be predicted.

What still remains to be done in order to pass judgement on the reliability of the whole pipe network, is to integrate the concepts that were discussed in the previous chapters into a singular, corrosion-based plan. Since the development of a complete mathematical model that is able to predict the reliability of the whole pipe network is not only formidable, but may even prove to be impossible, it is necessary to develop a corrosion-based plan.

The life expectancy of a section of pipe that is subjected to the combined effects of corrosion and internal pressure is mainly a function of the stresses present in the load-carrying material (i.e. the pipe wall). These stresses are dependent on the wall thickness of the pipe. Two parameters, k and n, describe the corrosion rate. The main reason for following a reliability approach is that the corrosive penetration varies from position to position and is not constant over the length of the section of pipe under investigation.

In order to determine the corrosion parameters, it is necessary to monitor the wall thickness of the pipe as it varies with time. In Chapter 2, it was suggested that a first-order approximation of the corrosion equation could be made if only two data points were available. This is not ideal, but by following the simulation approach, the uncertainty associated with the corrosion rate was accounted for.

The data points used to construct the penetration equation can only be obtained through physical measurement of either the corrosion rate (Tafel extrapolation) or of the wall thickness at a specific time and position. It should be noted that it is impossible to measure the wall thickness of the pipe at every position in the network.

The main objective of the corrosion-based plan is to identify critical areas in the network where the probability of system failure, at a specific time, is greater than that which is acceptable. Critical areas can be seen as the "weak links" in the network – areas where potential failure is of definite concern and of certain probability. By monitoring the corrosion rate and the condition of the pipe at the critical areas, the cost of analysis can be greatly reduced.

The magnitude of acceptable system reliability depends on various parameters. If the network must conform to certain technical standards and specifications, it can be expected that a maximum stress-level in the material, or a minimum wall thickness, will be specified. This wall thickness corresponds to a certain life expectancy and a specific reliability index.

However, if the network is not expected to conform to technical standards and specifications, the level of acceptable reliability will depend on company policy. If the required reliability is too high, it may result in the premature decommissioning of the pipe network (which is costly and unnecessary). On the other hand, specifying low reliabilities may result in unforeseen failures that can lead to frequent periods of downtime, loss of product and loss of income.

In this chapter, a procedure will be presented that should be helpful in the identification of the critical areas. It is not the be all and the end all, but is merely a suggested line of thought, presented through the medium of an illustrative, generic underground pipe network.

7.2. Decomposing the network into representative blocks

Consider the generic underground pipe network shown in Figure 7.1 (the width of the lines are directly proportional to the diameter of the pipe).

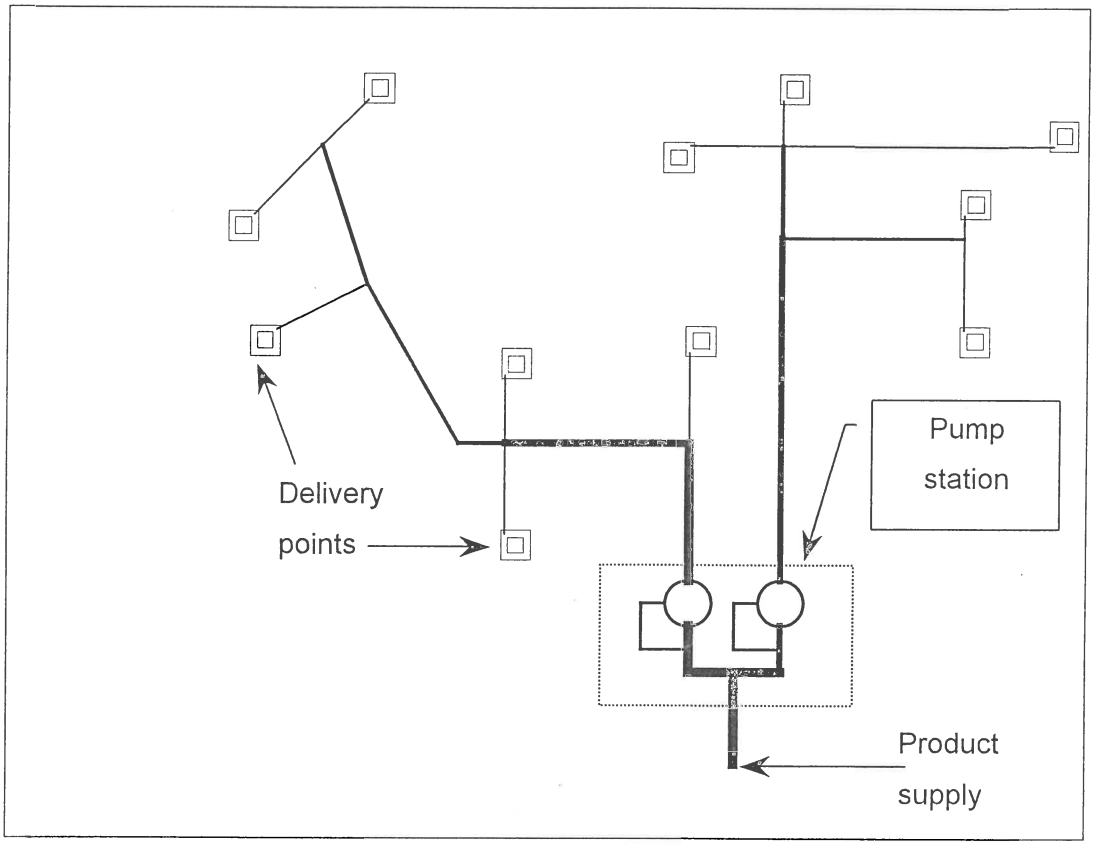

Figure 7.1. Generic underground pipe network

The network consists primarily of straight sections of pipe, and secondarily of pumps, valves, T-junctions and bends. The diameter of the pipes in the network and their respective working pressures do not remain constant over the whole network. The severity of corrosion might be constant in localised areas, but will vary from area to area. In order to predict the reliability of the network as a whole, it is therefore necessary to decompose the network into representative blocks that can be analysed separately.

The following criteria should be satisfied when the network is decomposed into these blocks:

1. the diameter of the section of pipe in the specific block should be fixed;

2. the working pressure of the pipe in a specific block should be nearly uniform (not necessarily constant) throughout its length. The differences in working pressure due to pressure drop effects (i.e. internal friction) can be ignored;
3. if possible, the blocks should be chosen in such a way that the corrosion rate remains nearly constant in the block. The corrosion parameters, k and n, should be representative of the corrosive attack experienced by the pipe, and
4. blocks should include only one type of piping component. Thus, straight sections of pipe and T-junctions should not be allowed in the same block.

Figure 7.2 shows the decomposition of the generic pipe network of Figure 7.1 (the blue circles indicate junctions, and the red ellipses indicate straight sections with approximately the same corrosion rates and service loads).

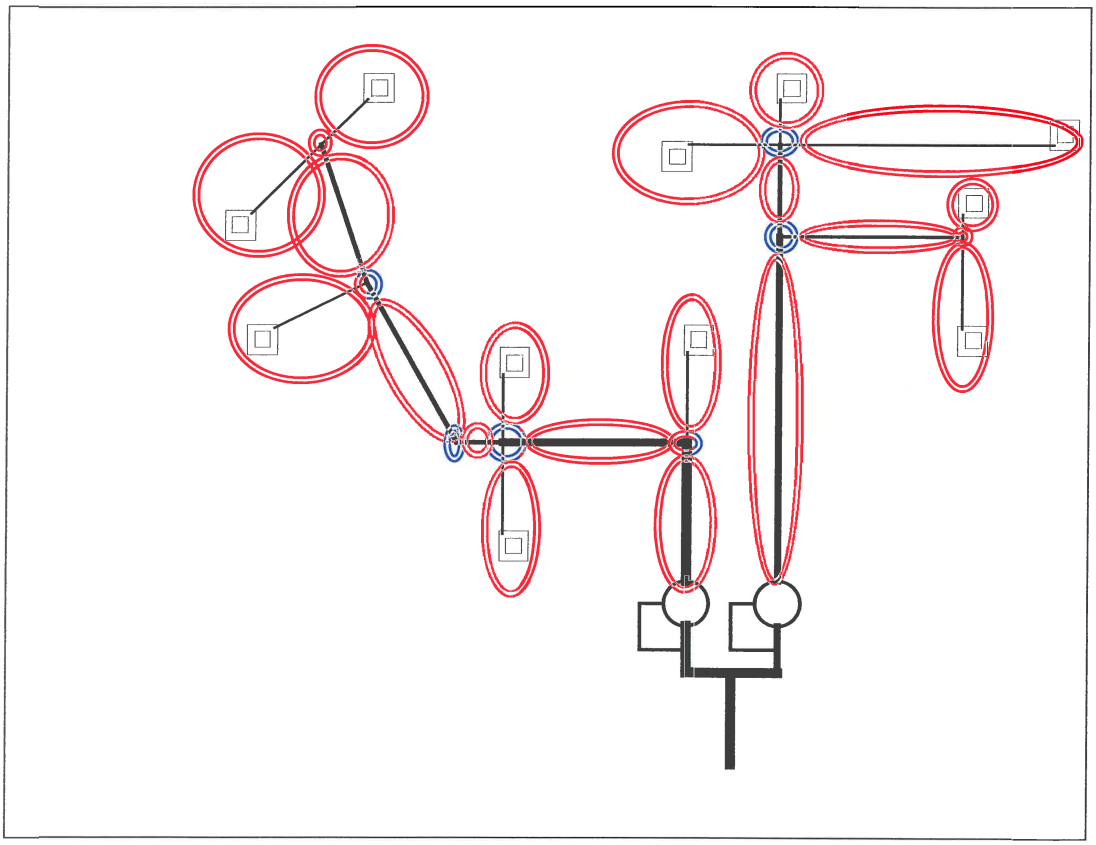

Figure 7.2. Decomposition of generic pipe network into representative blocks

7.3. Failure history

An analysis of the existing failure data of a pipe network is probably the most logical starting point in the process of identifying critical areas. If an adequate amount of failure data is available, the reliability of the network can be determined from basic statistical principles. However, in line with the reasoning that corrosion due to soil exposure is generally a slow process, it can be assumed that the amount of failure data that is required to confidently apply statistical models does not exist.

The sole objective of an analysis of the failure history is to indicate regions in the network where failure has frequently occurred in the past. If failures have occurred frequently in a specific region of the network, and if normal in-service loads caused these failures, it can be deduced that that region is, in fact, a critical area. It is impossible to indicate critical areas in the network if the failures are scattered randomly over the network.

An analysis of the existing failure data should reflect the following aspects:

1. the specific position where the failure occurred in the network should be documented;
2. an effort should be made to identify the cause of the specific failure. Failures caused by negligence (such as damage caused by drilling equipment) cannot be taken into account since they are not normal in-service loads, and
3. since important information can be obtained from the inspection of the area of failure, the region in the vicinity of the failure should be carefully inspected. By measuring a series of wall thicknesses in the vicinity of the failure, a great amount of data can be obtained that might be useful in determining the corrosion parameters, k and n. Subjective evaluation of the condition of the pipe may also prove to be very useful. If a pipe fails after 10 years in service and it has been observed that the extent of corrosive attack is insignificant, it can be deduced that a) a corrosion initiation period of at least 10 years exists, and b) that corrosion is not the predominant driving force behind failure in that particular region of the network.

7.4. Soil evaluation

As previously stated, a chemical analysis of the soil surrounding the buried pipeline can be used to indicate whether the soil is potentially corrosive towards a cast-iron pipe. These analyses are relatively cheap and might prove to be very helpful in indicating areas where the corrosion rate can be expected to be severe (see Section 3.7). By analysing a few soil samples from each representative block, it is possible to superimpose contours of varying corrosion potential onto a diagrammatic layout of the network, as shown in Figure 7.3.

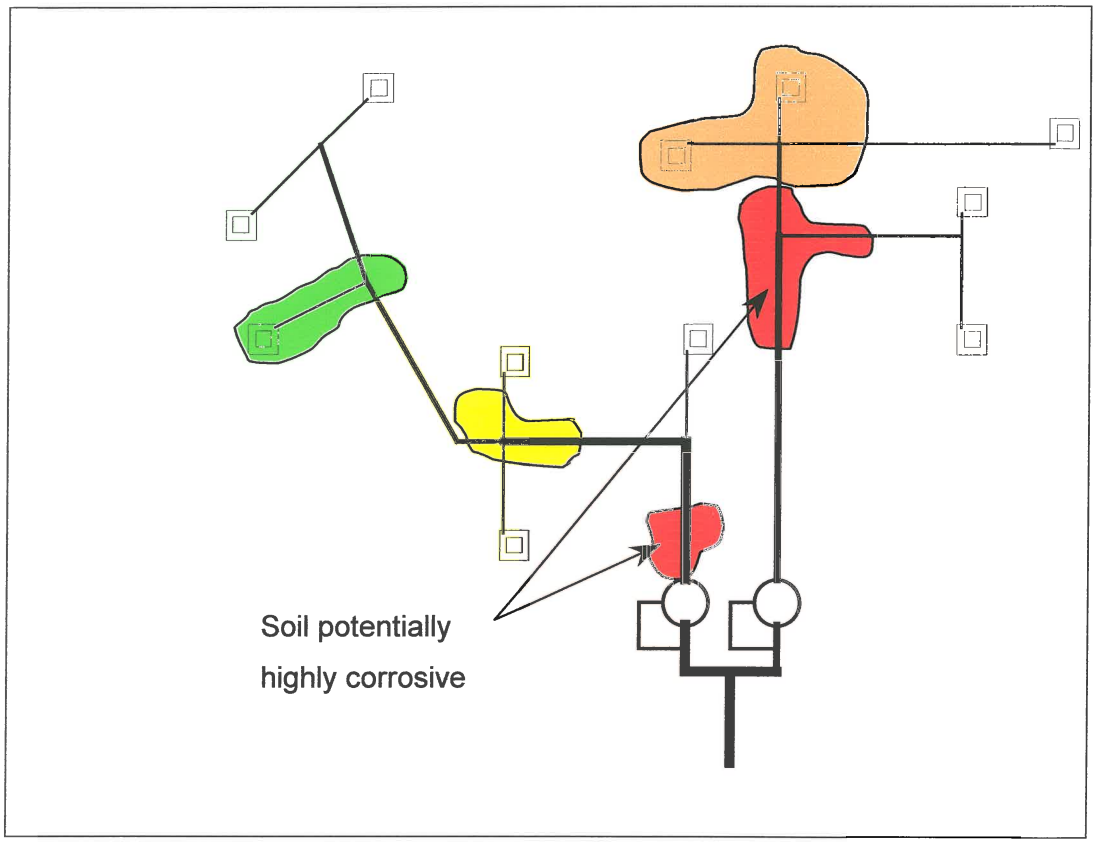

Figure 7.3. Contours of varying corrosion potential

Areas where the soil is potentially corrosive can be identified as critical areas where corrosive attack may be of concern. It might be appropriate to investigate whether these areas correspond in any way to areas where failures (if any) have previously occurred.

7.5. Galvanic areas

Galvanic corrosion was previously defined as the electrochemical process that occurs due to an electrical potential difference that exists between two dissimilar, conducting materials. The electrical contact between the two materials is usually established through a conducting electrolyte (i.e. the soil).

Thus, galvanic corrosion can be expected in areas where the pipe is either in direct or in indirect contact with other metallic structures. Typical examples of areas where galvanic corrosion can be expected are discussed below:

1. Galvanic corrosion might occur at positions where valves, manufactured from different materials than that of the pipe, are in direct contact with the pipe. The pipe will function as the corroding electrode (i.e. the anode) if the valve, which it is in contact with, is manufactured from a material that is more noble than the pipe material. This will happen when a pipe that is manufactured from iron (Fe) is in electrochemical contact with a valve manufactured from copper (Cu). The combined effects of galvanic and soil corrosion will increase the corrosion rate at that position in the network.
2. The basis of galvanic corrosion is the dissolution of the corroding material into its positive ions and into electrons ($M \rightarrow M^{n+} + ne^{-}$). It is a well-known fact that the corrosion rate can be decreased if an electrical current or potential difference is applied to the corrosion system in such a way that it counters the flow of electrons from the corroding anode to the reducing cathode. This method of corrosion prevention is commonly known as cathodic protection. Conversely, an electrical current or potential difference that aids the flow of electrons from the corroding anode to the reducing cathode will increase the corrosion rate. At certain positions in the network it might be possible that such electrical currents are present in the soil, and the corrosion rate at these positions will be increased. This process will occur when the corroding electrode (i.e. the pipe) has a positive potential with respect to the soil current. Therefore, areas where the pipe is in close contact with electrical systems (such as railway tracks and power transmission lines) should be monitored.

7.6. Areas of erosion corrosion

Erosion corrosion was defined as the acceleration of the rate of corrosion due to relative movement between the material and the corrosive. Metal is removed from the corroding surface as dissolved ions or it forms solid corrosion products that are mechanically removed from the surface. Typical areas where erosion corrosion might be of concern are pipe bends and tees (see Figure 7.4).

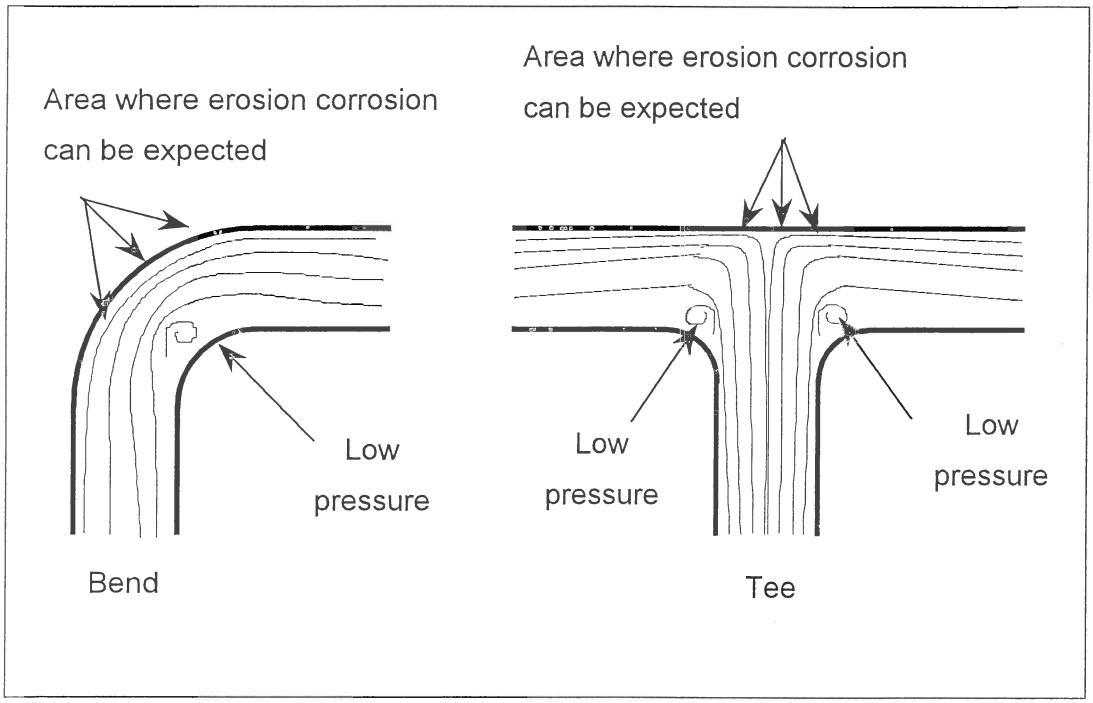

Figure 7.4. Positions in a bend and a tee where erosion corrosion can be expected

The blue lines in Figure 7.4 indicate the streamlines of the fluid. The streamlines are compacted by the momentum change that the fluid experiences in both the bend and the tee. The abrasive action of the fluid in these areas is accentuated by the increase in fluid velocity. The erosion corrosion process is an internal corrosion phenomenon, but a model representative of the combined effects of external and internal corrosion has been proposed in Chapter 6 and, subsequently it should not be difficult to incorporate it into the predictive model.

As was stated in Chapter 2, erosion corrosion can also be expected at the pump impeller, but since the pump itself is not modelled as part of the pipe network in this study, it will not be discussed any further.

7.7. Conclusion

It is impossible to measure or monitor the corrosion rate of the pipe at every possible position in the network. This necessitates the development of some sort of strategy or plan that indicates areas in the network where corrosive attack is problematic. A representative indication of the corrosive attack experienced by the network can be determined by monitoring the wall thickness of the pipe in these areas.

8. PENULTIMATE REMARKS

The following penultimate remarks, regarding the variable distributions and pipe stresses, are presented:

8.1. Revisiting the variable distributions

In Sections 5.6 and 6.5 it was assumed that each of the system variables varies according to the Normal distribution. However, it is not inconceivable that one (or more) of the variables might follow a different statistical distribution. This is, of course, not an unmanageable problem and a methodology for incorporating different statistical distributions is subsequently proposed.

Consider an arbitrary system variable that follows the statistical distribution function shown in Figure 8.1.

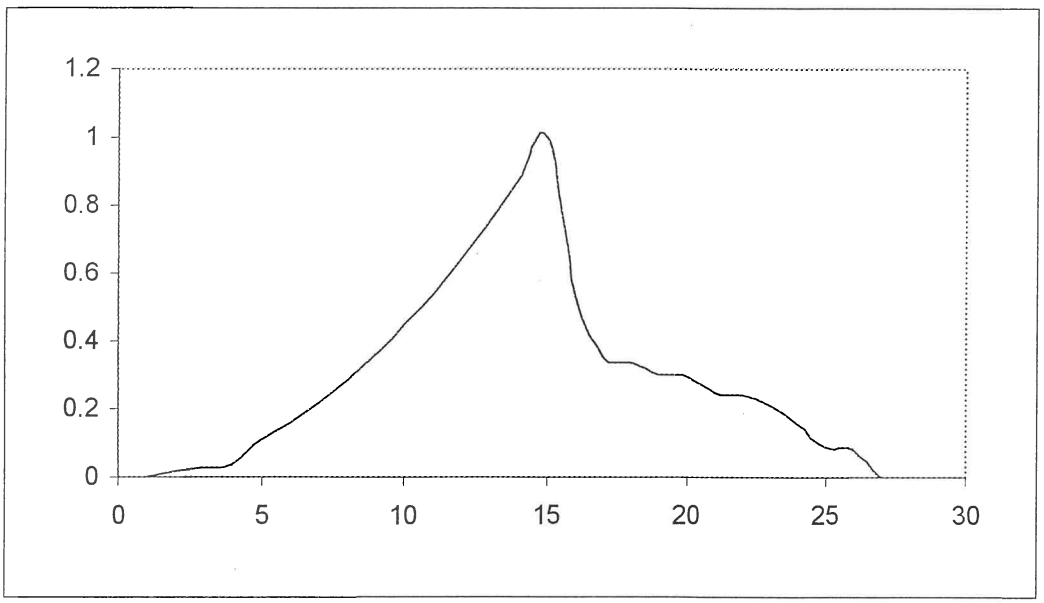

Figure 8.1. Statistical distribution function for an arbitrary system variable

When conducting a Monte Carlo simulation, one relies on the creation of a random number ($0 \leq r_1 \leq 1$) that lies between zero and one. This random number is a random probability draw and corresponds to a certain area

beneath the distribution function shown in Figure 8.1. This is graphically depicted in Figure 8.2.

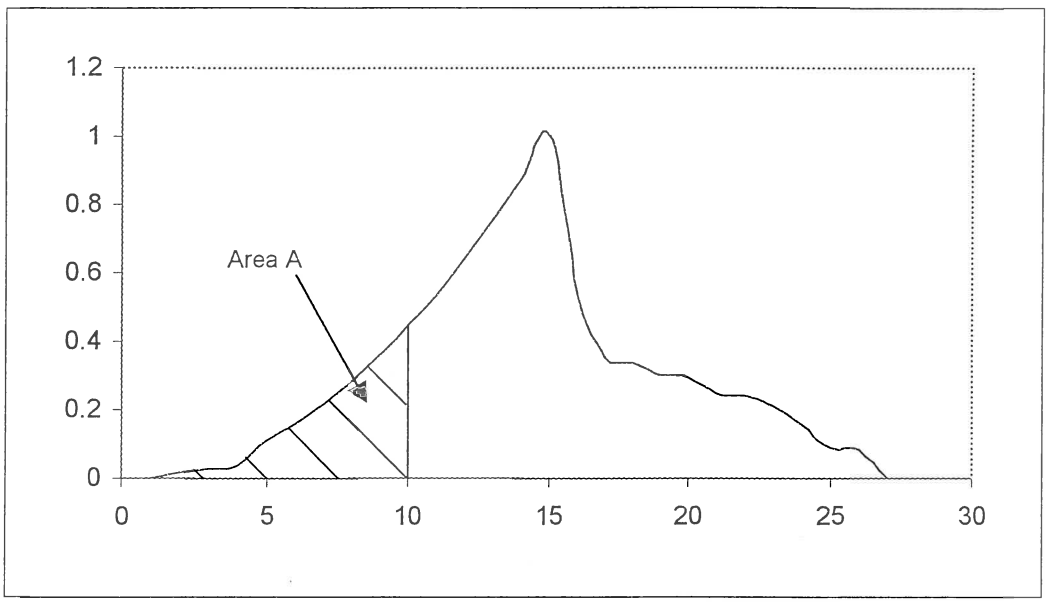

Figure 8.2. The random number as a random probability draw

Thus, the generated random number is equal to area A ($r_1 = A$). This implies that the area beneath the distribution function, between the lower defined limit (x_b) and an unknown upper limit (x_1) should be equal to $r_1 = A$. Formally it can be written as follows:

$$r_1 = A = \int_{x_b}^{x_1} f(x)dx$$

where $f(x)$ is the distribution function shown in Figure 8.2.

The random sampling magnitude created by the Monte Carlo simulation is therefore x_1. Thus, the Monte Carlo sampling point can be determined for any entity that follows any known statistical distribution by solving the above-mentioned integral with an iterative procedure.

8.2. Revisiting the proposed pipe stress relationships

The effects that pitting corrosion and uniform attack have on the stresses present in the pipe wall were approximated in Section 2.6 and presented in Sections 5.3 and 6.3. The modes of failure inherent to the stress states discussed in the above-mentioned sections are the following:

1. the longitudinal tearing of the pipe;
2. the blow-out of the remaining material plug at the pit root, and
3. static or fatigue failure due to the equivalent stress caused by a combination of the above-mentioned modes of failure.

Another noteworthy mode of failure was identified:

Bulging occurs when corrosion causes the pipe wall to thin over a large patch. A significantly large patch of reduced wall thickness behaves as a locally-clamped plate that is subjected to uniform surface pressure, and bending stresses would exist in the material due to bending moments induced on the plate. The author acknowledges this as a possible mode of failure, but feels that, since the pipe is buried, the soil pressure acting on the external pipe surface constrains the corroded patch in the outwardly radial direction and that the proposed plate behaviour might not occur.

Two finite element analyses (FEAs) are presented in this section to verify this statement.

8.2.1. Pit stress verification

A finite element model (FEM) of the generic pipe described in Section 2.6 has created with the following geometrical and load properties:

- the pipe is subjected to an internal pressure (p_i) of 5 MPa;
- the pipe has an internal radius (r_i) of 0.5 m, and
- the pipe has a wall thickness (t_w) of 21 mm.

Three pits, with different depths (see Table 8.1), have been modelled in the pipe wall and the Von Mises stresses solved. The analysis results are shown in Figure 8.3 and indicate that, although the pits have relatively large diameters, no bulging occurred and that the maximum Von Mises stress is approximately 310 MPa. In Section 2.6, the maximum shear stress (Tresca's criterion) present in the pit root was predicted to be in the order of 350 MPa for a pit with a depth of 15 mm. The FEA predicted the maximum Von Mises stress in the vicinity of the pit to be in the order of 310 MPa. An approximate relationship between shear stress and Von Mises stress is the following:

$$\sigma_{eq} = \sqrt{3} \times \tau_{MAX}$$

Based on the FEA results, the maximum shear stress in the vicinity of the pit can be approximated to be equal to:

$$\tau_{MAX}^{FEA} = \frac{\sigma_{eq}}{\sqrt{3}} = \frac{310}{\sqrt{3}} \approx 179MPa$$

Therefore, it can be concluded that, for the specific generic pipe, the stress approximation presented in Section 2.6 is conservative and indicative of the critical failure mode.

Table 8.1. Depths of the three modelled pits

Pit	Diameter [mm]	Depth [mm]
# 1	10	10
# 2	10	15
# 3	10	18

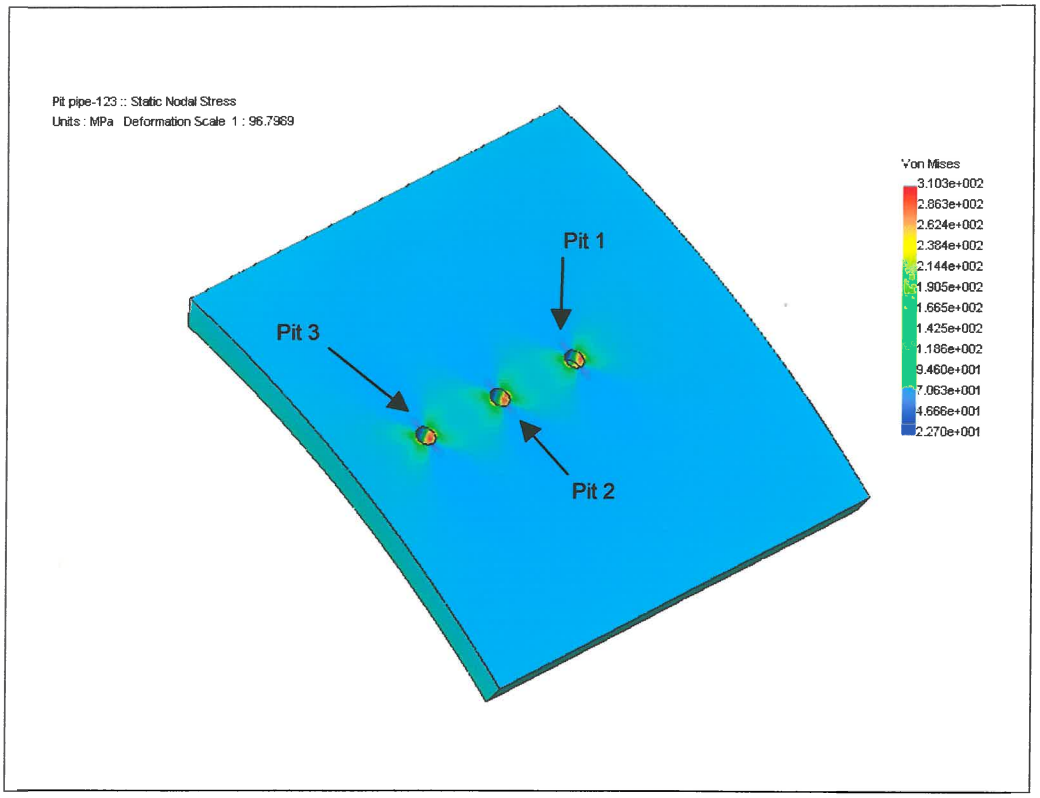

Figure 8.3. FEA results of three pits in a generic pipe

8.2.2. Uniform attack verification

A finite element model (FEM) of the generic pipe described in Section 6.3 has been created with the following geometrical and load properties:

- the pipe is subjected to a mean internal pressure (p_i) of 5 MPa;
- the pipe has an internal radius (r_i) of 0.5 m, and
- the pipe has a wall thickness (t_w) of 7 mm.

In Section 6.3 it was indicated that fatigue failure would become a definite concern when the wall thickness reached 2.7 mm. Quasi-stochastic external uniform attack was also modelled with a maximum penetration of 7 – 2.7 = 4.3 mm. The Von Mises stresses present in the pipe wall are shown in Figure 8.4 and it can be seen that the maximum Von Mises stress is approximately equal to 475 MPa. This stress is quite high and correlates well with the prediction made in Section 6.3 that fatigue failure would be a definite concern.

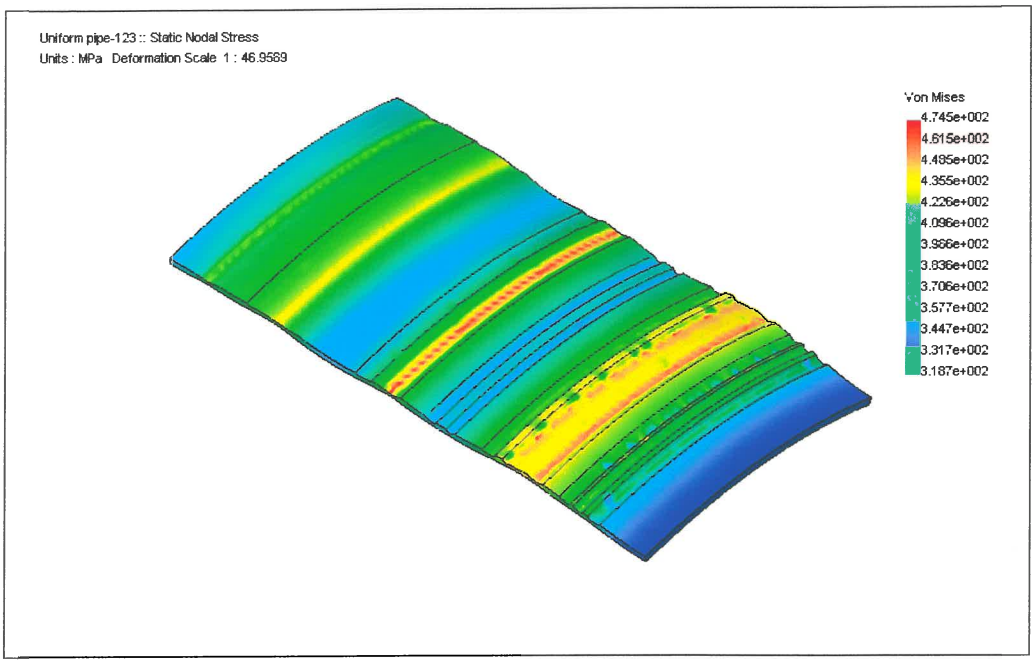

Figure 8.4. FEA results of quasi-stochastic uniform attack on a generic pipe

9. CONCLUSION

The extent of corrosive attack on an underground pipeline might be highly localised or might be fairly uniform over the length of the installation. An indisputable fact proved by research is that, since the pipe is buried, it will not only be a formidable task to quantify the external damage caused by corrosion singularly, but it may even prove impossible. A variety of techniques are used to survey pipelines and to detect anomalies. However, for large pipelines most of these techniques prove to be either inefficient or too expensive and there will always remain some uncertainty regarding the integrity of the pipeline.

The inherent uncertainty associated with the magnitude of various variables that influence the life of the pipeline necessitates the use of a reliability analysis. The reliability analysis was conducted through the use of the Monte Carlo simulation technique. The basis of this technique is to artificially conduct "experiments" or trials on the system by adjusting the system variables at random, within each specific variable's statistical boundaries, and to observe the outcome of each trial. An acceptance criterion (normally in the form of an acceptance domain or region), derived from the physical parameters regarding the system under investigation, is specified and each trial is compared with this criterion.

Two acceptance criteria were used in this study:

1. A static failure criterion valid for pipes subjected to near-constant internal pressures has been used. This criterion is specified in terms of a limit state function (z) that is a derivative of the Von Mises failure criterion. The analysis indicated that the probability of failure is fairly low for a generic pipe that is subjected to near-constant internal pressure. This is not an unexpected result. However, the model has one fundamental flaw – it simulates variations in internal pressure statistically and compares the result with a static failure criterion. The model is, therefore, not indicative of the real fatigue phenomenon. Another drawback of this model is that, since the probability of failure is determined directly by the simulation ($P_f = \frac{n(z \leq 0)}{N}$), it

becomes tedious to determine useful statistical derivatives such as the hazard rate function ($z_H(T)$).

2. A fatigue failure criterion valid for pipes subjected to varying internal pressure has been constructed. This criterion is also specified in terms of a limit state function (D_{CUM}) which is a derivative of Miner's damage rule. In order to determine the probability of failure, an expected life function was defined in Section 6.3 as:

$$Life = F(T, \underline{x}) = \frac{1}{D_{CUM.}(T)} = \frac{1}{\int_0^T (D/year)dT}$$

where T is time and $\underline{x}$ is the set of independent variables that describes the corrosion rate and the stresses in the pipe.

The dependence of the expected life on internal pressure magnitude was illustrated in Section 6.4 and Figure 6.11 indicated that, as can be expected, the life expectancy of a pipeline is a linear, decreasing function of internal pressure. A sensitivity analysis, in the form of the partial derivative of the life function with respect to each variable in the set $\underline{x}$, showed that the expected life is almost totally insensitive to changes in the elastic modulus of the pipe material. This is a key result since it indicates the necessity of using principles of strain-life fatigue analysis.

The variables in the set $\underline{x}$, with known statistics, were randomly changed through the use of the Monte Carlo simulation method. The expected life for each trial was recorded and a statistical distribution function was constructed for the life data. By integrating the distribution function, the probability of pipe failure was obtained. Furthermore, since the distribution function is known, it became possible to determine statistical derivatives such as the hazard rate function. The increasing nature of the hazard rate function indicates that use-based preventative maintenance may certainly be an effective maintenance strategy.

Conventionally, the management structure of an organisation is divided into three task levels:

1. the operational management level concerned with the day-to-day operation of the organisation;
2. mid-level management concerned with communicating strategic instructions from the top-level management to the operational level, as well as aiding the operational level with task execution (i.e. supplying the operational level with resources etc.), and
3. top-level management concerned with steering the organisation on a strategic course.

In terms of efficient functioning, each of these management levels relies on correct and reliable managerial information. In many cases, technical information forms the basis of managerial information. Without reliable information, meaningful and well-founded decisions regarding supply and demand, turnover and profit, cash flow, maintenance task scheduling and replacement programmes cannot be made.

The aim of the work presented in this study was the following:

1. to devise a mathematical model that is easy to implement and to use, and that describes the reliability of a pipeline subjected to the combined effects of internal pressure and external corrosion, and
2. to provide mid- and top-level management with reliable information that can be used to make meaningful and well-founded decisions. An example of this is the hazard rate function, as determined in Sections 6.5 and 6.6, that indicates that use-based preventative maintenance may certainly be an effective maintenance strategy.

An analysis of structural integrity, such as presented in this study, has the following advantages:

1. the risk and consequences of failure can be hedged by employing relevant maintenance strategies;
2. downtime can be minimised, and

3. future strategies regarding the system (i.e. increased supply etc.) can be scrutinised and judged with regard to the reliability and life expectancy of the pipeline.

Furthermore, the work presented in this study can easily be modified to determine the reliability of other structures:

1. by modifying the stress equations, the structural reliability of other stress-bearing components subjected to corrosion can be determined, and
2. by setting the penetration equation (i.e. $P = kT^n$) equal to zero (i.e. $k = 0$) and by modifying the stress equations, the structural reliability of other stress-bearing components that are not subjected to corrosion can be determined.

Finally, a Fracture Mechanics failure criterion was not proposed in this study since the surveillance techniques described in this paper, and used in the context of determining corrosion rate, do not lend themselves to finding cracks in pipelines.

10. REFERENCES

Ahammed, M. and Melchers, R. E. 1997. *Probabilistic analysis of underground pipelines subjected to combined stresses and corrosion*, Engineering Structures, Volume 19, No. 12, pp. 988-994.

ASTM, American Society of Testing and Materials, 1986. *Standard Practise for Examination and Evaluation of Pitting Corrosion.* G 46 – 76.

ASTM, American Society of Testing and Materials, 1989. *Standard Practise for Conventions Applicable to Electrochemical Measurements in Corrosion Testing.* G 3 – 89.

ASTM, American Society of Testing and Materials, 1984. *Standard Practise for Conducting Corrosion Coupon Tests in Plant Equipment.* G 4 – 84.

ASTM, American Society of Testing and Materials, 1987. *Standard Reference Test Method for Making Potentiostatic and Potentiodynamic Anodic Polarization Measurements.* G 5 – 87.

ASTM, American Society of Testing and Materials, 1989. *Standard Practise for Calculation of Corrosion Rates and Related Information from Electrochemical Measurements.* G 102 – 89.

ASTM, American Society of Testing and Materials, 1989. *Standard Guide for Applying Statistics to Corrosion Data.* G 16 – 88.

Bannantine, J. A., Comer, J. J. and Handrock, J. L. 1990. *Fundamentals of Metal Fatigue Analysis*. London:Prentice-Hall.

Brasunas, A.deS. 1984. *Corrosion Basics, An Introduction.* NACE.

Coetzee, Jasper L., 1997. *Maintenance*. Pretoria:Maintenance Publishers.

Denison, I. A., H. H. Uhlig, ed. 1948. *Soil Exposure Tests, Corrosion Handbook*. New York:John Wiley & Sons, p.1048.

Engineering Sciences Data Unit, 1975. *Stress and Strength Volume 6: Fatigue Strength of Material/Pipes.*

Fontana, M.G. and Greene, N.D. 1967. *Corrosion Engineering.* New York:McGraw-Hill.

Kendall, V.V., H. H. Uhlig, ed. 1948. *Water Pipe Service Tests, Corrosion Handbook.* New York: John Wiley & Sons, p.1058.

Kowaka, M. 1989. *Metal Corrosion Damage and Protection Technology.* Allerton Press, Inc.

Landrum, R.J. 1989. *Fundamentals of Designing for Corrosion Control*, NACE.

McAllister, T. P. and Ellingwood, B. R. 2002. *Evaluation of crack growth in miter gate weldments using stochastic mechanics.* Structural Safety. Article in press.

Melchers, R. E. 1999. *Structural Reliability Analysis and Prediction*, Second Edition. Chichester: John Wiley & Sons.

Mohammadi, J., Saxena, S. K. and Wang, Y.T. 1985. *Modelling Failure Probability of Underground Pipes*, in Advances in Underground Pipeline Engineering. New York: ASCE, pp. 193-205.

Osella, A., Favetto, A., López, E. 1997. *Currents induced by geomagnetic storms on buried pipelines as a cause of corrosion*, Journal of Applied Geophysics, Vol. 38, pp. 219-233.

Smith, W. F. 1993. *Principles of Materials Science and Engineering.* New York: McGraw-Hill.

Snyman, J. A. 2000. *Course Notes, Annual Short Course: Mathematical Optimization.*

Stephenson, D. 1976. *Pipeline Design for Water Engineers.* Elsevier.

Websites:

Cast Iron Soil Pipe Institute (CISPI), 2000.

http://www.cispi.org/internet/cispi/corrosion.htm

Chlorine Chemistry Council, 2000. Website:

http://c3.org/chlorine_knowledge_center/safepipes.html

APPENDICES

PROGRAM CODE	DESCRIPTION
APPENDIX A: PROGRAM CODES USED IN THE STATIC ANALYSIS	
MontCSTAT.m	Main program used to conduct a Monte Carlo simulation of a pipe subjected to near-constant internal pressure.
Solve.m	This function determines the value of ***x*** for a random number ***u***, generated by a random number generator. ***x*** is used to determine the sampling point ***r*** (refer to Section 5.6).
itegr.m	This function determines the value of ***x***, for a random number ***u***, by integrating the Normal Distribution Function. This function is called by *solved.m*
Fnormal.m	This function returns the Normal Distribution for a variable ***x***, with mean ***mu*** and standard deviation ***sigma***.
z.m	This function determines the value of the limit state function ***z***, for the set of input variables (refer to Section 5.3)
MontRES.m	This program displays the output of the Monte Carlo simulation for the static analysis.
APPENDIX B: PROGRAM CODES USED IN THE FATIGUE ANALYSIS	
MontCFAT.m	Main program used to conduct a Monte Carlo simulation of a pipe subjected to varying internal pressure.
zero.m	This script determines the time of zero wall thickness for a specific permutation of the corrosion parameters ***k*** and ***n***.
Morrow.m	This function is minimised in *MontCFAT.m* to yield the number of reversals ($2N_f$) to failure.
OutMCF2.m	This script displays the results of the Monte Carlo simulation for the fatigue analysis.
Weibull.m	This function is minimised in *outMCF2.m* to yield the β-parameter of the Weibull Distribution Function.

APPENDIX A: PROGRAM CODES USED IN THE STATIC ANALYSIS (CHAPTER 5)

A1. MAIN PROGRAM – MontCSTAT.m

```
% CG van Deventer
% MONTE CARLO SIMULATION of underground pipelines: Adapted from
% M Ahammed and RE Melchers
% Simulation program for determining probability of pipeline failure when subjected to %
combined stresses
% and corrosion.
% ONLY STATIC STRESSES : No Fatigue
% MontCSTAT.m
% 7/03/2001

clear;
clc;

% Define input variables mu=Mean of variables
% mu=[Le,Bd,Cd,Ct,E,F,Ic,k,kd,km,n,p,r,Sy,t,alpha,gamma,chi,mu,deltheta]
mu=[1000;760;1.32;0.12;201000;150000;1.25;0.066;0.108;0.235;0.53;5;225;400;7;
11.7E-6;18.9E-6;-1E-6;0.3;10];
COV=[0.1;0.1;0.2;0.15;0.033;0.1;0.2;0.56;0.15;0.15;0.26;0.1;0.04;0.05;0.06;0.1;0.1;
0.1;0.023;0.15]; % Coefficient of varation
StdDEV=mu.*COV; % Determine Standard deviation of each of the variables: Sigma(var)
time=[0 15 25 30 40 50 75 100 150 200 250 300];
tic
for counter1=0:11 % YEARLY LOOP STARTS HERE
  T=time(counter1+1) % year increments
  Indicator=0; % Start with empty indicator for each year
  clear P;
  rand('state',sum(100*clock));% Reset the random number generator for each yearly loop

  for counter2=1:50000 % PROBABLITY LOOP STARTS HERE
    counter2
    clear U;
    clear X;
    clear R;
    U=rand(20,1);
```

```
    X=solve(U);
    R=X.*StdDEV+mu;
    Z(counter2,counter1+1)=z([R;T
    if Z(counter2,counter1+1)<=0
        Indicator=Indicator+1
    end; % end if
    P(counter2)=Indicator/counter2;
  end; % end for
Pf(counter1+1)=P(counter2);save BackMCstat2;
end; % end for
save MCstat2;
figure(1);
plot(Pf)
computer_time=toc/60
```

A2. FUNCTION – solve.m

```
function X=solve(U)
for i=1:length(U)
  X(i)=itegr(U(i));
end;
X=X';
```

A3. FUNCTION – itegr.m

```
function out=itegr(u)
mu=0;
sigma=1;
A=100;
A2=0;
if u<0.0001 % Set a Limit on u to increase computational speed
  u=0.0001;
end;
delta=0.1;
x=5;% Starting position of integration
% Integrate from right to left
while A>u
  A2=A2+delta*fnormal(x,mu,sigma);
  x=x-delta;
  A=1-A2;
```

```
end;
out=x;
```

A4. FUNCTION – fnormal.m

```
function out=fnormal(x,mu,sigma)

K=1/(sigma*sqrt(2*pi));
K2=(x-mu)/sigma;
out=K*exp(-0.5*K2^2);
```

A5. FUNCTION – z.m

```
function Z=z(x)
% Usage: Z=z(x)
% x=[Le,Bd,Cd,Ct,E,F,Ic,k,kd,km,n,p,r,Sy,t,alpha,gamma,chi,mu,deltheta,T]
% Function z determines the value of the limit state function for an
% underground pipeline subjected to static stresses and uniform corrosion.
% Failure occurs if Z < 0 and the design is safe if Z > 0.
Le=x(1); Bd=x(2); Cd=x(3); Ct=x(4); E=x(5); F=x(6); Ic=x(7); k=x(8); kd=x(9); km=x(10);
n=x(11); p=x(12); r=x(13); Sy=x(14); t=x(15); alpha=x(16); gamma=x(17); chi=x(18);
mu=x(19); deltheta=x(20);
T=x(21);

Scf=p*r/(t-k*T^n);
Scs=6*km*Cd*gamma*(Bd^2)*E*(t-k*T^n)*r/(E*((t-k*T^n)^3)+(24*kd*p*(r^3)));
Sct=6*km*Ic*Ct*F*E*(t-k*T^n)*r/(Le*((E*((t-k*T^n)^3))+(24*kd*p*(r^3))));
Sc=Scf+Scs+Sct;

Slf=mu*Scf;
Slt=alpha*E*deltheta;
Slb=E*r*chi;
Sl=Slf+Slt+Slb;

% Define Limit state function: z
% Failure if z<0 and safe if z>0

Z=Sy^2-(Sc^2-Sc*Sl+Sl^2);
```

A6. OUTPUT PROGRAM – MontRES.m

```
% CG van Deventer
% Program for displaying results of MONTE CARLO SIMULATIONS
% ONLY STATIC STRESSES : No Fatigue
% MontRES.m
%
% 11/03/2001
clear;
clc;
load MCstat2
Pf1=Pf*100; % Convert to percent
k=mu(8);
n=mu(11);
T=0:0.1:300;
depth=k*T.^n;
% Display results
figure(1)
plot(T,depth)
xlabel('Elapsed pipeline life: Time (T) [years]');
ylabel('Pit depth [mm]');
title('PENETRATION OF CORROSIVE ATTACK vs TIME');
grid on

figure(2)
plot(time,Pf1)
grid on
xlabel('Elapsed pipeline life: Time (T) [years]');
ylabel('Probability of failure (Pf) [%]');
title('PROBABILITY OF FAILURE vs TIME (STATIC APPLIED LOADS)');

figure(4)
plot(P*100)
xlabel('No. of Trials');
ylabel('Probability of failure (Pf) [%]')
title('PROBABILITY OF FAILURE vs No. OF TRIALS');
```

APPENDIX B: PROGRAM CODES USED IN THE FATIGUE ANALYSIS (CHAPTER 6)

B1. MAIN PROGRAM – MontCFAT.m

```
% CG van Deventer
% MONTE CARLO SIMULATION of underground pipelines:
% Simulation program for determining probability of pipeline failure when subjected to
% combined stresses and corrosion.
% FATIGUE ANALYSIS : No Traffic Loads
% MontCFAT.m
%
% 16/04/2001

% START OF PROGRAM

clear all;
clc;
tic; % START TIMER
load IP; % Load the internal pressure signal from the file IP.mat
global c2 deltaEpsilon SigFk SigmaAVE E b EpsFk c k n% Define global variables

%   DEFINE INPUT VARIABLES mu=MEAN OF VARIABLES
%   mu=[r,t,km,Cd,gamma,Bd,E,kd,mu,alpha,deltheta,chi,Kk,nk,SigFk,b,EpsFk,c,k,n]

mux=[500,7,0.235,1.32,18.9E-6,760,201000,0.108,0.3,11.7E-6,10,-1E-6,1337,0.226,1117,
-0.11,0.338,-0.48,0.23909,0.6802];
COV=[0.04,0.06,0.15,0.2,0.1,0.1,0.033,0.15,0.023,0.1,0.15,0.1,0.03,0.03,0.03,0.03,0.03,0.03,
0.1504985,0.062379]; % Co-efficient of varia.
StdDEV=mux.*COV; % Determine Standard deviation of each of the variables: Sigma(var)

for c4=1:150
  rand('state',sum(100*clock));% Reset the random number generator for each trial
  clear U;
  clear X;
  clear R;
  U=rand(20,1);
  X=solve(U);
  MU=X'.*StdDEV+mux;
  r=MU(1);  t=MU(2);  km=MU(3);  Cd=MU(4);  gamma=MU(5);  Bd=MU(6);  E=MU(7);
 kd=MU(8);  mu=MU(9);  alpha=MU(10);  deltheta=MU(11);  chi=MU(12);  Kk=MU(13);
 nk=MU(14);  SigFk=MU(15); b=MU(16); EpsFk=MU(17);  c=MU(18);  k=MU(19);  n=MU(20);
```

```
clear time
clear time1
clear time2
zero
time2=0.5*floor(time1);
increment=floor(time2/7);
% TIME VECTOR from Zero to Time of Zero Thickness
time=0:increment:time2;
time(8:15)=time1*[0.52 0.55 0.58 0.6 0.62 0.8 0.9 1];

% START DAMAGE LOOP HERE
for c3=1:length(time)
  clear S1x S2x Sx S1y S2y S3y Sy %SigmaEq deltaSigma deltaEpsilon SigmaAVE
  Pit=depth(time(c3));
  if Pit>6.999
    Pit=6.999;
  end;
  % DETERMINE EQUIVALENT STRESSES FROM IP, PIT DEPTH, AND STRESS EQUATIONS
  for c1=1:120
    S1x(c1)=IP(c1)*r/(t-Pit); % Hoop stress due to internal pressure
    S2x(c1)=(6*km*Cd*gamma*Bd^2*E*(t-Pit)*r)/(E*(t-Pit)^3+24*kd*IP(c1)*r^3); % Hoop stress due to soil pressure
    Sx(c1)=S1x(c1)+S2x(c1); % Total hoop stress
    S1y(c1)=mu*S1x(c1); % Longitudinal stress due to Poisson effect (Longitudinal constraint)
    S2y(c1)=alpha*E*deltheta; % Longitudinal stress due to thermal difference
    S3y(c1)=E*r*chi; % Longitudinal stress due to longitudinal bending due to variation in soil bed height
    Sy(c1)=S1y(c1)+S2y(c1)+S3y(c1); % Total longitudinal stress
    SigmaEq(c1)=(Sx(c1)^2-Sx(c1)*Sy(c1)+Sy(c1)^2)^0.5; % Equivalent stress : Von Mises distortion energy theory
    SIGMAEQ(c1,c3)=SigmaEq(c1);
  end;

  % CALCULATE HYSTERIS CURVE
    SigmaEq(121)=SigmaEq(1); % Make sure that the block "closes"
  if max(SigmaEq)>=SigFk
    break
```

```
    end;

    TIME(c4,c3)=time(c3);

    for c2=1:120
      deltaSigma(c2)=abs(SigmaEq(c2+1)-SigmaEq(c2));
      deltaEpsilon(c2)=(deltaSigma(c2)/E)+(2*(deltaSigma(c2)/(2*Kk))^(1/nk));  %  Calculate
from Hysteris Curve Equation
      SigmaAVE(c2)=(SigmaEq(c2+1)+SigmaEq(c2))/2;
      SIGMAAVE(c2,c3)=SigmaAVE(c2);

      % DETERMINE THE LIFE BY USING MORROW'S STRAIN-LIFE EQUATION

     % SOLVE FOR 2Nf FROM THE FOLLOWING EQ. %%
    % deltaEpsilon(c2)/2=((SigFk-SigmaAVE(c2))/E)*(Nf2)^b+EpsFk*(Nf2)^c; % Nf2 = 2*Nf %

      x=1E12;% Starting point of optimization procedure in safe region (1 million cycles ???)
      if c3>10
        x=1000;
      end;
      f=inline('100000*(morrow(Nf2))^2');
      [xx]=fminsearch(f,x);
      check(c2)=morrow(xx);
      Nf2(c2)=xx;
      ReversalDamage(c2)=1/Nf2(c2);
    end;
    BlockDamage(c3,c4)=sum(ReversalDamage);

    BlockLife(c3,c4)=1/BlockDamage(c3,c4); % No of blocks to be expected before failure
    noBlocksYear=60*24*365.25; % No of Blocks per year;
    TimeLifeYear(c3,c4)=BlockLife(c3,c4)/noBlocksYear; % No of years (continuous service)
to be expected before failure
    YearDamage(c3,c4)=BlockDamage(c3,c4)*noBlocksYear; % Damage caused in 1 year

  end;
  save MCF
end;

computer_time=toc/60 % END TIMER
save MCF
```

```
%%%%%%%% END OF MAIN PROGRAM %%%%%%%%
```

B2. DETERMINE TIME OF ZERO WALL THICKNESS – zero.m

```
% DETERMINE TIME OF ZERO WALL-THICKNESS

time1=0;
Pit=depth(time1);
while Pit<t
  time1=time1+10;
  Pit=depth(time1);
end;
while Pit>t
  time1=time1-1;
  Pit=depth(time1);
end;
while Pit<t
  time1=time1+0.1;
  Pit=depth(time1);
end;
while Pit>t
  time1=time1-0.01;
  Pit=depth(time1);
end;
```

B3. FUNCTION – morrow.m

```
function out=morrow(Nf2)

global c2 deltaEpsilon SigFk SigmaAVE E b EpsFk c

out=deltaEpsilon(c2)/2-((SigFk-SigmaAVE(c2))/E)*(Nf2)^b-EpsFk*(Nf2)^c;
```

B4. OUTPUT PROGRAM – outMCF2.m

```
%%%% OUTPUT %%%%
% FATIGUE SIMULATIONS no. 1%
% Filename: outMCF2.m
clear all
clc
gcl

global N ExpLife

load MCF2
DAMAGEyear(:,1:150)=YearDamage;
TIME1(:,1:150)=TIME';
CumDamage=zeros(12,150);

for i=1:150
  indicator=max(find(TIME1(:,i)));
  p=12-indicator+1;
  CumDamage(p:12,i)=cumtrapz(TIME1(1:indicator,i),DAMAGEyear(1:indicator,i));
  TIME2(p:12,i)=TIME1(1:indicator,i);
end;
CumLife=1./CumDamage;
for j=1:150;
  index=max(find(CumDamage(:,j)<=1));
  ExpLife(j)=TIME2(index,j);
end;

% Determine Weibull parameters out of ExpLife
N=length(ExpLife);
x=2; % Starting point of minimization
% solve beta by minimizing weibull
f=inline('100000*(weibull(beta))^2');
[xx]=fminsearch(f,x);
beta=xx;
eta=((sum(ExpLife.^beta))/N)^(1/beta);
```

```
% Distribution functions
tt=0:0.1:250;
for k=1:length(tt)
  ff(k)=((beta/eta)*(tt(k)/eta)^(beta-1))*exp(-(tt(k)/eta)^beta);
  F(k)=1-exp(-(tt(k)/eta)^beta);
end;
figure(1)
plot(TIME2,CumDamage);
xlabel('Time [years]');
ylabel('Cumulative Damage year');
title('CUMULATIVE DAMAGE vs. YEAR');
axis([0 350 0 30]);

figure(2)
plot(TIME2,CumLife);
title('EXPECTED LIFE vs. YEAR');
xlabel('Elapsed Time [years]');
ylabel('Remaining Life [years]');
axis([0 350 0 12E8]);

figure(3)
hist(ExpLife,30)
axis([0 300 0 25]);
xlabel('Elapsed Time [years]');
ylabel('Number of Occurrences');
title('HISTOGRAM OF EXPECTED LIFE');

figure(4)
plot(tt,ff);
xlabel('Time [years]');
ylabel('f(T,mu,sigma)');
title('WEIBULL DISTRIBUTION FUNCTION')
axis([0 250 0 0.012]);

figure(5)
plot(tt,F*100);
xlabel('Time [years]');
```

```
ylabel('Probablilty [%]');
title('CUMULATIVE DISTRIBUTION FUNCTION')
grid on
axis([0 250 0 100]);
figure(6)
plot(tt,ff./(1-F));
xlabel('Time [years]');
ylabel('z');
title('HAZARD RATE FUNCTION (z = f(t)/R(t))')
axis([0 250 0 0.09]);
```

B5. FUNCTION – weibull.m

```
function out=weibull(beta)

global N ExpLife

out=(1/N)*sum(log(ExpLife))-(sum(ExpLife.^beta.*log(ExpLife)))/(sum(ExpLife.^beta))+1/beta;
```